The regular and chaotic dynamics of structures in fluid flows

M. I. Rabinovich and M. M. Sushchik

Institute of Applied Physics of the Academy of Sciences of the USSR, Gor'kiĭ
Usp. Fiz. Nauk **160**, 3–64 (January 1990)

"Order in chaos" is not an abstraction. It is a characteristic of real disordered processes and can be formulated quantitatively. In application to turbulence the term "order in chaos" means the existence of localized metastable states—structures. In this review experiments demonstrating that the nonlinear dynamics of these structures can be both regular and chaotic are discussed. Models on the basis of which it is possible to construct a theory of spatial-temporal chaos in an ensemble of structures and thereby to discuss turbulence with small and moderate values of the critical parameter (relative Reynolds number) are studied.

1. INTRODUCTION

The question of what state of a nonequilibrium medium or field is realized when the threshold of stability of the trivial equilibrium is exceeded by a finite amount is interesting for different fields of physics. Even recently it was believed that either completely ordered or completely disordered (turbulent) states of a field are typically established. In the first case different elementary excitations self-coordinate with one another in the process of nonlinear interaction and as a result a regular (in space and time) nontrivial formation—a structure which is stable in a finite region of parameters—arises. In the second case any definite combination of elementary excitations is unstable and spatial-temporal disorder—turbulence—is established.

Although physicists have always been interested in the problem of the relationship between chaos and order the theory of nonlinear structures (self-organization) and the theory of turbulence until recently largely coexisted independently of one another. The remarkable progress made in nonlinear dynamics and fundamentally new approaches to experimental studies of turbulence have made it possible only in the last few years to come close to understanding the problem of the interrelationship of structures and turbulence. It has been found that ordered structures exist even very far above threshold, when everything points to the formation of disorder. These ordered structures are often localized in space and they can be regarded as concentrated objects—particles. In analyzing the interaction of localized structures one necessarily encounters an important general-physical problem, in some sense opposite to the traditional problem. For example, in the quantum theory of fields particles and forces are unified, i.e., they are described on the same footing; here, however, localized states—structures—and the forces acting on them must be set apart on the basis of the nonlinear field equations. The transfer from continuous equations to discrete equations (for localized structures or their ensembles) is possible in those cases when the fields of individual structures decay rapidly enough from the center toward the periphery. The existence of a small parameter, equal to the ratio of the fields of the ith and jth structures in the region of the maximum of the field of the jth structure, makes it possible to apply the asymptotic method and to derive equations describing the dynamics of individual structures which are coupled with one another by a weak interaction.

This paper is devoted to the problem of structures in turbulence. It will be shown that real turbulence can often be regarded as the chaotic dynamics of nonlinearly interacting structures; moreover, the more developed chaotic dynamics, i.e., motion on a stochastic set of higher dimension, corresponds to more strongly developed turbulence. Although many of the results of the qualitative theory of turbulence which are presented below are common to fields of different nature the main attention is devoted to hydrodynamic flows, since it is precisely for these flows that, thanks to the exceptional possibilities of the method of visualization, inspiring experiments illustrating the existence of structures not only near a transition but also in developed turbulence have been performed.

2. THE DIVERSITY AND UNIVERSALITY OF STRUCTURES

Structures form in hydrodynamic flows as the result of the development of a hierarchy of instabilities as the critical parameter (the relative Reynolds number, Rayleigh's number, etc.) increases. In the process both the scales of the structures and their spatial and temporal symmetry change. In spite of the enormous diversity of structures and paths by which simple structures can transform into more complicated structures the existing experimental and theoretical (predominantly numerical) results make it possible to discern a general pattern.

2.1. Restructuring of the spatial symmetry of a flow. Rayleigh-Bénard thermal convection

When the uniform state of simple flows, such as, in particular, thermal convection and Taylor-Couette flow between rotating cylinders, becomes unstable spontaneously, i.e., without an external forcing, ordered structures in the form of different types of lattices appear (a honeycomb or chain of rolls accompanying thermal convection; Taylor vortices in the flow between rotating cylinders; square lattices of Faraday ripples in a layer of liquid on a vibrating substrate, etc.). As the degree of nonequilibrium of the medium increases further the regular lattices become more complicated (also spontaneously). For thermal convection under conditions of small Rayleigh numbers this increase in complexity is often unrelated with the change in the temporal dynamics and is manifested as a change in only the spatial symmetry of the flow. Although the scenarios of the destruction and change in the spatial symmetry of different flows

 0038-5670/90/010001-35$01.00

are extremely diverse we can try to identify the two most typical ones. The first scenario is related with the increase in the complexity of individual structures as the critical parameter increases and with the development of a secondary instability; the second scenario is connected with the appearance of dislocations in an ordered lattice of structures. We shall discuss these scenarios for the example of thermal convection.

Thermal convection in a thin layer of liquid heated from below is described by the equations of hydrodynamics and heat conduction in the Boussinesq approximation (see, for example, Ref. 1):

$$\mathrm{Pr}^{-1}\left(\frac{\partial \mathbf{u}}{\partial t} + \mathbf{u}\nabla\mathbf{u}\right) = -\frac{\nabla p}{\rho} + \theta\mathbf{z} + \nabla^2\mathbf{u}, \tag{2.1}$$

$$\nabla\mathbf{u} = 0, \tag{2.2}$$

$$\frac{\partial\theta}{\partial t} + \mathbf{u}\nabla\theta = \mathrm{Ra}(\mathbf{zu}) + \nabla^2\theta \tag{2.3}$$

with the boundary conditions at $z = \pm 1/2$

$$u_z = \partial_z u_z = \theta = 0$$

in the case of solid boundaries and

$$u_z = \partial^2_{zz} u_z = \theta = 0$$

in the case of free boundaries; here $\mathbf{z}$ is a unit vector directed opposite of the force of gravity; $\mathbf{u}$ is the velocity vector; p is the pressure; and, θ is the deviation of the temperature from the equilibrium value. The Rayleigh number $\mathbf{Ra} = \gamma g(T_2 - T_1)d^3/\nu\varkappa$ and the Prandtl number $\mathbf{Pr} = \nu/\varkappa$ depend on the kinematic viscosity ν and the thermal conductivity $\varkappa$; γ is the thermal expansion coefficient; and, g is the acceleration of gravity. The thickness of the layer d, the heat diffusion time $d^2/\varkappa$, and the temperature difference $T_2 - T_1$, where T_2 and T_1 are the average temperatures at the bottom and top boundaries, are chosen as the length, time, and temperature scales, respectively.

One can see from Eqs. (2.1)–(2.3) that the conditions for instability of static equilibrium $u = 0$, determined from the linearized system, depend solely on the Rayleigh number. At a small distance above the threshold of stability $\mathbf{Ra}_c$ ($\mathbf{Ra}_c = 1707.76$ in the case of solid boundaries and $\mathbf{Ra}_c \approx 657$ in the case of free boundaries) for an unbounded layer there exists an infinite number of stationary solutions which are periodic in space.[2-4] Analysis (including also numerical) of the system of equations (2.1)–(2.3) shows that in the case when the critical parameter $\varepsilon = \mathbf{Ra}/\mathbf{Ra}_c - 1$ is small only solutions corresponding to a periodic chain of parallel two-dimensional rolls with the characteristic spatial period $\lambda \equiv 2\pi/k \sim d$ can be stable.

The problem of determining the stability of one or another nontrivial regime of thermal convection, requiring an analysis of the behavior of secondary excitations (developing on the background formed by the starting excitations), is extremely unwieldy. It reduces to finding the spectrum of the eigenvalues of an inhomogeneous boundary-value problem with variable coefficients and can be solved analytically in only rare cases. We shall not dwell on this question in detail; we shall present only some results that demonstrate the diversity of structures which arise on the background of the starting convective rolls as the critical parameter increases.

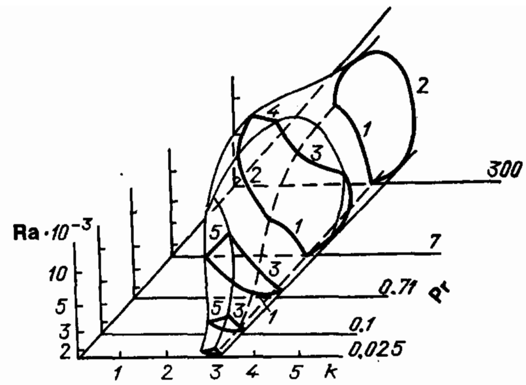

FIG. 1. The surface Σ determining the values of the parameters $\mathbf{Ra}$, $\mathbf{Pr}$, and k for which the convective rolls become unstable; the heavy lines show the intersection of the surface Σ with the planes $\mathbf{Pr} = \text{const}$ (see Ref. 1).

Figure 1 (see Ref. 1) shows the boundary Σ of the region of stability of two-dimensional rolls which was constructed using numerical methods. As the critical parameter $\varepsilon = \mathbf{Ra}/\mathbf{Ra}_c - 1$ is increased in the case of large Prandtl numbers two basic types of secondary instabilities can be identified. Near the part 1 of the surface Σ the two-dimensional structure of the flow becomes unstable with respect to disturbances of the type oblique rolls. In the experiment of Ref. 5 these secondary rolls are established at angles of $\pm 40°$ with respect to the starting rolls (zigzag instability). The development of this instability leads to the formation of new stationary structures, which look like sinusoidally deformed primary rolls. An instability of the cross-roll type appears near the other part 2 of the surface Σ.[6]

For lower Prandtl numbers (near the part 3 of the surface Σ) an instability of the type varicose expansions becomes important.[6,7] On the top part 4 of the surface Σ this instability, like the cross-roll instability, transforms into a knot instability, engendering more complicated structures. For low Prandtl numbers ($\mathbf{Pr} < 1.1$ for rigid and $\mathbf{Pr} < 3.5$ for free boundaries) a purely two-dimensional mechanism of instability appears on the bottom part of the surface Σ—two two-dimensional disturbances grow simultaneously; the wave number for one of them is much larger than and the wave number for the other is much smaller than for the starting rolls (Eckhaus instability[8-10,1]; see the list of remarks appended to the end of the paper). Finally, near the part 5 of the surface Σ there occurs a transition to structures which oscillate in time (oscillatory instability) with wavy transverse motions of the walls.[12,13] For large Prandtl numbers the transition to the oscillatory instability is observed only after purely three-dimensional structures have formed.

The second path by which the symmetry of flows can change spontaneously as the critical parameter increases is connected not with individual structures forming a lattice becoming more complicated but rather with the appearance of defects in the lattice. There is a deep analogy between the studied defects arising in the structures of nonlinear fields and defects in condensed media (crystals, magnets, etc.)—*the properties and symmetry of the defects are determined* primarily by the properties of the lattice.[14,15] Although such defects appear spontaneously as a result of the development of instability as the critical parameter increases, in order to create or destroy them in a steady-state flow a finite forcing

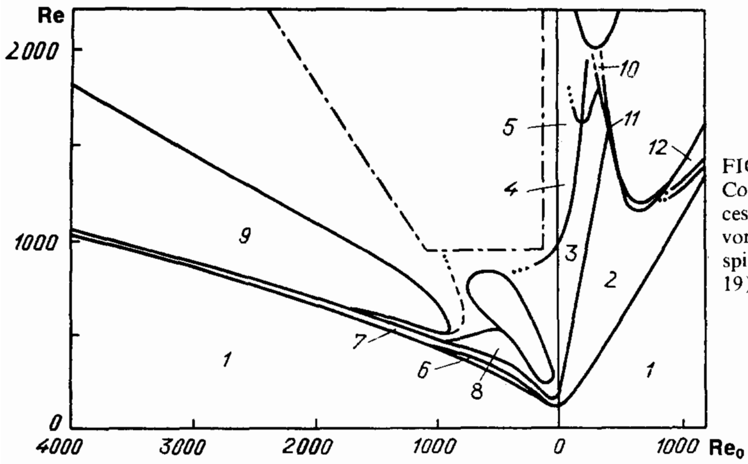

FIG. 2. The regimes of flow between independently rotating cylinders. 1–Couette flow; 2–Taylor vortex flow; 3–azimuthal waves on Taylor vortices; 4–modulated azimuthal waves on Taylor vortices; 5–turbulent Taylor vortices; 6–spiral Taylor vortices; 7–interpenetrating spirals; 8–wavy spirals; 9–spiral turbulence (the structures 10–12 are described in Ref. 19).

must be applied,[16] i.e., defects are stable formations and they can be regarded as independent structures (this will be discussed below).

2.2. Increase in the complexity of the temporal dynamics–appearance of oscillations and "temporal chaos." Taylor vortices

The appearance of nontrivial temporal behavior in different flows happens either as a result of a change in the intrinsic dynamics of individual structures or owing to the appearance of collective excitations in the ensemble of structures. In the process complex behavior and even chaotic dynamics can appear in spatially ordered flows without a change of the flow structure. It is obvious that transitions from simple to complicated dynamics in which the spatial structure is preserved are in no way different from the well-known bifurcations in systems with lumped parameters and the results of the theory of finite-dimensional dynamical systems are valid for them unconditionally (see, for example, Refs. 17 and 18). In particular, this pertains to the dynamics of the azimuthal modes on Taylor vortices in flow between rotating cylinders.

The diagram in Fig. 2, [19] constructed based on experimental data for a fixed value of the Reynolds number $\mathbf{Re}_0 = b(b-a)\Omega_0/\nu$ of the outer cylinder and a slow (quasistatic) increase of the Reynolds number of the inner cylinder $\mathbf{Re} = a(b-a)\Omega/\nu$, illustrates the diversity of structures arising in such a flow. Here $b = 59.46$ mm and $a = 52.5$ mm are the radii while Ω_0 and Ω are the angular rotational velocities of the outer and inner cylinders, respectively (the length of the cylinders $L \approx 30(b-a)$; the covers at the ends of the cylinders rotate together with the outer cylinder).

If the cylinders rotate in the same direction, then Taylor vortices form after the Couette flow becomes unstable (region 2 in Fig. 2); as **Re** is further increased these vortices in their turn become unstable. However even significantly above their threshold of stability the Taylor vortices are not completely destroyed—disturbances in the form of azimuthal waves arise on them (the regions 3, 10, 11, and 12). For low rotational velocities of the outer cylinder ($\mathbf{Re}_0 < 40$, region 3) these disturbances look like periodic (as a function of the azimuthal angle) inflections of the Taylor vortices. As **Re** is increased (region 4) periodic modulation appears in the azimuthal waves, and two independent frequencies and their combinations can be seen in the spectrum. The representation of such a flow in the phase space of the equivalent dynamical system is an open winding on a two-dimensional torus. It is well known[20,21] that as the critical parameter is increased the appearance of new frequencies and the decomposition of the N-dimensional torus for $N \geqslant 3$ can result in the appearance of a strange attractor—a transition to chaos through quasiperiodicity. This process is in fact observed under certain conditions (region 5) in a Taylor-Couette flow—previously excited azimuthal waves on Taylor vortices become stochastic, though in the process new spatial modes are not excited.[22] Even significantly above the threshold of stochastization the flow retains the distinct structure of Taylor vortices with azimuthal modes excited on them.[22]

2.3. Turbulent spots. Plane Poiseuille flow

Together with staged transitions, associated with a successive increase in the number of excited degrees of freedom, flows of other type—sharper transitions, directly transferring the flow from a stationary (or even static) state into a chaotic state in time together with a significant increase in the complexity of the spatial structure—are also encountered (see, for example, Ref. 23). Such transitions with formation of solitary turbulent structures are characteristic for strictly parallel flows, for example, planar Poiseuille flow.

The planar Poiseuille flow (in which the longitudinal component of the average velocity cross the channel $U = U_0[1-(z^2/h^2)]$, h being the half-width of the channel) becomes unstable at $\mathbf{Re} = \mathbf{Re}_c = 5772$ with respect to an infinitesimal disturbance (see Refs. 24 and 25). With respect to two-dimensional finite-amplitude waves, however, the flow is also unstable for $\mathbf{Re} < \mathbf{Re}_c$ (subcritical instability).[25] These waves, in their turn, are unstable with respect to three-dimensional infinitesimal disturbances.[2)] Moreover, numerical[25] and physical[26] experiments show that the instability with respect to three-dimensional disturbances also remains for two-dimensional waves for Reynolds numbers such that the flows are decaying (for $700 \lesssim \mathbf{Re} \lesssim 2900$). Since the characteristic decay times of a two-dimensional wave are longer than the growth times of three-dimensional disturbances there is enough time for them to build up before the primary wave decays. As the experiments of Ref. 27 show, this cascade is then repeated, and because of the nonuniformity of the initial disturbances and the amplitude dependence of the threshold for small values of **Re** solitary turbulent spots, surrounded by laminar flow, usually appear.

Although the turbulent spots in a planar Poiseuille flow are not identical and change with time they are characterized by universal properties associated with the manifestation of their characteristic dynamics. Figure 3 shows a schematic diagram of a turbulent spot and a photograph of this spot, which were obtained with visualization of the flow.[27] For **Re** = 840–1500 turbulent spots have the form of a triangular wing with a flare angle of 15–20°, and as they are carried downstream they grow in size. A turbulent vortex motion arises inside the spot; this motion can be regarded as resulting from the strong interaction of oblique waves. At the boundary of the spot waves are emitted into the laminar region of the flow. Initially these waves are quite regular, but then because of the secondary instability they decay, thus leading to growth of the turbulent nucleus. For smaller Reynolds numbers (**Re** < 840) there is not enough time for fully developed turbulent spots to form—they are transformed into longitudinal vortex structures which decay with time. An increase in the critical parameter results first in an increase in the number of randomly distributed turbulent spots and then (for **Re** > 1500) in the entire flow becoming turbulent. The transition to turbulence occurs in a similar manner (i.e., through turbulent structures—spots) in planar Couette flow and in axisymmetric Poiseuille flows (see, for example, Ref. 28).

2.4. Small-scale structures. Boundary layer

The small-scale turbulence, arising as a result of a sequential cascade of a large number of spatial and temporal bifurcations, ultimately turns out to be structurally so complicated that, strictly speaking, it becomes impractical to represent it in the form of an ensemble of structures (especially since the number of different types of structures also increases at the same time). It turns out, however, that in strongly nonuniform and anisotropic flows such as, for example, two-dimensional boundary and free shear layers, cascade-free generation of small-scale structures is possible (as a result of a small number of bifurcations). In this case their symmetry is substantially affected by the dynamical and kinematic restrictions connected with the geometry of the flow, and such structures turn out to be comparatively simple and easily identifiable in an experiment. Examples of such structures are: a small groove on Taylor vortices, which arises near the wall of the outer cylinder in Taylor-Couette flow;[19] longitudinal vortices in shear flows generated near saddle points of the velocity field of large-scale structures;[29–34] ripples and "horse shoes" on spiral vortices in flow past rotating bodies;[35,39] etc.

To understand the nature of turbulence it is essential that such structures persist not only near a transition but also in fully developed turbulent flow. From this viewpoint the structure of a turbulent boundary layer is instructive–a significant part of its three-dimensional vorticity is concentrated in "spoke-like" vortices, which accumulate downstream at an angle of about 45°, are carried off by the flow with approximately the same velocity, and interact comparatively weakly with one another.[40] The transverse dimen-

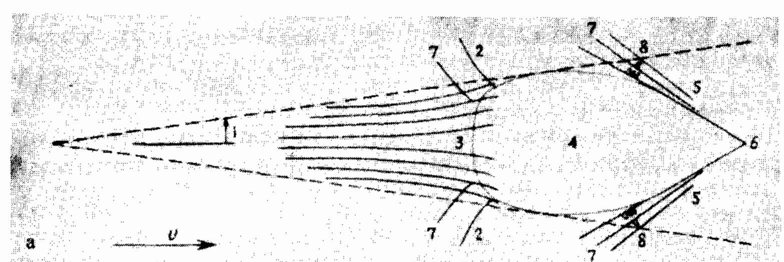

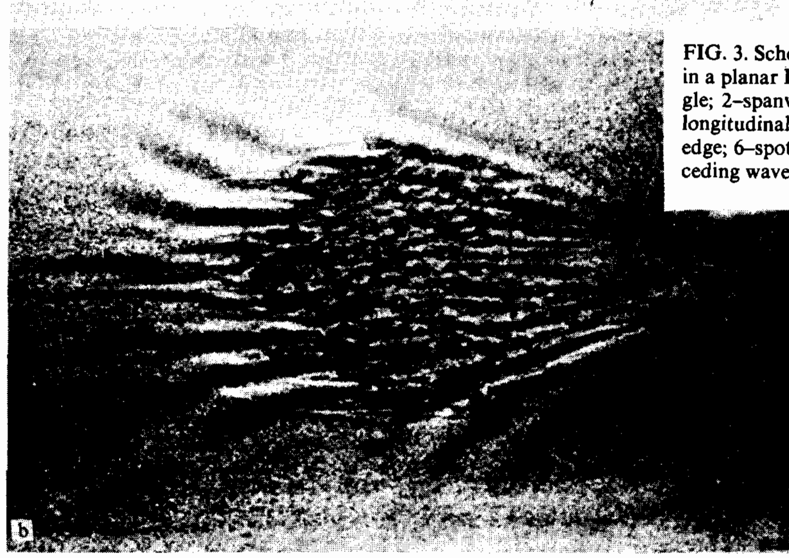

FIG. 3. Schematic diagram (a) and visualization (b) of a turbulent spot in a planar Poiseuille flow. **Re** = 10^3, $x/h = 64$. a) 1–Spreading half-angle; 2–spanwise tips; 3–streaks consisting of structures oriented in the longitudinal direction; 4–region of small-scale turbulence; 5–spot leading edge; 6–spot front; 7–waves receding from the spot; 8–excitations on receding waves (see Ref. 27).

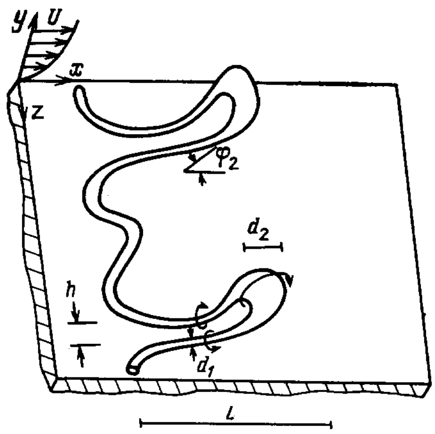

FIG. 4. Horseshoe-shaped vortex, forming in the transitional region of the boundary layer on a flat plate. The angle of inclination of the horseshoe $\varphi \approx 45°$, the width of the horseshoe $h \approx (50\text{–}60)\nu/U_\tau$, the length of the vortex along the flow $L \approx 10^3\ \nu/U_\tau$, the diameter of the vortex at the base $d_1 \approx (30\text{–}40)\ \nu/U_\tau$, and the diameter of the vortex at the top of the horseshoe $d_2 \approx (10\text{–}40)\ \nu/U_\tau$ (see Ref. 41).

sions of such vortices[41] $\sim (10\text{–}100)\nu/U_\tau$ are much smaller than the thickness of the boundary layer $\delta \sim 10^3\nu/U_\tau$, where

$$U_\tau = \left(\nu \frac{\partial U}{\partial y}\bigg|_{y=0}\right)^2$$

is the friction velocity, which depends on the tangential stresses at the wall $y = 0$ (Fig. 4). The model of a boundary layer in the form of a statistical ensemble of such structures gives a correct overall description of the relationship between the form of the average velocity profile, the distribution of the turbulence intensity, and the turbulence spectra.[42]

Although the mechanisms of formation of spoke-like vortices have not yet been completely studied it nonetheless follows from analysis of experiments[43–45] that the appearance of such vortices is indeed preceded by a small number of bifurcations. Downstream the following occur in succession:[3)] instability of the boundary layer and development of two-dimensional waves; appearance of three-dimensionality on the background of these waves and generation of longitudinal vorticity near the critical layer (see Ref. 46); removal of low-velocity liquid and formation of thin three-dimensional shear layers; and, development of nonviscous instability of the three-dimensional shear flow accompanied by formation of a horseshoe-shaped vortex and its subsequent stretching in the field of the deforming velocity of the large-scale flow.

2.5. Secondary structures. Shear flows

Here we shall demonstrate using the example of shear flows that large-scale coherent formations can exist in a stable fashion in a nonstationary nonuniform medium also, in particular, in a turbulent shear flow. This situation is typical for hydrodynamics, if the characteristic scales L of instability are much greater than the scales l of the background turbulence of the flow ($l \ll L$).

The experimentally realizable shear layers usually develop in space—along the flow behind a plate separating two flows with different velocities. If the shear layer was formed by merging of laminar flows, then for sufficiently large Reynolds numbers the characteristic times of the nonviscous instability are much shorter than the viscous diffusion times, and for this reason quasistationary structures—a chain of two-dimensional vortices—form first (under the influence of the nondissipative mechanism of stabilization of the instability). Turbulence in the incident flow does not affect the character of the process—it merely introduces a small correction to the increment of the nonviscous instability and turbulent diffusion; this can be observed only at large distances downstream. However the processes determined by the dynamics of the large-scale structures become important much earlier—the chain of turbulent vortices formed at the starting stage is in its turn unstable with respect to perturbations with longer wavelength, equal primarily to twice the spatial period (see Ref. 47). The development of this instability farther downstream leads to merging (predominantly pairwise) of primary structures and formation of a new chain, etc. Amplification of three-dimensional disturbances—a competing process which could destroy the two-dimensional structures— is suppressed owing to such mergings.[48–50] For this reason, even when the incident flow or the boundary layer on the plate separating flows are made artificially turbulent or when a device generating three-dimensional vortices is placed on the plate the degree of two-dimensionality of the large-scale structures increases after the first several mergings, i.e., downstream.[50] As a result large-scale coherent structures (i.e., structures which are dynamically stable with respect to the action of small-scale turbulence) are observed in shear layers at all distances downstream for which laboratory measurements have now been performed, right up to $x = 5000\theta \approx 3$ m (see Ref. 15), where θ is the momentum thickness of the shear layer near the edge of the plate.

In the other limiting case, when the increments of instability of the mean flow are small or the flow, generally speaking, is stable the existence of small-scale structures or small-scale turbulence can play a qualitatively different role. In particular, analysis[52–61] of the solutions of the Navier-Stokes equations

$$\frac{\partial \mathbf{u}}{\partial t} + \mathbf{u}\,\nabla \mathbf{u} = -\frac{\nabla p}{\rho} + \nu \nabla^2 \mathbf{u} + \mathbf{f}(\mathbf{r}), \tag{2.4}$$

$$\nabla \mathbf{u} = 0 \tag{2.5}$$

with the external force $\mathbf{f}(\mathbf{r})$, giving a stationary small-scale flow which is periodic in space, shows that large-scale structures can form spontaneously as a result of the development of the long-wavelength instability, owing precisely to the microstructure of the flow.

The transfer of energy from small scales (which, as a rule, are three-dimensional) to larger scales, as follows from a linear analysis of the stability of structured flows,[57–61] requires that such flows be quite strongly anisotropic. Numerical calculations[59] show that in the process the formation of large-scale structures once again results in the destruction of the starting symmetry of the flow, and the energy in the large-scale secondary flow resides predominantly in the velocity components which have in the primary flow the highest energy. Aside from the anisotropy, spirality of the small-scale turbulence and weak compressibility also can affect the reverse cascade of energy transfer.[55,56]

Of course, in real experiments it is difficult to separate the mechanisms of formation of secondary structures associated directly with small-scale turbulence and with the instability of the average temperature, velocity, etc. profile. Nonetheless the fact that small-scale turbulence can have a nontrivial effect on secondary structures can be confirmed in some flows. Thus in the case of developed turbulent convection with $\mathbf{Ra} \sim 10^7$ the mechanism of formation of almost stationary structures, reminiscent of hexagonal cells, is apparently substantially different from the mechanism of formation of such cells in the absence of small-scale structures—now there is no preference for cold or hot liquid at the center of the cell, and cells of both types can usually be found in different parts of the layer.[62] Other well-known examples of large-scale secondary structures are turbulent Taylor vortices, which are observed right up to $R \sim 10^8$ (see Refs. 63 and 64), and large-scale drift flows in thermal convection.[65,66]

2.6. Generalized Ginzburg-Landau equation

Experiments show that flow restructuring which results in the formation and transformation of structures very often occurs with very low values of the critical parameter ε. Therefore the increments of the spatial disturbances determining the formation of structures are small. In addition, as ε increases the flow becomes more complicated, usually as a result of successive transformations–bifurcations with $\varepsilon = \varepsilon_i$ $(i = 1,2,...)$. This means that Landau's scheme can be employed to construct the theory of formation of structures at the first stage.[67] For example, if after the first bifurcation the flow field can be represented in the form $u(\mathbf{r},t) = A(t)f(\mathbf{r})\exp(i\omega t)$ (the spatial structure of the field $f(\mathbf{r})$, determined by the geometry of the problem, is fixed), Landau's equation[24,67] is obtained for $A(t)$:

$$\frac{\mathrm{d}|A|^2}{\mathrm{d}t} = 2\gamma|A|^2 - l|A|^4. \tag{2.6}$$

Here the increment γ is determined from the linear approximation, while l is Landau's constant, which for $l > 0$ characterizes the nonlinear stabilization in the lowest order of perturbation theory.

In unbounded flows the spatial spectrum of the growing disturbances is obviously continuous, and for this reason for any small excess above the threshold of stability the spatial structure of the flow should be determined from the solution of the nonlinear problem. At a finite excess above the threshold of stability this is also valid for bounded but quite extended flows. For such flows quite accurate models based on the asymptotic analysis of the starting equations (2.1)–(2.3) or (2.4) and (2.5) can be constructed only with some restrictions on the spatial structure of the velocity field.

In models of flow which have been studied in greatest detail up to now the change in the velocity (temperature) along one of the coordinates z is given $(\sim \xi(z))$, while in the (x, y) plane normal to the z axis it is determined by a narrow packet of modes, for example, describing the slightly curved rolls in Rayleigh-Bénard convection, quasi-two-dimensional Tollmien-Schlichting waves in a boundary layer, etc. With these restrictions a slow envelope field $A(x, y, t)$ will be described by a quite general model–the two-dimensional analog of the complex Ginzburg-Landau equation (GL) (see, for example, Refs. 68 and 69). We shall briefly discuss the derivation of this equation for the case when the conditions for rotational symmetry are satisfied in the linear approximation [at least for small angles of rotation relative to the main wave vector of the packet k_0 in the horizontal (x, y) plane]. The starting problem will be the problem of linear stability

$$L\left(\frac{\partial}{\partial t};\ -\nabla^2;\ \frac{\partial}{\partial z};\ \mathrm{Re}\right)\mathbf{u}(x, y, t)\,\xi(z) = 0,$$

whose solution can be written in the form

$$u_i(x, y, t) = u_{i,0}\exp(i\mathbf{k}\mathbf{r} + \gamma t - i\omega t),$$

where

$$L\{\gamma(\mathbf{k}, \mathrm{Re}) - i\omega(\mathbf{k}, \mathrm{Re});\ k^2;\ \mathrm{Re}\} = 0,$$

$$\mathbf{r} = (x, y), \quad \mathbf{k} = (k_x, k_y).$$

The curve $\gamma(\mathbf{k},\mathbf{Re}) = 0$ is the curve of neutral stability, the minimum value $\mathbf{Re} = \mathbf{Re}_c$ on which determines the mode $\mathbf{k} = \mathbf{k}_c$ excited by the first mode when the flow becomes unstable. The packet of modes centered at $\mathbf{k}_0 = \mathbf{k}_c$ [for definiteness $\mathbf{k}_c = (k_c, 0)$ with $\mathbf{Re} = \mathbf{Re}_c(1 + \varepsilon)$ close to $\mathbf{Re}_c$ $(\varepsilon \ll 1)$ can be approximated by the following expression (for one component of the velocity field):

$$u(x, y, t) = \varepsilon^{1/2}A(X, Y, T)\exp[i(k_c x - \omega_c t)] + \varepsilon u_2 + \varepsilon^{3/2}u_3 + \dots$$

Here the envelope A is a slowly varying function of space and time: $X = \varepsilon^{1/2}x$, $Y = \varepsilon^{1/4}y$, $T = \varepsilon^{1/2}t$. The substitution of this solution into the starting nonlinear equations generates a system for the perturbed field $\sim \varepsilon^{1/2}A(X,Y,T)$ and corrections to it $\sim \varepsilon^{n/2}$. The generalized Ginzburg-Landau equation (GL) for the function $A(X,Y,T)$ follows from the condition that the derived system be solvable:

$$\frac{\partial A}{\partial t} + \omega_c'\frac{\partial A}{\partial x} - i\frac{\omega_c}{2k_c}\nabla^2 A + \frac{1}{2}[\gamma'' - i(\omega_c'' - \omega_c' k_c^{-1})] \left(\frac{\partial}{\partial x} - \frac{i}{2k_c}\frac{\partial^2}{\partial y^2}\right)^2 A = \gamma A - lA^2A^*, \tag{2.7}$$

where ω_c' is the group velocity of the packet along the x-axis, ω_c'' and ω_c'/k_c characterize the diffusion spreading of the packet, γ'' is a negative constant determining the decrease in the increments when the wave numbers k deviate from the wave number k_c of the most unstable mode, whose increment is equal to γ; and, $l = l_r + il_i$ is the complex Landau constant, characterizing saturation and nonlinear modulation of the wave.

In spite of the fact that the generalized GL equation was derived for a flow forming near the first bifurcation–instability of the stationary flow, it is also useful for studying subsequent transitions, if in the process the amplitudes of the disturbances remain small. In a number of cases (for example, in binary mixtures and liquid crystals) the complex properties of the flows are already manifested for small values of ε, and the "slow" equations obtained can even be used to describe the transition to turbulence.

2.7. Autostructures. Discrete analog of the Ginzburg-Landau equations.

For all their diversity hydrodynamic structures—spatial–temporal formations in continuous media—can naturally be divided into three groups by making use of the analogy with oscillations in lumped systems. It is well known that oscillations can be divided into free, forced, and self-excited oscillations. The free structures are, for example, vortices in shear flows of an ideal liquid (i.e., as $\mathbf{Re} \to \infty$); an example of forced structures are rolls in Rayleigh-Bénard convection, whose shape is identical to that of the boundary of the cylindrical container with small diameter (see Ref. 70), or more complicated vortex formations which form under conditions of flow over shallow depressions on a smooth surface.[71] Autostructures are a much less trivial object; these objects are localized spatial formations which are stable in dissipative and nonequilibrium media and do not depend (within finite limits) on the boundary or initial conditions.[72] In the same way that self-excited oscillations can have as generating solutions a family of conservative (free) oscillations, among which the introduced small dissipation and pumping of energy only select a definite motion while preserving its form, autostructures in weakly nonequilibrium media can inherit the properties of free structures in nonviscous flows. Examples of such quasiconservative structures are well known: for example, self-maintained solitons, in particular, Rossby solitons, of which the great red spot on Jupiter could be an example.[73,74] We stress, however, that in most hydrodynamic experiments one does not observe individual structures, but rather an ensemble of structures (chains of Taylor vortices, lattices of hexagonal or rectangular cells, etc.), and the presence of neighbors is of fundamental importance for their formation and dynamics. Such flows can in many cases nonetheless be regarded as ensembles of coupled autostructures (see below). At the same time it is natural to regard defects in such ensembles–lattices of structures–as secondary autostructures.

To elucidate the mechanism responsible for the creation of convective autostructures we shall study the following two-dimensional model:

$$\frac{\partial u}{\partial t} = [(v-\alpha) - (1+\nabla^2)^2]\,u + \beta u^2 - u^3, \tag{2.8}$$

$$\mu \frac{\partial v}{\partial t} = v - lv^3 + \delta u + D\nabla^2 v. \tag{2.9}$$

It can be shown[75] that for small values of β ($\beta \ll 1$) this system admits stationary solutions in the form of disks, whose characteristic sizes and steady-state intensity are determined solely by the parameters in the equations and do not depend on the boundary and initial conditions. The number and mutual arrangement of autostructures is determined by the initial conditions, but the distance between them cannot be less than L_c, which corresponds to the characteristic size of the region which adjoins the autostructure and where the field u becomes negative (Fig. 5). In the general case ($\beta \sim 1$) other nontrivial structures can also form; this is determined by the diversity of initial excitations, which serve as a seed for subsequent nonlinear growth and formation of autostructures. The simplest nontrivial structures with a center of symmetry are polyhedra. They are engendered by two modes of a circular membrane–radial and azimuthal.

One can see from Fig. 5 that in the autostructures formed the effect of the field v on the field u reduces to creating a profile of the degree of nonequilibrium of the medium [the terms $\sim u$ in Eq. (2.8)]. On the other hand, numerical modeling[75] and experiments on thermal convection with nonuniform heating[76] show that stable autostructures also form in the case where the field $v(x, y)$ is not self-consistent,

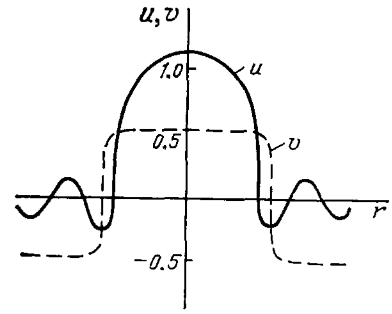

FIG. 5. The distribution of the field in localized structures described by the model (2.8) and (2.9) with $\beta = 0.9$, $\gamma = 4$, $\delta = 0.15$, and $D = 0.3$ (see Ref. 75).

but rather is fixed externally. In this case subtle details of the field $v(x, y)$ have virtually no effect on the topology of such structures.

To describe analytically the weakly supercritical localized convective structures in a situation close to that in the experiment with nonuniform heating [76] we shall assume that the critical parameter is a radially symmetric function

$$\begin{aligned} \varepsilon(r) &= \varepsilon_0 \geqslant 0, \quad r \leqslant r_0, \\ &= \varepsilon' < 0, \quad r > r_0. \end{aligned} \tag{2.10}$$

For $\varepsilon \ll 1$ Eqs. (1.1)–(1.3) reduce to Eq. (2.8) in which $v - a \equiv \varepsilon(r)$, the variable u is the deviation of the temperature θ from the equilibrium temperature, and the quadratic term is related, for example, with the temperature dependence of the capillary tension and (or) viscosity (Haken's equation[77]). Making the formal assumption that the nonlinearity is weak $|u|^2 \ll 1$ we shall seek the solution of (2.8)–(2.10) in the form of a superposition of the eigenfunctions of the problem linearized near $u = 0$; we represent the solution of this problem in the form

$$u(r, t) = \sum_n F_n(r) \sin(n\varphi) \cdot \exp(\lambda_n t),$$

where the functions $F_n(r)$ satisfy the conditions $F_n(r) \to 0$ as $r \to \infty$ and $|F_n(r)| < \infty$ as $r \to 0$. The eigenfunctions $F_n(r)$ can be found by joining the solutions of Laplace's equation at the boundary $r = r_0$. However only those functions which correspond to disturbances which grow in time, i.e., functions with $\lambda_n > 0$, are of interest. Outside the region where ε is positive ($r > r_0$) only Neumann's functions with complex argument $K_n(i\bar{k}r)$ ($\bar{k}^2 = -1 + iq$) can satisfy this condition. Within the region $r \leq r_0$ the Bessel functions with real argument $J_n(kr)$ satisfy this condition. The quantities q and k must satisfy, by virtue of the fact that the λ_n are real, the relation $\lambda_n = \varepsilon_0 - (1 - k^2)^2 = q^2 > 0$ and are determined from the dispersion equation

$$\frac{J_n(kr_0)}{kJ_n'(kr_0)} = \frac{\operatorname{Re} K_n(i\bar{k}r_0)}{\operatorname{Re}(i\bar{k}K_n'(i\bar{k}r_0))}.$$

This equation follows from the conditions of continuity of F_n and dF_n/dr at the boundary $r = r_0$.

We shall now assume that the parameters r_0 and ε_0 are such that several of the exponents λ_n, corresponding, for example, to axisymmetric disturbances with $n = 0$ and azimuthal disturbances with $n = 3$, are positive. Then substituting into Eq. (2.8) a solution in the form $u(r,\varphi,t) = A_0(t)F_0(r) + A_3(t)F_3(r)\sin 3\varphi$ and making the assumption that the amplitudes of the disturbances are slowly-varying functions of the conjugate system we obtain for A_0 and A_3 a second-order system of equations of the following form:[78,79]

$$\frac{dA_0}{dt} = \lambda_0 A_0 + c_1 A_0^2 + c_2 A_3^2 - c_3 A_0^3 + c_4 A_0 A_3^2,$$

$$\frac{dA_3}{dt} = \lambda_3 A_3 + d_1 A_0 A_3 - d_2 A_0 A_3 - d_3 A_3 A_0^2.$$

For $c_1, d_1 \neq 0$ [i.e., in the presence of quadratic nonlinearity in Eq. (2.8)] this system has a stable stationary solution with $A_0, A_3 \neq 0$, to which the solitary hexagonal cell corresponds. In those cases when the number of such interacting modes exceeds two the equations for the amplitudes of these modes can have stable motions with nontrivial (including also chaotic) dynamics. This situation apparently describes the regime, observed in the experiment of Ref. 6, of aperiodic creation and vanishing of cells. Similar solutions in the form of a solitary cell can also be obtained for a uniform but two-component medium described by the system (2.8) and (2.9).

The physical mechanisms lying at the basis of the spontaneous formation of localized structures—two- and three-dimensional structures associated with the character of the interaction of the components u and v and with spatial dispersion of the field—are quite general and can be realized in the most diverse nonequilibrium media. Three-dimensional stable structures are already observed on the basis of the model (2.8) and (2.9) with $\nabla^2 = \partial^2/\partial x^2 + \partial^2/\partial y^2 + \partial^2/\partial z^2$. Localized structures—particles with different topology—have been studied with the help of computer experiments.[60] Three "elementary" structures have been observed: sphere, torus, and "baseball" (Fig. 6a). The orientation of elementary structures in space is arbitrary—it is determined solely by the initial conditions, while the topology and dimensions are universal and do not change when the boundary conditions and dimensions of the region change. Stable formations in the form of coupled elementary structures—identical or different (Fig. 6b)—were realized with appropriately chosen initial conditions. In a definite region of starting conditions the nonlinear field (2.8) and (2.9) admits formations which are not directly connected with the states of the elementary structures (for example, Fig. 6c). Such formations are not, however, attractors (in this case—equilibrium states) of the system under study and in the limit $t \to \infty$ they transform into coupled states of elementary structures.

The topology and character of the interaction of localized structures turned out to be virtually independent of the concrete form of the coupling between the fields u and v. In particular, the elementary structures shown in Figs. 6a—sphere, torus, and "baseball"—have also been observed in a model medium in which these fields are coupled linearly:[4)]

$$\frac{\partial u}{\partial t} = [\bar{\varepsilon} - (1 + \nabla^2)^2] u + \beta u^2 - u^3 + qv \equiv -\frac{\delta F}{\delta u},$$
$$\mu \frac{\partial v}{\partial t} = (1 + D\nabla^2) v - \gamma v^3 + qu \equiv -\frac{\delta F}{\delta v}. \qquad (2.11)$$

The structures shown in Fig. 6a are observed in this medium, for example, with $\bar{\varepsilon} = -0.007$, $\beta = 1$, $q = 0.15$, $\mu = 0.1$, $D = 0.06$, and $\gamma = 4$.

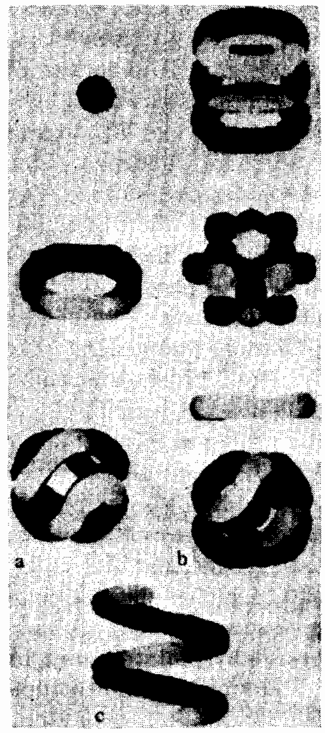

FIG. 6. Three-dimensional localized structures with $\alpha = 0.5$, $\beta = 1.5$, $0.05 \lesssim \mu \lesssim 0.1$, $\gamma = 0.15$, and $D = 0.1$, forming under different initial conditions.[80]

The universality of the observed localized formations indicates that the model equations, on the basis of which the localized solutions that are found exist and are stable, must follow from the most general assumptions about the character of the fields (symmetry, uniformity, isotropy, etc.). Indeed we shall seek the solutions in a class of gradient systems $\partial u/\partial t = -\delta F/\delta u$, whose energy density

$$\mathcal{F}\left(F = \int_V \mathcal{F}\, dV\right)$$

admits a series expansion in powers of the field and powers of the gradient of the field near the point of instability of the uniform state. Assuming that the real scalar field u can become unstable not only in a "soft" but also in a "hard" manner and, in addition, keeping in mind that the instability can be manifested not at the maximal but rather at finite scales, we must retain, aside from the traditional leading order terms in the expansion, the terms of next highest order also. As a result we obtain

$$\mathcal{F} = \frac{\alpha}{2} u^2 - \frac{\beta}{3} u^3 + \frac{1}{4} u^4 + \frac{1}{2} [(k_0^2 + \nabla^2)^2 u]^2. \qquad (2.12)$$

The sought equation, corresponding to (2.12), has the form

$$\frac{\partial u}{\partial t} = -\alpha u + \beta u^2 - \gamma u^3 - (k_0^2 + \nabla^2)^2 u. \qquad (2.13)$$

This is a generalization of the well-known Swift-Hohenberg equation,[81] which has localized solutions for $\alpha < 0$, $\beta > 0$, and $\gamma > 0$ (the case of soft self-excitation). However, they are unstable and transform into periodic structures. If hard loss of stability is characteristic for the medium ($\alpha > 0$, $\beta > 0$, and $\gamma > 0$), then the situation changes—in this case isolated structures can exist.

The stability of individual autostructures, and in some cases also the relative autonomy of their dynamics (see, for example, Ref. 82), permit transferring in the description of their interaction and dynamics of ensembles from partial differential equations for fields to ordinary or differential-difference equations for the parameters of the structures. We call attention to the fact that for different parameters of a nonequilibrium system the regular spatial lattice of identical elements can be either an ensemble of weakly coupled autostructures or it is simply the result of a resonance interaction of a small number of excited media (usually harmonic). The clearest and simplest example is the hexahedral Bénard cells. For small excess above threshold, as is well known,[70] they form owing to synchronization of the phases of three plane waves, turned relative to one another at an angle of 60°. As the critical parameter (and, therefore, the nonlinearity also) increases a large number of harmonics of these waves is created, and the lattice of hexahedra, which remains similar to the starting lattice, now transforms into a collection of individual hexahedra which are weakly coupled with one another. Long-range action effects are no longer important now. The situation here is reminiscent of the formation of a periodic chain of solitons from a stationary sinusoidal wave as the excitation energy increases, for example, in the Korteweig-de Vries equation. It is natural to regard such a chain of solitons as a discrete ensemble of weakly coupled elements.

We shall give an example of the description of the interaction of coupled "elementary particles" of the type of spheres in the model (2.8) and (2.9), where $\nabla^2 = \partial^2/\partial x^2 + \partial^2/\partial y^2 + \partial^2/\partial z^2$. Using the asymptotic method an ordinary differential equation of the following form can be derived for the coordinates of the centers of the spheres $\mathbf{r}_{0j}(x_{0j}, y_{0j}, z_{0j})$:[83]

$$\frac{d\mathbf{r}_{0j}}{dt} = \nabla \mathbf{r}_{0j} \sum_{l\neq j} \mathrm{Re}\, \frac{\exp(ik|\mathbf{r}_{0j} - \mathbf{r}_{0l}|)}{|\mathbf{r}_{0j} - \mathbf{r}_{0l}|}.$$

If there are only two spheres, then according to these equations they will move along a straight line connecting their centers until a stable equilibrium state—a bound state—is established. For two "particles" and especially for several particles there is an infinite number of stable bound states. These could be regular polyhedra consisting of spheres (see Fig. 6b), different types of lattices—periodic and "quasicrystalline," etc.

In the conservative system

$$\frac{\partial^2 u}{\partial t^2} = [(v - \alpha) - (1 + \nabla^2)^2]\, u + \beta u^2 - u^3,$$
$$\frac{\partial^2 v}{\partial t^2} = v - \gamma v^3 + \delta u + D\nabla^2 v,$$

the stable static solutions of which are identical to those studied above, the dynamics and character of the interaction of the "elementary particles" is much richer. In particular, they can rotate relative to one another, forming planet-like systems, chaotically approaching one another and moving apart, etc.[83]

Although a rigorous proof of such a transition "from fields to structures" is a quite difficult problem, which has only been solved in a few cases (see Refs. 72 and 84), the qualitative considerations lying at the basis of the phenomenological approach are quite transparent. The above-described experiments as well as the numerical solutions of the starting hydrodynamic equations (2.1)–(2.3) or (2.4) and (2.5) show that as a result of the development of primary instabilities there quite often forms, for example, a chain of structures in the form of two-dimensional vortices, Bénard convective rolls, Taylor vortices, spirals on rotating bodies in a flow (Fig. 7),[35-39] transverse vortices in a boundary layer,[85] vortex streets in a wake behind a cylinder[86] (Fig. 8), etc. Secondary excitations for small ($\varepsilon \ll 1$) and moderate ($\varepsilon \sim 1$) values of the critical parameter result in modulation of these structures—vortices, i.e., their internal dynamics is manifested. It is natural to suppose that the procedure for deriving the equations for the slow amplitude of the secondary excitations on the jth solitary vortex once again will lead to the GL equation (2.7), but now in a one-dimensional variant (the y coordinate varies along the vortex):

$$\frac{\partial A_j(y, t)}{\partial t} = \Phi(A_j(y, t), \varepsilon) + \xi \frac{\partial^2 A_j(y, t)}{\partial y^2}, \qquad (2.13')$$

where ξ is a complex parameter.

If the description of the interaction of excitations on neighboring vortices is restricted to only the linear approximation $\sim \varkappa(A_{j+1} - A_j)$ and $\sim \gamma(A_{j-1} - A_j)$ (see, for ex-

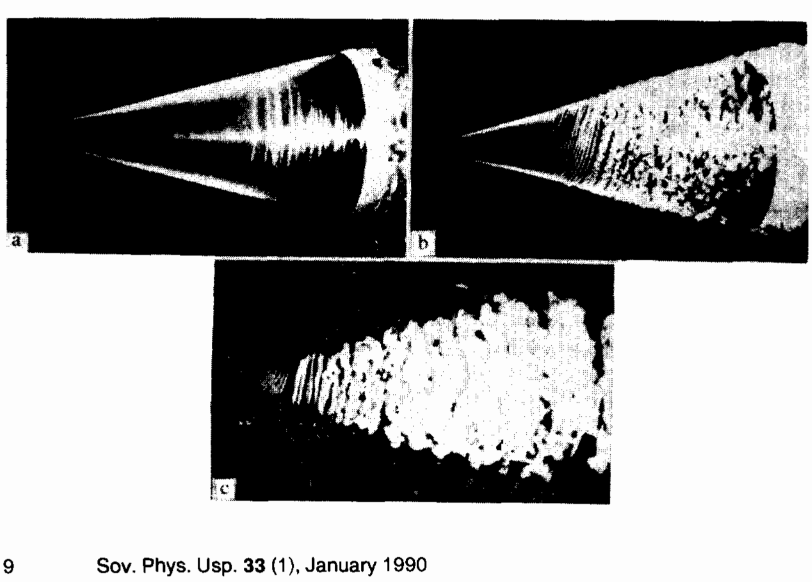

FIG. 7. The development of disturbances on spiral vortices formed in flow around a rotating cone. a—$U = 2.05$ m/s, $n = 300$ rpm; b—$U = 1.7$ m/s, $n = 670$ rpm; c—$U = 1$ m/s, $n = 1200$ rpm (see Ref. 36).

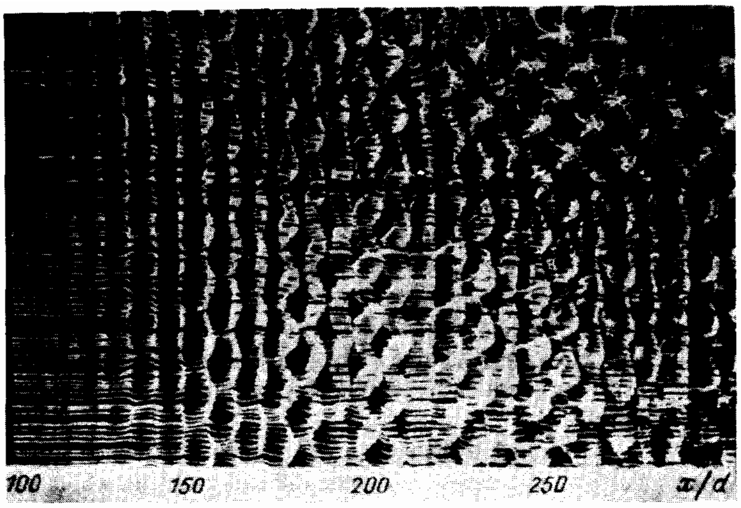

FIG. 8. The development of three-dimensional disturbances in the wake behind a circular cylinder with **Re** = 150 (see Ref. 86).

ample, Ref. 84), then we arrive at the model[87]

$$\frac{\partial A_j(y,t)}{\partial t} = \Phi(A_j,\varepsilon) - \gamma(A_j - A_{j-1}) + \varkappa(A_{j+1} - A_j) + \xi\frac{\partial^2 A_j}{\partial y^2}. \qquad (2.14)$$

The equations (2.14) can be greatly simplified, if the structure of the excitations on the vortices is assumed to be given. Thus, for example, for ring vortices, assuming that only one azimuthal mode is excited, it is possible to transform to a model described by Eqs. (2.14) with $\xi = 0$.

2.8. Structures with singularities. Defects

In the case when the secondary excitations on structures which have already been formed are periodic, lattices which are similar to those shown in Fig. 9 can form (see Refs. 88 and 89). Such regular lattices are, however, the

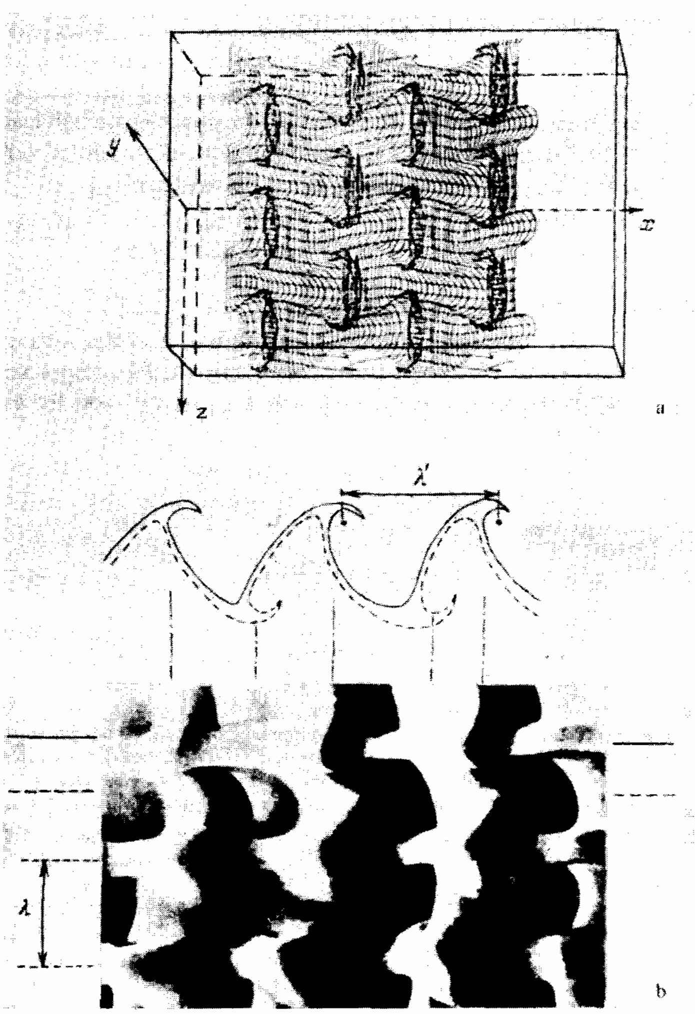

FIG. 9. Visualization of a vortex lattice in a wake behind a flat plate with sinusoidal back edge in numerical (a) and physical (b) experiments. The solid and dashed lines show the sections of the lattice by planes parallel to the (x, y) plane (see Ref. 88).

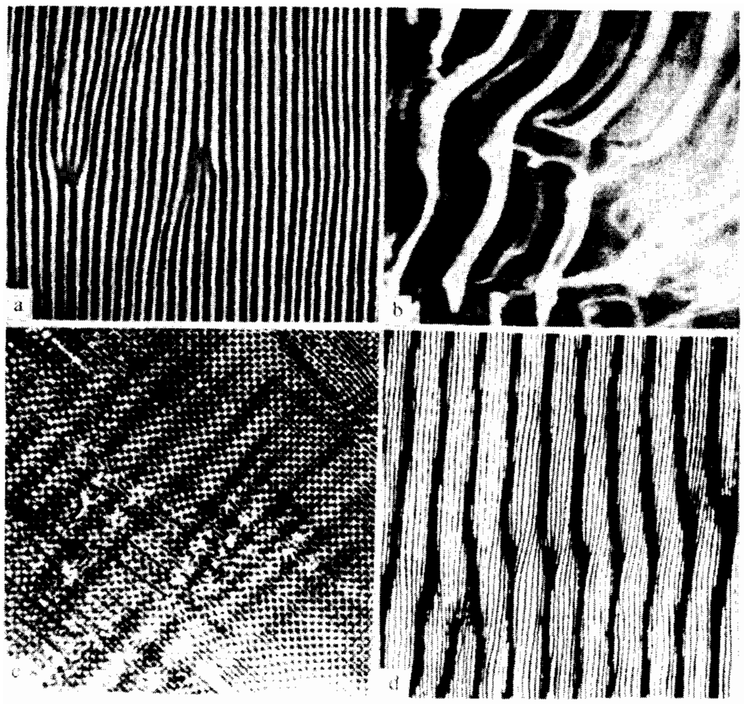

FIG. 10. Dislocations: a–arising with the electrohydrodynamic instability in liquid crystals;[92] b–in waves of modulation of Faraday ripples;[93] c–in the wake behind a cylinder;[94] d–in a shear layer.[95]

exception and not the rule. Thus, for example, under the conditions of thermal convection in extended thin layers ordered islands of rolls, coupled with one another by dislocations of different types, are most often observed. In spite of the fact that the concrete properties of such defects are determined by the type of flow, in an ensemble of structures which has a wavy nature the mechanism responsible for their formation can be quite general. Imagine that for the same values of the parameters periodic excitations—modes or waves—with different wave numbers can exist in a stable fashion in the flow (multistability). If these modes compete strongly with one another, then some definite regime depending on the starting conditions, is established.[90,91] If, however, the competition is not strong enough (or one of the "weak" modes is maintained by the nonuniformity of the medium or external excitation), then the modes can coexist in space. On the line of contact of the modes with different wave numbers the "extra" phase fronts must obviously be cut off. As a result dislocations similar to those presented in Fig. 10a will be observed; these dislocations appear as a result of the development of the electrohydrodynamic instability in liquid crystals when a spatially periodic voltage is applied.[92] Dislocations of modulation waves (Fig. 10b) against the background of capillary ripples—Faraday ripples (see Ref. 93 and the discussion in Sec. 3.7)—have an analogous appearance. As a result of the coexistence of excitations with different spatial periods in neighboring regions the formation of dislocations can also be clearly observed in the wake behind a cylinder with variable diameter.[94] If the diameter of the cylinder varies slowly enough along the axis of the cylinder, then a cellular structure of the flow appears in the wake—Kármán vortices, whose repetition period is related with the local Strouhal frequency $f_s \sim U_0/d$ and varies from cell to cell, form in each cell. Because the repetition period of the vortices is different in neighboring cells defects appear at the locations where the cells join (Fig. 10c).[94]

The discussed mechanism of formation of dislocations is also manifested in the same manner in a different shear flow—a solitary shear layer which is nonuniform along the width.[95] It is interesting that dislocations can also appear in the case when the repetition periods of the vortices in separate cells are identical but the vortices form at different moments. Figure 10d shows an example of such dislocations in a shear layer. The layer is excited by an external acoustic field near the edge of the plate forming the layer; the frequency of the field is the same everywhere along the edge but at some point of the layer its phase changes sharply by 180°.

It is obvious that dislocations in lattices consisting of stable structures are also often stable—a quite strong action is required in order for them to form or decompose in an established flow.[16] For this reason they can be regarded as secondary autostructures arising on the background of regular cellular lattices.

Although the description of dislocations is in itself a complicated problem the flow at large distances from them can be calculated quite accurately. The situation here is similar to that arising in the hydrodynamics of an incompressible ideal liquid—in the presence of localized regions of concentrated vorticity the flow outside these regions can be regarded as a potential flow, and the vortex regions themselves can be regarded as defects of the medium in which the "potential nature" of the medium breaks down. Thus there arises the problem—common to both the usual and structured flows—of representing the hydrodynamic fields in terms of their singularities and finding the law of motion of these singularities. This description is based on the formalism associated with the representation of the solutions of partial differential equations for a complex field in terms of its singularities, in particular, the poles.

The simplest example are the solutions[96,97]

$$u(x,t) = -2\Gamma \sum_{\alpha} (x - z_\alpha(t))^{-1}, \qquad \dot{z}_\alpha = -2\Gamma \sum_{\beta \neq \alpha} (z_\alpha - z_\beta)^{-1},$$

$$z_\alpha = x_\alpha + i y_\alpha$$

for the integrable Burgers equation

$$\frac{\partial u}{\partial t} + u\frac{\partial u}{\partial x} = \nu \frac{\partial^2 u}{\partial x^2}.$$

The representation of analogous solutions[98] for the nonintegrable dissipative Benjamin-Ono equation

$$u(x, t) = -(i\beta + \nu) \sum_{j=1}^{n} (x - x_j)^{-1} + \text{c. c.},$$

$$\dot{x}_j = -i\mu - (i\beta + \nu) \sum_{l \neq j}^{n} 2(x_j - x_l)^{-1} + (i\beta - \nu) \sum_{l=1}^{n} 2(x - x_l^*)^{-1}$$

which models the turbulence of internal waves in a stratified liquid, is not much more complicated. In the case of a collection of periodic chains of poles $x_{l,j} = x_l \pm 2j\pi$, $j = 1, 2, \ldots$,

$$\frac{\partial u}{\partial t} + \mu H \frac{\partial u}{\partial x} + \beta H \frac{\partial^2 u}{\partial x^2} - \nu \frac{\partial^2 u}{\partial x^2} + 2u\frac{\partial u}{\partial x} = 0,$$

$$Hf(x) = \frac{1}{\pi} \int_{-\infty}^{\infty} \frac{f(x')}{x - x'}\, dx',$$

and

$$u(x, t) = -\frac{i\beta + \nu}{2} \sum_{j=1}^{n} \operatorname{ctg} \frac{x - x_j(t)}{2} + \text{c. c.},$$

$$\dot{x}_j(t) = -i\mu - (i\beta + \nu) \sum_{l \neq j}^{n} \operatorname{ctg} \frac{x_j - x_l}{2} + (i\beta - \nu) \sum_{l=1}^{n} \operatorname{ctg} \frac{x_j - x_l^*}{2}.$$

This representation of the solution $u(x,t)$ is superficially reminiscent of the expansion in linear modes, but with the fundamental difference that the nonlinear modes are not independent and truncating the sum for some n gives an exact solution. These solutions describe wave structures of the soliton type, which remain in the asymptotic limit and whose form is almost restored after collisions. However the motion of these structures and the changes in their parameters can be very complicated, including also chaotic. Unlike conservative solitons they can grow or decay, and their collisions are not elastic (these and other properties of the solutions as well as the questions of stability and completeness are studied in detail in Ref. 98).

For a classical ideal liquid, described by the Euler equations

$$\frac{\partial \mathbf{u}}{\partial t} + \mathbf{u}\nabla\mathbf{u} = -\frac{\nabla p}{\rho}, \quad \nabla\mathbf{u} = 0,$$

the representation of the two-dimensional velocity field by means of a discrete collection of singularities—point-like vortices[99]

$$u^* = \frac{1}{2\pi i} \sum_{\alpha} \Gamma_\alpha (z - z_\alpha)^{-1}, \qquad \dot{z}_\alpha^* = \frac{1}{2\pi i} \sum_{\beta \neq \alpha} \Gamma_\beta (z_\alpha - z_\beta)^{-1}$$

$$\times\ (u = u_x + i u_y, \quad z = x + iy)$$

is an idealization, since now the singularities are located in the real space occupied by the flow. For some formulations of the problems this leads to fundamental difficulties (see, for example, Refs. 97 and 100); nonetheless there are numerous examples of flows in which the vorticity is indeed concentrated in thin filaments. In particular, such vortex filaments have been observed under conditions of thermal-convective[101,102] and turbulent[103] mixing of a liquid in a rotating vessel.

The simplest defects of structured flows are planar fronts, separating stable and unstable states of flows with small excess above threshold, which can be described on the basis of the GL model. Such fronts are formed, for example, from localized disturbances when the nonequilibrium state is switched on rapidly—a spatially periodic flow is first established in the region occupied by the disturbance and then gradually encompasses the remaining part of the space that is still occupied by flow in the unstable state.[104,105] The velocity of the stationary front is determined uniquely by the linear part of the GL equation, and its form is determined by the solution of the corresponding ordinary differential equation.[106] Analogous results also hold for a wider class of solutions.[107–109] For sufficiently weak starting excitations the time-dependent asymptotic structure of the solutions can be related with the data for the Cauchy problem. Experiments confirm that when the nonequilibrium state "is switched on" rapidly and the initial conditions are nonuniform the formation of stationary and nonstationary structured flows proceeds precisely through the motion of fronts: Rayleigh-Bénard thermal convection,[105] Taylor-Couette flow,[104] and capillary ripples accompanying parametric excitation.[109]

In a more general case curved fronts or fronts propagating at an angle with respect to one another can form in the flow. Their collision and interaction leads to the formation of defects, whose motion determines the further dynamics of the structured flows. The description of fields engendered by such defects and their dynamics depends on the type of flow to a greater extent than in the case of regular cell structures. Such a description requires taking into account not only the dispersion and nonlinear properties of elementary excitations, forming the structures, but also the so-called "drift flows," associated with the component of vorticity which is oriented transverse to the plane of the lattice and which always arises in the presence of dislocations or curving of convective rolls.[110,111] The difficulties in deriving simplified equations for this problem are largely due to the existence of several spatial-temporal scales with different orders of magnitude. An approximate description of the component of the vorticity Ω normal to the plane of the lattice in different flows requires, as a rule, the use of terms with different orders in perturbation theory. When the excess above threshold is small taking into account the average drift velocity determined by the vertical vorticity (or pressure gradient, as, for example, in the case of plane Poiseuille flow) nonetheless leads to equations for the amplitudes which are similar even for apparently completely different flows: a plane shear layer, Rayleigh–Bénard thermal convection, Taylor-Couette flow, and plane Poiseuille flow near a Hopf bifurcation point (see, for example, Ref. 112). For a uniform shear layer the corresponding equations have the following form:[112]

$$\frac{\partial A}{\partial t} = \varepsilon A + \frac{\partial^2 A}{\partial x^2} + \xi \frac{\partial^2 A}{\partial y^2} - |A|^2 A - iBA; \tag{2.14'}$$

$$\frac{\partial \Omega}{\partial y} = -\nabla^2 B, \quad \left(\frac{\partial}{\partial t} - \nu\nabla^2\right)\Omega = \sigma \frac{\partial}{\partial y}\left(A^* \frac{\partial A}{\partial x} + \text{c. c.}\right). \tag{2.15}$$

The equations describing thermal convection in a layer with free boundaries are similar (the notation of Ref. 113 is employed):

$$\frac{1+\mathrm{Pr}}{\mathrm{Pr}}\frac{\partial A}{\partial t}=\frac{3\pi^2}{8}\varepsilon A+\left(\frac{\partial}{\partial x}-\frac{i}{2q_0}\frac{\partial^2}{\partial y^2}\right)^2 A-\frac{1}{8}|A|^2A-iq\frac{1+\mathrm{Pr}}{\mathrm{Pr}}BA, \tag{2.16}$$

$$\frac{\partial\Omega}{\partial y}=-\nabla^2 B,\quad \left(\frac{\partial}{\partial t}-\mathrm{Pr}\,\nabla^2\right)\Omega=2\frac{\partial}{\partial y}\left[A^*\left(\frac{\partial}{\partial x}-\frac{i}{2q_0}\frac{\partial^2}{\partial y^2}\right)A+\mathrm{c.c.}\right]. \tag{2.17}$$

The differences in the structure of the differential operators in Eqs. (2.14′) and (2.15) and Eqs. (2.16) and (2.17) in the coordinates x and y are due to the different properties of the spatial symmetry of the corresponding flows.[112]

It is obvious from Eqs. (2.16) and (2.17) that in the presence of defects in the lattice of convective rolls ($B\neq 0$) for finite Prandtl numbers the equations for the order parameter A and the vertical component of the vorticity Ω are coupled with one another. The role of this coupling for large values of the critical parameter remains unclear, but in the case of moderate values of critical parameter ($\varepsilon\lesssim 1$), as was found in Refs. 110 and 111, the amplitude equations with $B=0$ describe correctly the motion of dislocations—no qualitative differences which could be ascribed to the effect of Ω and finite **Pr** were found, though the quantitative dependences start to differ when $\mathbf{Pr}\lesssim 60$. The reason for this qualitative similarity of the results of the more and less accurate descriptions is connected with the fact that drift flows do not change the topology of the structures and therefore they do not affect the mechanism of formation of defects. This, in particular, makes it possible to explain them using the topological approach, which is largely based on the symmetry properties and is analogous to that employed for describing defects in liquid crystals (see, for example, Ref. 14).

To analyze the dynamics of structured flows with defects it is convenient to generalize the amplitude equation so that it would describe both cellular structures and defect structures. In the case of convective rolls, which are described by Eq. (2.7) with real coefficients, this can be done by introducing the real function $\psi=A(x,y,t)\times\exp(ik_c x)+$ c.c. (by analogy to the theory of phase transitions it is called the order parameter). Then the simplest equation for it, transforming for slowly varying $A(x,y,t)$ into Eq. (2.7), will have the form of the Swift-Hohenberg equation:[81]

$$\tau_0\frac{\partial\psi}{\partial t}=\varepsilon\psi-\frac{\xi_0^2}{4k_c^2}(\nabla^2+k_c^2)\psi-g\psi^3. \tag{2.18}$$

One of the remarkable properties of this equation (as also of the Ginzburg-Landau equation (2.7) with real coefficients with $\omega_c'=0$) is that it can be written in the gradient form

$$\tau_0\frac{\partial\psi}{\partial t}=-\frac{\delta F}{\delta\psi}, \tag{2.19}$$

$$F=\int d^2r\left\{\frac{1}{2}\varepsilon^2-\frac{1}{2}\varepsilon\psi^2+\frac{1}{4}g\psi^4+\frac{1}{2}\frac{\xi_0^2}{4k_c^2}[(\nabla^2+k_c^2)\psi]^2\right\}, \tag{2.20}$$

where $\delta F/\delta\psi$ is a variational derivative, while the free energy is a Lyapunov functional

$$\frac{dF}{dt}=-\tau_0\int d^2r\,(\dot\psi)^2\leqslant 0. \tag{2.21}$$

The problem of finding the stable stationary states thus reduces to finding the minima of F.

The dynamics of defects has been studied in greatest detail for potential systems of the form (2.19) and (2.20).[14,110,111,114–117] The motion of the defects in such systems always terminates with the establishment of one of the stationary states corresponding to a local minimum of the functional F (the defects either stop or vanish). The change in the free energy in this case can be regarded as the work performed by some force which, by analogy to the force acting on a dislocation in a crystal when a pressure is applied, is called the Peach-Koehler force (see Ref. 14). For simple dislocations, in particular, dislocations representing a transition from a roll structure with the wave number $2\pi(n+1)/L$ to a lattice with the wave number $2\pi n/L$ (as in Fig. 10), this force can be easily calculated.[115] The change in the free energy F in the case under study is

$$dF\sim\frac{dF}{dk}\frac{2\pi}{L}dy,$$

and the force acting on the dislocation is

$$f_{\mathrm{PK}}=\frac{dF}{dy}\sim\frac{dF}{dk}.$$

The defect will obviously continue to move until the force f_{PK} is equal to the friction force f_v, which depends on the magnitude of the diffusion in the nonequilibrium medium, acting on the defect.[115] Thus the motion of a defect is similar to the motion of a small sphere along the uneven bottom of a tank filled with viscous liquid.

2.9. Formation of lattices

For hydrodynamic flows described by equations in the gradient form of the type (2.19) and (2.20) strong degeneracy and the presence of numerous local minima F, corresponding to different locally stable states, is characteristic (Fig. 11).[114] In the presence of quite strong background noise such structured states will relax to a single globally stable state, corresponding to the absolute minimum of F. In systems with low noise levels, however, states corresponding to local minima can also be stably observed. In this case the final state is determined by the character of the starting exci-

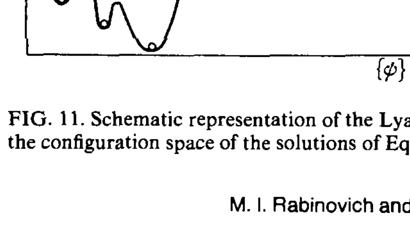

FIG. 11. Schematic representation of the Lyapunov functional (2.20) in the configuration space of the solutions of Eq. (2.18).

tation. For example, if the Rayleigh number increases rapidly, because the thermal diffusion time is short convection is established independently in separate regions. In addition, the rolls in each region can be oriented differently. As convection develops different regions come into contact and form patterns with dislocations which can exist indefinitely.

Near the threshold of instability ($\varepsilon \ll 1$) for sufficiently far-removed boundaries ($\varepsilon^{1/2} L/d \gg 1$) F can be represented as a sum of three components $F = F_B + F_S + F_D$ (see Refs. 116 and 117). The volume contribution

$$F_B \approx \varepsilon \xi_0^2 \int d^2 r \left[(k - k_c)^2 + \frac{1}{4} k_c^{-2} (\nabla \mathbf{k})^2 \right]$$

is primarily determined by the square of the deviation of the local wave number $(k(\mathbf{r}) - k_c)^2$ and the square of the divergence of the wave vector $(\nabla \mathbf{k})^2$, characterizing the curvature of the convective rolls. The suppression of convection near the side walls is determined by the term

$$F_S \approx \frac{2\sqrt{2}}{3} \varepsilon^{3/2} \xi_0^2 \oint \frac{(\mathbf{ks})}{k} \, dl,$$

which is minimum in the case when the convective rolls are oriented perpendicular to the side wall ($\mathbf{s}$ is a unit vector normal to the side wall). Finally the contribution of F_D, determined by the defects, can be approximately represented in the form

$$F_D \approx \frac{1}{2} \varepsilon^2 N_D \pi r_c^2,$$

where N_D is the number of point defects and r_c is the characteristic distance over which ψ is strongly distorted by these defects. The competition between these three terms is what determines the (local) minimum of the functional. The model based on the variational principle, as a comparison with experiment showed,[78,118] adequately describes the above-noted properties of thermal convection, including also quantitatively for moderate excesses above the instability threshold of the static equilibrium $0.3 < \varepsilon < 2.0$.

It is obvious that the same flow structures can be formed along different paths and the paths depend on the initial conditions. A good example is the process whereby a regular hexahedral lattice is established in the model (2.8) with $v - \alpha = \text{const} = \varepsilon$, which describes Bénard-Marangoni convection in a flat layer of liquid heated from below:

$$\frac{\partial \psi}{\partial t} = [\varepsilon - (1 + \nabla^2)^2]\, \psi + \beta \psi^2 - \psi^3. \tag{2.22}$$

In the case of the periodic boundary condition studied here

$$\psi(x, y, t) = \psi(x + L, y + L, t) \tag{2.23}$$

the limiting regimes are static and are determined by the minimum of the Lyapunov functional for Eq. (2.22):

$$F = \int d^2 r \left\{ -\frac{\varepsilon}{2} \psi^2 - \frac{\beta}{3} \psi^3 + \frac{1}{4} \psi^4 + \frac{1}{2} [(1 + \nabla^2)^2 \psi]^2 \right\}. \tag{2.24}$$

Analysis of this functional shows[78,118] that for not too small values of ε it has many local minima corresponding to different stable spatial forms—rolls ($\beta < \beta^*$) or hexahedra ($\beta > \beta^*$). Local minima correspond to lattices with different defects, realized with different initial conditions. In all

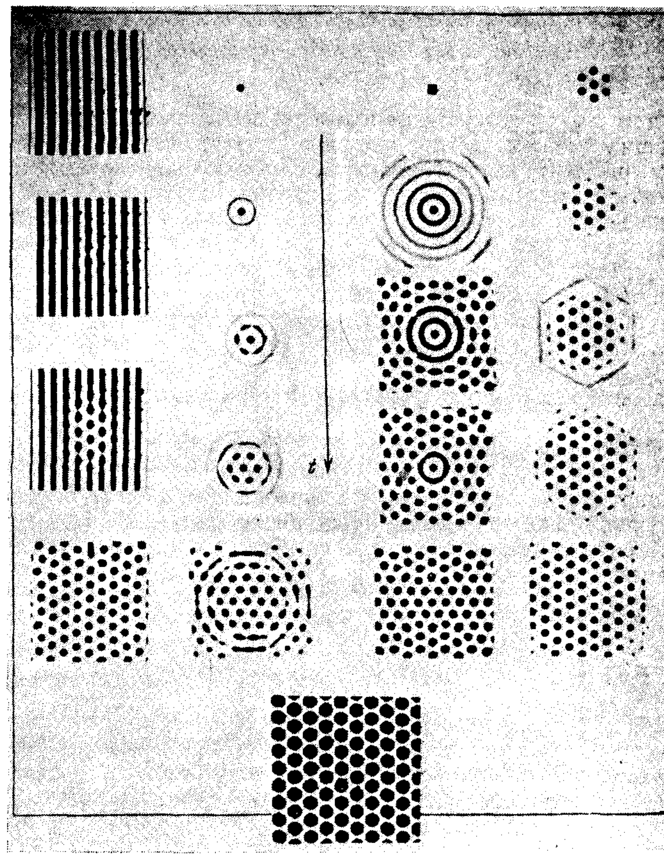

FIG. 12. Different paths by which a regular lattice is established in the model (2.22) and (2.23) (see Ref. 78). Transfer from row to row corresponds to increasing time t.

cases, however, when the initial conditions contain a localized disturbance (including also on the background formed by a periodic disturbance) a transition of the system into the same state with the lowest free energy $F = -38$ occurs.

Figure 12 shows the results of a numerical experiment,[118] illustrating the multiplicity of the paths by which a hexahedral lattice forms. In some cases, such as, for example, accompanying the formation of a lattice from a standing wave and close to a point-like disturbance (see Fig. 12), a lattice of hexahedra forms owing to the successive development of instabilities of the main wave and then the modulation wave. We shall illustrate this for the example of the development of a hexahedral lattice from a localized disturbance with a cylindrical form. Linearization of Eq. (2.22) gives an equation for the disturbance $a(x, y, t)$ in the form

$$\frac{da}{dt} = [\varepsilon - (1 + \nabla^2)^2]\, a. \tag{2.25}$$

Its solution in a cylindrical coordinate system with the boundary conditions $a|_{r=R} = 0$ has the form of cylindrical waves

$$a(r, t) = A_0 e^{ct} J_0([1 - (\varepsilon - c)^{1/2}]^{1/2} r), \tag{2.26}$$

where J_0 is a zeroth-order Bessel function, and the constant c is determined from the relation

$$c = -\left[\left(\frac{\alpha_j}{R}\right)^2 - 1\right]^2; \tag{2.27}$$

and, α_j is the jth root of the Bessel function. We are interested only in solutions of the form (2.26) which grow in time, i.e., the solutions which correspond to positive values of c. Thus for $R = 32$ $c > 0$ only for $\alpha = \alpha_1$ ($c \approx 0.04$). We shall prove that for sufficiently large β the cylindrical waves which arise are unstable with respect to azimuthal disturbances $b(\varphi, t) \sim \exp[i(\omega t - n\varphi)]$. It is this secondary instability that leads in the limit $t \to \infty$ to the formation of a hexahedral lattice under the initial conditions studied. We shall explain the problem directly in the nonlinear formulation. To this end we shall represent the solution of Eq. (2.22) in the form of a cylindrical wave on which azimuthal disturbances are given:

$$a(r, \varphi, t) = A_0(t) J_0(k_0 r) + A_3(t) J_3(k_3 r) \sin 3\varphi. \tag{2.28}$$

To satisfy the boundary conditions it is necessary that $J_0(k_0 r_0) = 0$ and $J_3(k_3 r_0) = 0$. Near the boundary of instability of the cylindrical wave $A(t)$ and $A_3(t)$ can be regarded as slowly varying functions of time. Then, substituting the expression (2.28) into the starting equation (2.22) and using the asymptotic method we obtain for A_0 and A_3 equations of the form

$$\begin{aligned} \frac{dA_0}{dt} &= \lambda_0 A_0 + c_1 A_0^2 + c_2 A_3^3 - c_3 A_0^3 + c_4 A_0 A_3^2; \\ \frac{dA_3}{dt} &= \lambda_3 A_3 + d_1 A_0 A_3 - d_2 A_0 A_3 - d_3 A_3 A_0^2, \end{aligned} \tag{2.29}$$

where the quadratic terms with A_0^2 and $A_0 A_3$ are proportional to the parameter β. Even in the presence of a decrement in the mode A_3 the azimuthal waves will grow for sufficiently large β, and as t increases a hexahedron appears—see the second and third rows in the second series on the left side of Fig. 12.

The static, in particular, the topological characteristics of the defects arising on the background of regular lattices in different fluid flows (see Fig. 10), as already mentioned, are very similar to the corresponding defects in crystals, where they have been studied in detail.[119] The specific nature of nonequilibrium media consists here of the fact that topological defects of the field continuously move, are created, and decay, i.e., for fields in nonequilibrium media the nonlinear dynamics of defects is of the main interest. In particular, turbulence in such media can, in a certain range of values of the critical parameter, be regarded as the chaotic dynamics of defects (see. Sec. 3.7).

3. CHAOTIC DYNAMICS OF STRUCTURES AND TURBULENCE

3.1. The fractal nature of turbulent flow and of a "phase" liquid

The concept of a "phase liquid," which is widely employed in the theory of dynamical systems and which is intended to make more tangible the vector field in the phase space of the system, is in reality more than simply an analogy. The point is that under conditions which are easily established in each specific case the motion of particles of impurity in real stationary flows is described by the dynamical equations

$$\frac{d\mathbf{r}}{dt} = \mathbf{u}(\mathbf{r}), \tag{3.1}$$

whose trajectories in phase space in the literal sense coincide with the trajectories of impurity particles in the flow. For this reason many results, in particular, about the possibility of the appearance of chaos, pertaining to dynamical systems are also valid for the transfer of particles. For example, the formation of regions of chaotic mixing of an impurity is possible already in the comparatively simple velocity field[120]

$$\mathbf{u} = (A \sin z + C \cos y,\ B \sin x + A \cos z,\ C \sin y + B \cos x), \tag{3.2}$$

satisfying Euler's equations

$$\frac{\partial \mathbf{u}}{\partial t} + \mathbf{u}\nabla\mathbf{u} = -\frac{\nabla p}{\rho}, \qquad \nabla\mathbf{u} = 0, \tag{3.3}$$

or the Navier-Stokes equations (2.4) and (2.5) with an external force. Mixing of an impurity can also become chaotic in a two-dimensional regular velocity field, if it is nonstationary, for example, periodic in time $\mathbf{u}(x, y, t) = \mathbf{u}(x, y, t + T)$ (see Refs. 97 and 121–127). Figure 13 shows the distribution of dye in a liquid which is put into motion by an alternate periodic rotation of the inner and outer cylinders.[125] The figure also shows the two-dimensional map of the corresponding dynamical model. The flow pattern observed in this case with mixed (tangled) particle trajectories is, of course, not turbulence. Turbulence is usually regarded as the spatially and temporally irregular behavior of the velocity field itself. Here, however, the velocity field is strictly periodic. Such pseudoturbulence is sometimes called "Lagrangian turbulence." Nonetheless analysis of the chaotic motion of an impurity makes it possible to get an idea of

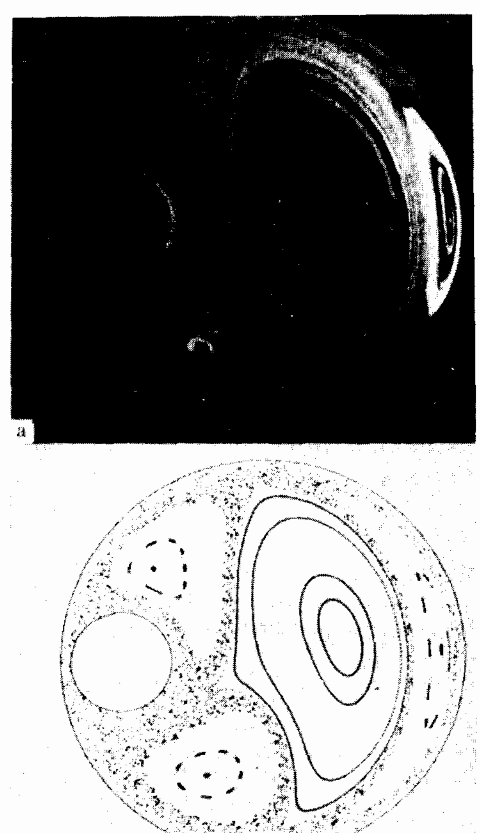

FIG. 13. Comparison of the distribution of dye in a physical experiment (a) and points of the Poincaré map (b) in the corresponding model of flow between cylinders rotated alternately in time (see Ref. 125).

the mechanisms responsible for the appearance of "real turbulence." Thus, in particular, under certain assumptions singularities or localized structures of the velocity field itself (for example, vortices) can play the role of impurities, and in this case the velocity field becomes chaotic in space and time by the same mechanisms by which the transport of particles becomes chaotic.[121-123,128-131] These analogies qualitatively explain why the structure of turbulent flows is as complicated as the structure of the phase space of dynamical systems with chaotic behavior. In particular, as experiments indicate,[132] turbulent flows have a fractal structure.

Fractal sets, whether they are complicatedly organized sets of trajectories of particles of liquid of the turbulent flow in real space or strange attractors in phase space, are described by special characteristics. The most important of these characteristics is the dimension of the realization and the associated dimension of the dynamical system which completely reproduces the properties of the flow. A turbulent flow, like also "strictly noise pulsations," is characterized by a continuous Fourier spectrum and a decaying autocorrelation function. However dynamical turbulence is distinguished from random fluctuations precisely by the fact that it can be engendered by a dynamical system with a finite, though large, number of degrees of freedom (while the generation of "true" noise requires that the system excite an infinite number of degrees of freedom). It is precisely the determination of the dimension of the number of degrees of freedom required to reproduce a turbulent flow that permits distinguishing dynamical turbulence from, say, random hydrodynamic fluctuations.

It is well known[21] that the physical nature of irregular entangled behavior of a finite-dimensional system is associated with the instability of all (or most) individual motions with finite energy. In phase-space language this can be explained as follows: unstable trajectories are distributed in a bounded region, owing to instability they separate from one another, and owing to the finiteness of the region in which they are distributed they become entangled in a very complicated fashion. This complexity of a stochastic set can be described quantitatively.

For definiteness we shall talk about a three-dimensional phase space. Imagine an attractor in a volume bounded by the surface of a two-dimensional torus. Consider a bundle of trajectories on the way to the attractor (they describe transient regimes of the motion of the system leading to establishment of "stationary" chaos). The trajectories (more precisely, their tracks on the intersecting plane) lie in a definite region in the transverse cross section of the bundle; we shall follow the change in the size and shape of this region along the bundle. We take into account the fact that an element of the volume in a neighborhood of the saddle-point trajectory is stretched in one (transverse) direction and compressed in the other direction; because of the dissipative nature of the system the compression is stronger than the stretching—the volumes should decrease. These directions must change along the trajectories, otherwise the trajectories would recede to infinity. All this will result in the fact that the cross-sectional area of the bundle will decrease and the cross section will acquire a flattened and at the same time bent shape. But this process must occur not only with the cross section of the bundle as a whole but also with each element of its area. As a result the cross section of the beam is divided into a system of strips embedded into one another and separated by voids. With time (i.e., along the bundle of trajectories) the number of strips grows rapidly, and their widths decrease. The attractor arising in the limit $t \to \infty$ is a nondenumerable set of layers—surfaces, which do not touch one another and on which saddle trajectories pass. These layers connect with one another in a complicated manner on their sides and ends; each trajectory belonging to the attractor wanders over all layers and after the passage of a sufficiently long time will pass quite close to any point of the attractor (the property of ergodicity). The total volume of the layers and the total area of their sections is equal to zero. Such sets are Cantor sets in one of the directions.[21] It is precisely the Cantor nature of the structure that must be regarded as the most characteristic property of an attractor in the more general case of an n-dimensional ($n > 3$) phase space also.

The volume of a strange attractor in the starting phase space is always equal to zero. But it will be nonzero in a different space—a space of lower dimension. The latter is defined as follows. We divide the entire n-dimensional space into small cubes with edge ε and volume ε^n. Let $N(\varepsilon)$ be the minimum number of cubes which together completely cover the attractor. We define the dimension D of the attractor as the limit

$$D = \lim_{\varepsilon \to 0} \frac{\ln N(\varepsilon)}{\ln(1/\varepsilon)}. \tag{3.4}$$

The existence of the limit (3.4) means that the volume of the attractor in the D-dimensional space is finite: for small ε we have $N(\varepsilon) \approx V\varepsilon^{-D}$ (where V is a constant), whence it is obvious that $N(\varepsilon)$ can be regarded as the number of D-dimensional cubes which cover the volume V in the D-dimensional space. The dimension defined according to (3.4) obviously cannot exceed the total dimension n of the phase space, but it can be less than the latter and, unlike the customary dimension, it can be fractional; for Cantor sets it is fractional.[5)]

We call attention to the following important fact. For established motion on an attractor the dissipation of energy is on the average compensated by the energy applied by the source of nonequilibrium of the system. Therefore if the evolution of an element of "volume" belonging to the attractor is followed in time (in some space whose dimension is determined by the dimension of the attractor), then this volume will on the average be conserved—its compression in one direction will be compensated by stretching owing to the divergence of the close trajectories in other directions. This property can be exploited to determine in a different manner the dimension of the attractor.

For attractors having the property of ergodicity of the motion the average characteristics can be established by analyzing the motion along one unstable trajectory belonging to the attractor. The individual trajectory will reproduce all properties of the attractor, if one moves along it for an infinitely long time.

Let $\mathbf{X} = \mathbf{X}_0(tg)$ be the equation of such a trajectory, one solution of the starting nonlinear equations

$$\dot{\mathbf{X}} = \mathbf{F}(\mathbf{X}). \tag{3.5}$$

Consider the deformation of a "spherical" element of volume as it moves along this trajectory. Such a deformation is determined by Eqs. (3.5), linearized with respect to the difference $\boldsymbol{\xi} = \mathbf{X}(t) - \mathbf{X}_0(t)$—the deviation of trajectories neighboring the given trajectory. These equations, written out in terms of components, have the form

$$\dot{\xi}_i = A_{ik}(t)\,\xi_k, \qquad A_{ik}(t) = \left.\frac{\partial F_i}{\partial X_k}\right|_{\mathbf{X}=\mathbf{X}_0(t)}. \tag{3.6}$$

Along the trajectory the element of volume is compressed in some directions and stretched in other directions, and a sphere transforms into an ellipsoid. Along the trajectory both the direction and length of the semiaxis of the ellipsoid change; we denote the lengths by $l_j(t)$, where j enumerates the directions. The Lyapunov characteristic exponents are the limiting values

$$\Lambda_j = \lim_{t\to\infty}\left(\frac{1}{t}\,\frac{\ln l_j(t)}{\ln l(0)}\right), \tag{3.7}$$

where $l(0)$ is the radius of the starting sphere (at a moment arbitrarily chosen as $t = 0$). The quantities so determined are real numbers and their number is equal to the dimension of the n-space. One of these numbers (corresponding to the direction along the trajectory itself) is equal to zero.[6)]

The sum of the Lyapunov exponents determines the average change, along the trajectory, of an elementary volume in phase space. The local change in volume at each point of the trajectory is given by the divergence $\operatorname{div}\mathbf{X} = \operatorname{div}\boldsymbol{\xi} = A_{ii}(t)$. It can be shown that the average value of the divergence along the trajectory is

$$\lim_{t\to\infty}\left(\frac{1}{t}\int_0^t \operatorname{div}\boldsymbol{\xi}\,dt\right) = \sum_{j=1}^{n}\Lambda_j. \tag{3.8}$$

For a dissipative system this sum is always negative—arbitrary volumes in the n-dimensional phase space are compressed. We arrange the Lyapunov exponents in the order $\Lambda_1 \geqslant \Lambda_2 \geqslant \ldots \geqslant \Lambda_k \geqslant 0 \geqslant \Lambda_{k+1} \geqslant \ldots \geqslant \Lambda_n$ and take into account as many stable directions as required in order to compensate the stretching by compression. If the sum $\Sigma_{j=1}^{m}\Lambda_j$ obtained in the process were to vanish identically, then the integer m would be the dimension of the attractor determined through the Lyapunov exponents. However the sum of an integer number of exponents usually does not vanish, and to satisfy the requirement that "the phase volume on an attractor be conserved" we must take into account some fraction of the next $(m+1)$th "compressing" exponent. Thus the dimension of the attractor will lie between $m+1$ and m, where m is the number of exponents in the indicated sequence, whose sum is still positive but which after adding Λ_{m+1} becomes negative.[7)] The fractional part $d<1$ of the dimension $D_\Lambda = m + d$ is found from the equality[133]

$$\sum_{j=1}^{m}\Lambda_j + d\Lambda_{m+1} = 0. \tag{3.9}$$

Since only the least stable directions are taken into account in calculating d (the negative exponents Λ_j, which are largest in absolute magnitude and correspond to rapid motions, at the end of their sequence are dropped) the estimate of the dimension given by D_Λ is, generally speaking, an upper limit.

3.2. Dimension of realization

The dimensional characteristics of stochastic motion are extremely important from different viewpoints. On the one hand they make it possible to begin to understand the essence of randomness, and on the other hand they are very useful for applied problems, associated with signal processing (encoding, recognition, etc.). Indeed, with the help of the traditional analysis of a random signal (spectral, correlation) it is usually difficult to say anything about the source of the signal. In particular, is the signal of the nature of noise in the usual sense (i.e., not reproducible with the help of an algorithm) or is the signal generated by a determinate, though very complicated, system? If, however, the dimension of this signal can be determined in some manner (see below), then this problem can be solved. A finite dimension D_Λ means that the signal can in principle be constructed with the help of a dynamical system of order no higher than $2D_\Lambda + 1$ (see Ref. 134). Thus the value of the dimension D_Λ gives an estimate of the number of degrees of freedom of the system (medium) involved in the formation of the stochastic signal under study. As the dimension of the realization increases (approaches infinity) a chaotic signal approaches increasingly more closely to an absolutely random signal. From this viewpoint a source which we have become accustomed to regard as random can be regarded as the motion of a dynamical system toward an infinite-dimensional strange attractor.

The ideas of processing random signals in order to reconstruct the properties of the sources engendering them were put forth comparatively recently by Takens.[135] They are based on the viewpoint that if a chaotic signal is generated by a finite-dimensional dynamical system, then it is first possible to reconstruct the corresponding limiting set (in particular, of the strange attractor) in some effective phase space and then to determine on this set the characteristics of the motion, such as the entropy and dimension. The fundamental step in the development of these ideas and their practical fruition was taken in 1983 by Grassberger and Procaccia.[136] They proposed that limiting sets not be studied at all in phase space, but rather the entire diagnostics procedure should be constructed solely on the processing of a concrete (sufficiently long) temporal realization of the physical quantity under study.

Usually there is only one observable, for example, one component of the velocity field of a hydrodynamic flow, measured as a function of time at one point. Since the effective phase space, in which the stochastic set corresponding to this realization is embedded, has a dimension M' it is necessary to have M' independent functions of time $u^{(k)}(t)$. Takens suggests that they be obtained as follows: the observable is studied at discrete times $t, t+\tau, \ldots, t+k\tau, \ldots, t+(M'-1)\tau$; these values of $u^{(k)}(t)$ describe the coordinate of a point in an M'-dimensional space corresponding to the time t. As t varies a trajectory, reproducing some set, is obtained in this space. The dimension D of this set can be calculated from the formulas (3.4) or (3.9). The next step consists of analyzing the dependence of D on M'. It is obvious that for small M' as M' increases the dimension $D(M')$ should also increase. If the signal is a noise signal, then this growth will occur without saturation. If, however, the signal is produced by the dynamical system, then for some $M' = M$

growth stops—the quantity $D(M)$ is the dimension of the limiting set, in particular, of the strange attractor reconstructed in this manner. We note that the formulas (3.4) or (3.9) are inconvenient for calculating the dimension of the reconstructed attractor (in particular, it is not clear how much ε should be decreased). Investigations performed over the last few years have shown that it is much more effective to use the correlation integral.[136-145] This integral is given by the approximate expression:[8)]

$$C(\varepsilon) = \frac{1}{N^2} \sum_{i=1}^{N} \sum_{j=1}^{N}{}' H(\varepsilon - \|\mathbf{u}_i - \mathbf{u}_j\|)$$

$$= \frac{1}{N^2} \sum_{i=1}^{N}{}' N_i(\varepsilon) = \frac{N(\varepsilon)}{N}; \tag{3.10}$$

here $\mathbf{u}_j = (u^{(1)}(j\tau); u^{(2)}(j\tau);...)$ is a point on the trajectory in an M'-dimensional space, N is the total number of points in the processed time segment of the observable, H is the Heaviside function, and $\|\mathbf{u}_i - \mathbf{u}_j\|$ is the distance between a neighboring pair of points. Thus the correlation integral is the average number of pairs of points in the realization, the distance between which in the space $\mathbf{u}_j$ is less than ε. For small values of ε the correlation integral depends on ε in a power-law fashion:[142]

$$C(\varepsilon) = \varepsilon^{\nu} e^{-KM'\tau} \tag{3.11}$$

(K is Kolmogorov's entropy). The correlation dimension ν can be introduced according to (3.10) and (3.11):

$$D = \lim_{\varepsilon\to 0} \frac{\ln N(\varepsilon)}{\ln(1/\varepsilon)} = \lim_{\varepsilon\to 0}\left(\nu + \frac{\ln N - KM'\tau}{\ln(1/\varepsilon)}\right) \equiv \nu. \tag{3.12}$$

In the actual processing of experimental data the dimension is usually calculated approximately—directly from the slope of the function $\ln C$ versus $\ln \varepsilon$. These functions behave differently for signals of different origin; this is what makes it possible to perform diagnostics of signals of unknown nature and, in some cases, to distinguish the dynamical (i.e., having a finite dimension) component of the signal from the noise component.

In attempting to determine the slope of the curve $\ln C = f(\ln \varepsilon)$ for practically any concrete situation we immediately encounter a surprise: the graphs have different slopes for different intervals of ε (Fig. 14). Which slope should be regarded as the "true" dimension? Before answering this question we shall think about why changes in slope occur on our graph. We can say immediately that they can be "instrumental," i.e., caused by the technical characteristics of the procedure employed to process the realization (for example, inadequate time duration), or fundamental, i.e., owing to the dynamical characteristics of the system generating the given realization.

If, for example, an attractor in the effective phase is nonuniform (the image point falls into some sections more often than others), then the value of ν will be different for different values of ε.[9)] For sufficiently large N, however, the density of points on the attractor will indeed reflect its structure. Thus the "nonuniformity" of the attractor leads to instrumental, in principal removable, changes in slope. We stress here that the required length of the realization is associated with the measured dimension. The larger the dimension the longer the realization must be in order to obtain the required filling of the attractor with points. The empirical estimate $\ln N \sim \nu(\varepsilon_{\max} - \varepsilon_{\min})$, where $(\varepsilon_{\min}, \varepsilon_{\max})$ is the interval of ε in which $C \sim \varepsilon^{\nu}$ [see Eq. (3.11)], is well known.[143]

The existing changes in slope in the correlation interval are most often due to the "structured nature" of the observable, i.e., the presence of components with different dimension in the signal. These components are correspondingly engendered by different systems, including noise systems (for example, a noisy communication channel). In the simplest case the structured signal is $u(t) = v_0(t) + \delta_1 v_1(t) + ... + \delta_k v_k(t)$, where $v_k(t)$ is generated by a dynamical system the dimension of whose attractor is equal to ν_i, and in addition $1 > \delta_1 > \delta_2 > ... > \delta_k$, $\nu_0 < \nu_1 < ... < \nu_k$. Then as ε is further reduced components with increasingly smaller amplitudes δ_i will appear in the correlation interval, and in this manner we shall observe on the graph intervals $(\varepsilon_i', \varepsilon_i'')$, the tangent of whose slope angle will be $\sim \nu_i$. It is natural to term the number of breaks $(k-1)$ for such a signal the degree of structure. We stress that increasing the length of the realization does not eliminate such changes in slope; quite the contrary, it makes them sharper.

Since any observable corresponding to a real process contains noise which produces precisely this observable the dynamical system must be infinite-dimensional. If the signal-to-noise ratio is not too small, the correlation integral for a real signal must necessarily have a change in slope which separates the scale of the dynamical component from the small scales ε, where the dimension is not determined by the noise. This makes it possible to separate the chaotic signal of dynamical origin from the adaptive white noise by analyzing the local slopes of the graph $\ln C = f(\ln \varepsilon)$. An example illustrating this algorithm is presented in Fig. 14, where the correlation integral and the local slopes are presented for different values of ε for Hénon's map with noise.

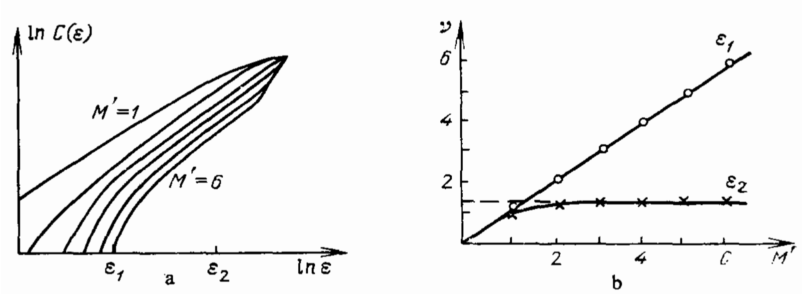

FIG. 14. The correlation integral (a) and the local slope $d \ln C / d \ln \varepsilon$ (b) for different values of ε for the Hénon map with noise.

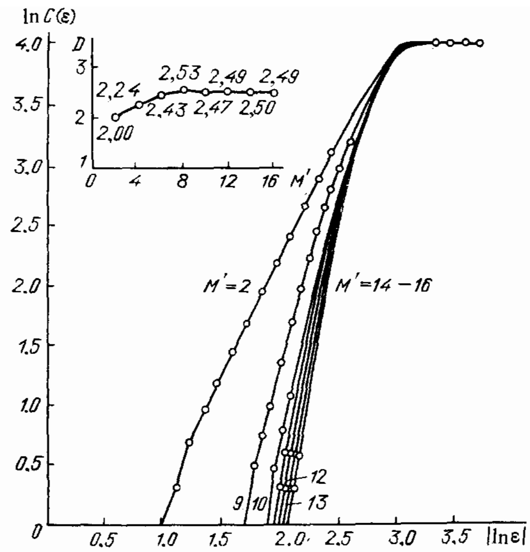

FIG. 15. The dependences $\ln C = F(\ln \varepsilon)$ and $D = D(M')$ with $M = 16$, calculated from the realizations of the velocity on the axis of the open working part ($300\times300\times1200$ mm^3) of a wind tunnel with a closed return channel for $U_0 = 24.2$ m/s (see Ref. 146).

3.3. Flow dimension. Spatial development of turbulence

Experiments with internal flows[18,144,145] not only confirm the idea that a chaotic (in time) velocity field in a flow of a viscous liquid can be described in the limit $t\to\infty$ by a finite (small) number of spatial functions, but they have also made it possible to determine the rate of growth of the dimension of turbulent motion (the number of effective excitations) as a function of the critical parameter immediately beyond the point where turbulence appears.[145] Moreover, it was established in Refs. 146–148 that open flows of the type of shear layers and jets can also contain, in the presence of feedback transporting disturbances upstream, chaotic pulsations of the velocity which correspond to motion on an attractor of low dimension.

Figure 15 shows values of the dimension D measured based on the signal from a one-filament gauge of a hot-wire anemometer on the axis of a jet in the open working part of a wind tunnel for Reynolds numbers $\mathbf{Re}\sim10^5$ (see Ref. 146). Feedback in the flow under study appeared owing to the acoustic field exciting the jet in the return channel of the tunnel. Because of the existence of comparatively strong feedback the disturbances encompassed by the global feedback made the main contribution to the velocity pulsations, and for this reason the dimension remained practically unchanged over the entire length of the jet (the length of the open working part $L = 1200$ mm; the dimensions of the starting cross section of the jet were 300×300 mm^2).

If the dynamical theory can indeed be used to describe a real flowing liquid, then it should describe the phenomenon of the appearance and spatial development of "disorder" downstream. Obviously, this is of greatest importance for shear flows (boundary layers, submerged jets, wakes, etc.). How does self-production of dynamical chaos along the flow occur? Are the scenarios of its appearance similar to those observed in simple systems when the controlling parameter is changed? What is the role of the structures in the flow? We shall attempt to answer these questions.

To describe nonuniform flows adequately we introduce the concept of flow dimension—the dimension of the temporal realization as a function of the spatial coordinates. Suppose that the temporal realization of the field $u(x,t)$ measured by the sensor is produced at each point along the flow by a dynamical system whose motion in the M'-dimensional phase space is described by the trajectory $\mathbf{U}(x,t) = \{u(x,t), u(x,t+\tau),\dots,u(x,t+(M'-1)\tau)\}$. To calculate the dimension we shall employ the correlation integral [analogously to (3.10)]:

$$C(x,\varepsilon) = \frac{1}{N^2}\sum_{i=1}^{N}\sum_{j=1}^{N} H(\varepsilon - \|\mathbf{U}_i(x) - \mathbf{U}_j(x)\|). \qquad (3.13)$$

In the finite interval $\varepsilon\in[\varepsilon_i', \varepsilon_i'']$ the correlation integral can be approximated by the expression

$$C(x,\varepsilon) \sim \varepsilon^{\nu_i(x)}. \qquad (3.14)$$

The functions $\nu_i(x)$ are the flow dimension in which we are interested. The soundness of these characteristics is confirmed by direct experiments.

The development of turbulence and the change in dimension along a flow excited at the boundary by regular pulsations were studied in a group of experiments.[149–151] It was established that both in a cylindrical jet with a parabolic initial profile[149] ($\mathbf{Re}_d = 500$) and in a boundary layer[150,151] ($\mathbf{Re}_x = 10^5$) the development of coherent structures and the appearance of low-dimensional chaos precede the transition to turbulence. In both cases the presence of ordered structures was correlated with the low measured dimension of the realization of the velocity signal.

We note that for flow systems, in particular, a boundary layer, the interpretation of the dimension of the realization is different from the traditional interpretation. The point is that in such systems the development of excitations is often determined not only by the absolute but also by the convective (or only by it) instability, and the structures formed in the process are carried off downstream. The reconstruction of the "intrinsic" dynamics of such structures requires a realization obtained in a moving system of coordinates,[152] in which measurements cannot always be performed in practice. At the same time the results of measurements of the dimension in a stationary coordinate system in the presence of an average flow always depend on the properties of the incident flow, the dimensions of pulsations in which is determined by its history and can be too large. However the presence of quasiordered repeating structures in many flows indicates that not all disturbances of the incident flow participate in the formation of these structures (see, for example, Ref. 148), rather their contribution depends on the distance downstream—nontrivially in the general case (compare curves *1* and *2* in Fig. 16). Thanks to the successive (downstream) development of new instabilities on the background of nonlinear structures new disturbances grow in the flow (including disturbances which decayed on the starting section) and as a result of restructurings (bifurcations) turbulence arises in the flow along the x axis. Since the dimension is calculated based on a realization measured with finite accuracy (or in a deliberately coarse realization, as in the construction of curve *2* in Fig. 16) it takes into account only excitations which make the greatest contribution to the total signal, and it may be finite. In this situation it

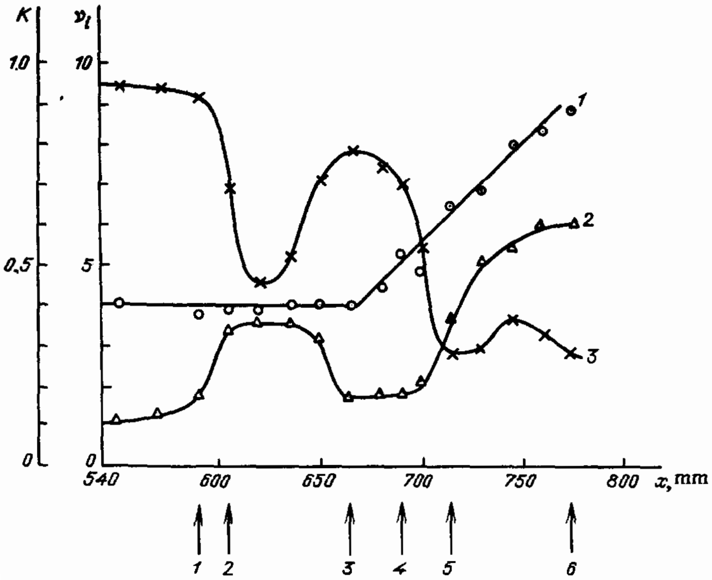

FIG. 16. The change in the characteristics of the realization of $u(t)$ in the direction of flow in a boundary layer. 1–Correlation dimension $\nu_1(x)$, calculated based on small scales in the phase space of the dynamical system with $M' = 12$; 2–the same for large scales–$\nu_2(x)$; 3–the mutual correlation coefficient K of the signal $U(t)$ and the signal applied to a vibrating ribbon. [The flow velocity $U_0 = 9.18$ m/s and the distance from the hot-wire anemometer sensor to the surface of the plate is 3 mm (see Ref. 150)].

is natural to employ the dimension $\nu(x)$ [or a function of the dimension $\nu(x,\varepsilon)$; see Ref. 87] as one of the characteristics describing the spatial development of the flow. It is not a universal characteristic in the sense that it characterizes a given **concrete** flow and becomes universal for flows of the same type, in the development of which absolute instabilities are the dominant factor. The construction of general models and the study of their scaling properties are of greatest interest precisely for such flows.

Detailed measurement of the dependence of the dimension on the downstream coordinate was performed in the case of a boundary layer.[150,151] In these measurements the correlation integral over finite intervals $\varepsilon\in[\varepsilon_i',\nu_i'']$, corresponding to different scales in phase space, was approximated by a power-law function (3.14) and the dimension was determined directly based on the dependence $\mathbf{d}\ln C/\mathbf{d}\ln\varepsilon$.

The measured value of the dimension depends on the studied range $[\varepsilon_i',\varepsilon_i'']$ of velocity pulsations. Changes in the pulsations which are much less than ε_i do not contribute to the computed values of ν_i. The existence of such differentiability of the contributions of different scales $u(t)$ makes it possible to determine the number of modes or, in the presence of additional information, even identify these modes; this is important for constructing a dynamical model of the downstream development of the flow.

Figure 16 shows the measured dimension of the realization versus the longitudinal coordinate for two intervals $[\varepsilon_{1,2}';\varepsilon_{1,2}'']$, each extending over ≈ 10 dB and each separated by approximately the same interval. Analysis of these dependences and the spectra (Fig. 17) established that in the experiment under discussion the realization at the starting section of the plate $x\lesssim 590$ mm (even taking into account the "fine" measurements of the realization—curve *1* in Fig. 16) can be represented as the result of excitation of four modes: modes generated by a ribbon at the frequency of the external forcing (≈ 87 Hz), at the frequency of the interference (50 Hz), at the frequency of characteristic oscillations of the ribbon in the flow (≈ 60 Hz), and the mode excited by vibrations of the plate (≈ 3 Hz). These modes are actually independent. The large changes in velocity, however, are associated only with one mode, excited at the frequency of the external forcing; as one can see from Fig. 16 (see curve *2*), for $x < 590$ mm $\nu_2 = 1$.

In the region 590 mm $< x <$ 665 mm all four modes ($\nu_2 = 4$) must be taken into account even for a rough approximation of $u(t)$. Downstream ($x\approx 665$ nm), however, in the region of formation of "spikes" characteristic for transitions to turbulence of the catastrophic (Klebanov) type, the dimension in the same approximation of the realization decreases to two. As follows from the measurements the cross-correlation signal applied to the ribbon and the signal from the hot-wire anemometer (curve *3* in Fig. 16) Tollmien-Schlichting waves at the frequency of the external forcing of 87 Hz and its phased harmonics make the main contribution to the formation of the spikes.

It is well known (see, for example, Ref. 153) that strong negative spikes on the velocity oscillograms indicate local stopping of the liquid and formation of points of inflection on the velocity profile, a consequence of which is the formation of secondary instability. The position along the flow ($x\approx 665$ mm) where new modes in the flow are excited as a result of the development of this instability is determined by the change in the behavior of the function $\nu(x)$. Farther downstream ($x > 700$) these modes become determining in the formation of pulsations with large amplitudes and their scales become chaotic. It is interesting that, as follows from visual observations of the flow, the breakdown of two-dimensional structures and formation of three-dimensional structures occur precisely for this value of the coordinate $x\approx 700$ mm in the boundary layer.

3.4. Generation of turbulence in structured flows. Scaling

One of the most important results in the theory of finite-dimensional dynamical turbulence was the observation of

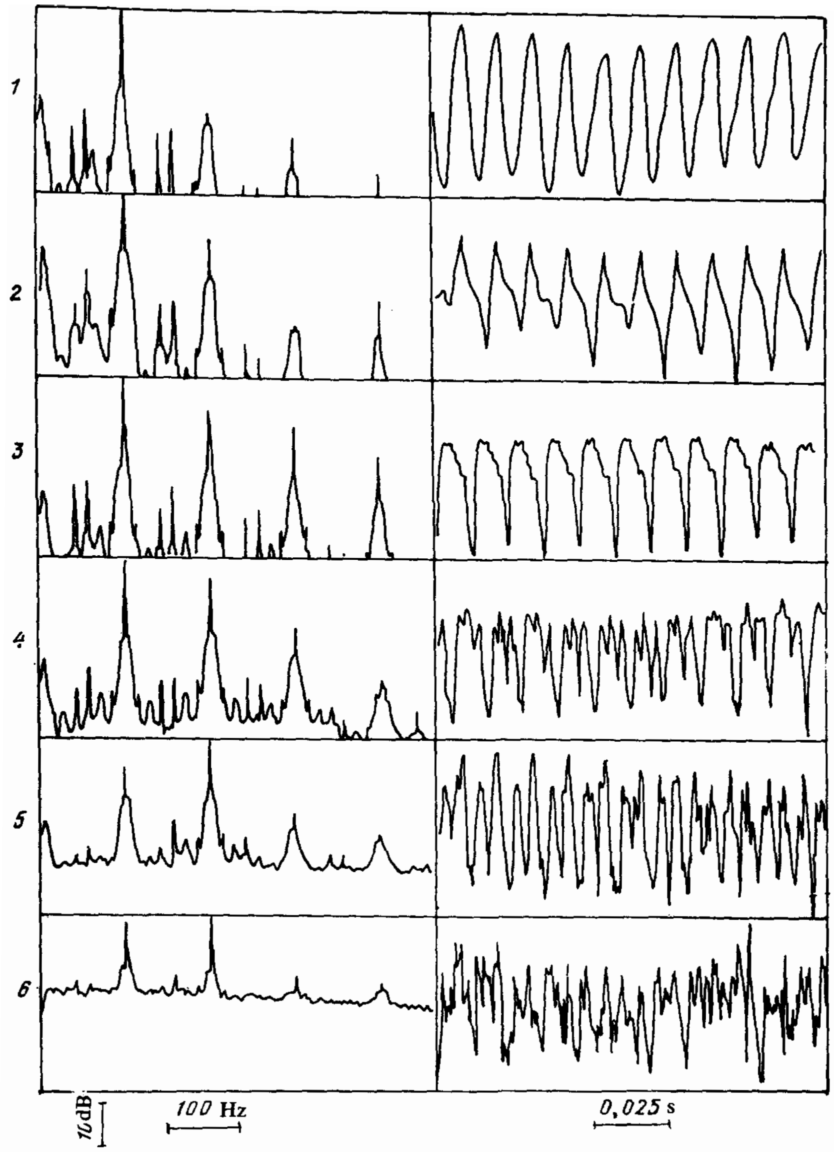

FIG. 17. The spectra and realizations of the signal $u(t)$ at the points x indicated in Fig. 16.

universality in the basic scenarios of the "order-chaos" transition. These universal properties are determined by the type of dynamical system (properties of the flow) and do not depend on its details, in the same way that the properties of a transition in critical phenomena do not depend on the specific form of the Hamiltonian of microscale motions. The nature of this universality is associated precisely with the closeness of the systems demonstrating it to the critical point. Indeed, we shall study the behavior of a system with close values of the parameter $\varepsilon = \varepsilon_1 = \varepsilon_{cr} - \mu$ and $\varepsilon = \varepsilon_2 = \varepsilon_{cr} + \mu$ ($\mu \ll \varepsilon$). In view of the continuous dependence on the parameter the equations corresponding to these situations will be identical, to within corrections $\sim\mu$ on the right sides. For the same starting conditions the behavior of the system with $\varepsilon = \varepsilon_1$ and $\varepsilon = \varepsilon_2$ will be distinguishable only after a very long time T, and $T \to \infty$ as $\mu \to 0$. The quantity T is the characteristic time scale on which the difference between the regular dynamics with $\varepsilon = \varepsilon_{cr} - \mu$ and the chaotic dynamics with $\varepsilon = \varepsilon_{cr} = +\mu$ appears. This time (as $\mu \to 0$) can exceed by as much as desired all characteristic times of our dynamical system. It is precisely for this reason that from the viewpoint of the transition to chaos the details of the behavior of a concrete system which are local in time may be assumed to be unimportant. Thus the characteristics of the transition to chaos near the critical point should be universal. From this universality it follows, in particular, that the simplest models demonstrating the basic paths of the transition to chaos can be employed to describe the basic types of critical behavior. On the basis of these models it is possible to obtain the quantitative characteristics of the universal behavior—similarity constants[10)] and critical exponents. In this situation the renormalization-group ideas, developed in the theory of critical phenomena and the theory of fields, and first applied by Feigenbaum[154] to study the transition to chaos through a sequence of doubling bifurcations (see also Ref. 155) turned out to be very effective in this situation. Later the renormalization group method was employed to study the scaling properties of the transition to turbulence through intermittency[156] and through the decay of quasiperiodic motions.[157,158] Here the largest Lyapunov exponent plays a fundamental role. Changes in this exponent demonstrate universal properties, analogous to the properties of the order parameter near the critical point—it equals zero below the threshold of the transition to chaos and depends in a power-law fashion on the critical parameter above threshold.

The most complicated and as yet least studied properties are the scaling properties of the transition to turbulence which develops in space in flows such as, for example, jets, shear layers, flows behind unstreamlined bodies, etc. Although the observation of quasicoherent structures in these flows indicates that models in the form of an ensemble of structures with comparatively simple (low-dimension) dynamics can in principle be constructed, the available information about their properties is still inadequate for performing a concrete analysis. For this reason the studies of the scaling properties of transitions in space are still limited only to those models which in the uniform approximation demonstrate the same properties of critical behavior as low-dimensional dynamical systems. In particular, a renormalization group description of the spatial development of turbulence in flow systems has been given for two types of critical behavior and a theory of the transition through intermittency into spatially uniform isotropic ensembles of structures has been constructed.[87,159]

In constructing a dynamical model of the spatial development of turbulence we shall keep in mind the fact that structures analogous to those shown in Figs. 7–9, the collective dynamics of whose excitations is what leads later to the appearance of spatial-temporal disorder—turbulence, formed as a result of the development of primary instabilities in a medium with flow. In the simplest formulation, discussed in Sec. 2.7, we shall employ the system of equations (2.14), setting $\xi = 0$ (i.e., the spatial dependence of the excitation on the structure is assumed to be given), to describe the one-dimensional chain of structures:

$$\frac{dA_j}{dt} = \Phi(A_j, \varepsilon) + \gamma(A_j - A_{j-1}) + \varkappa(A_{j+1} + A_{j-1} - 2A_j); \tag{3.15}$$

here $\Phi(A_j,\varepsilon)$ characterizes the dynamics of excitation on an elementary structure; γ determines the action of one element on another downstream; and, the feedback upstream depends on $\varkappa$. The equation (3.15) is supplemented by boundary conditions, for example, $A_0(t) = A\exp(i\omega t) + \text{c.c.}$—this corresponds to excitation of a flow which is periodic in time.

Neglecting diffusion ($\varkappa = 0$) the problem of the generation of spatial-temporal chaos along the flow reduces to the problem of the appearance of a strange attractor in a chain of elements which act successively on one another and whose individual dynamics is regular. The existence of spatially nonuniform stationary solutions $A_j(t) = \overline{A}_j$, determined by the relation $\overline{A}_{j-1} = (\Phi(\overline{A}_j,\varepsilon) + \gamma\overline{A}_j)/\gamma$, is characteristic for such a "discrete flow." If such a spatial distribution is stable, then chaos does not arise along the flow—the motion remains laminar. If, however, for some $j = j^*$ the solution becomes unstable, then for $j > j^*$ a more complicated motion is established (in the general case this motion is characterized by a large dimension). This motion, for example, quasiperiodic motion, can become unstable for $j = j^{**}$ and thus the motion can become more complicated along the flow, until finally chaos arises for some $j_{\rm cr}$. More precisely, this means that in the phase space of a system of $j = j_{\rm cr}$ dynamical elements (under the boundary conditions studied) there exists an attractive limiting set—a strange attractor. In this theory the values determining the nonuniform spatial distribution of the field are the parameter which controls the transition to dynamical chaos along the chain. In typical situations this parameter enters into the problem of determining the characteristic Lyapunov exponents along j similarly to the controlling parameter ε. From here there naturally follows the hypothesis that the scenarios of the transition to chaos in a point system as ε changes are similar to the scenario, unfolding in space (along j), of the generation of dynamical turbulence in the flow system.

To study the appearance and development of chaos downstream—to determine the number of spatial bifurcations and to find the similarity laws corresponding to them, etc.—we shall simplify the problem as much as possible, making the assumption that the structures are not carried off by the flow. This situation is encountered quite often, for example, in hydrodynamics—the boundary layers on rotating and fluted surfaces, flows above depressions, etc. In analyzing the interaction of "fixed" structures in a flow the feedback "upstream" is neglected, i.e., $\varkappa$ is set equal to zero in (3.15) and the problem of the appearance of a strange attractor along j is rigorously formulated.

We shall study the case when the development of chaos along the chain occurs through a sequence of period doublings. Keeping in mind the fact that the dynamics of individual elements can also be described with the help of maps we shall employ, aside from (3.15) with $\varkappa = 0$, the system

$$A_j(n+1) = f_0(A_j(n), \varepsilon) + \gamma_1(A_j(n) - A_{j-1}(n)) + \gamma_2(A_j^2(n) - A_{j-1}^2(n)) \tag{3.16}$$

with the boundary conditions $A_0(n) = A_0$; here γ_1 is responsible for the "inertial" coupling and γ_2 is responsible for the "dissipative" coupling. By specifying the form of the functions $f_0(A_j,\ \varepsilon)$ we shall be able to study transitions in chains whose individual elements have different dynamics.

Setting $f_0(A_j,\varepsilon) = \varepsilon - A_j^2(n)$, we write Eq. (3.16) in the more general form

$$A_j(n+1) = f_0(A_j(n)) + \gamma\varphi_0(A_j(n),\ A_{j-1}(n)) = F_0(A_j(n),\ A_{j-1}(n)). \tag{3.17}$$

We shall assume that the coupling is weak $|\gamma| \ll 1$, and with respect to $\varphi(A_j,A_{j-1})$ we set $\varphi_0(u,u) = \varphi_0(0,0) = 0$. Because the elements are identical the weakness of the coupling guarantees that the stationary state will be a smooth function of the coordinate j in the interval from one spatial bifurcation to another. Since we specified the type of critical behavior (period doubling), we shall be interested in the development of chaos along the chain from the starting 2^N periodic regime. This behavior of chaos through a sequence of period doublings is realized when on all elements

$\varepsilon - \varepsilon_{cr} > 0^{(11)}$, while on the first element $-\varepsilon(1-\gamma) < \varepsilon_{cr}$ (we assume for definiteness that $A_0 = 0$). In the process a stable 2^N periodic regime, which transforms into a chaotic regime as j increases, is realized at the start of the chain.

To construct the renormalization-group equations we perform on (3.16) a scale transformation (doubling transformation): we express the variables in terms of two units of discrete time [$A_j(n+2)$ in terms of $A_j(n)$] and make the substitution $A_j \to A_j/a$. Applying this procedure N times we obtain the equation of the renormalization group (RG)

$$A_j(n+2^N) = F_N(A_j(n),\ A_{j-1}(n))$$
$$= f_N(A_j(n)) + \gamma\varphi_N(A_j(n),\ A_{j-1}(n)) + O(\gamma^2),$$

which decomposes into two equations:

$$f_N(A_j(n)) = af_N f_N\left(\frac{A_j(n)}{a}\right), \tag{3.18}$$
$$\varphi_{N+1}(A_j,\ A_{j-1}) = af'_N f_N\left(\frac{A_j}{a}\right)\varphi_N\left(\frac{A_j}{a},\ \frac{A_{j-1}}{a}\right)$$
$$+\varphi_N\left[f_N\left(\frac{A_j}{a}\right),\ f_N\left(\frac{A_{j-1}}{a}\right)\right].$$

The first equation in (3.18) is a particular case of the universal operator equation of the renormalization group

$$F_{N+1}U = S^{-1}F_N F_N SU, \tag{3.19}$$

in which, however, on transferring to a map through two units of time the scale transformation is applied not only to the functions (operators) determining the dynamics of an individual element but also to the spatial coordinates.[12)] Here we have introduced the notation $S = S_1S_2$, $S_1U = U/a$; $S_2U = U/b$. In the general case the variable U can be a vector or a matrix. In Eq. (3.18), because the coordinate j is discrete, the change in the spatial scale is achieved by renormalizing the coupling γ. As will be shown below, in the long-wavelength limit Eq. (3.18) gives the same similarity laws as does Eq. (3.19).

The goal of applying the renormalization-group method in this case is to find the critical exponents and the scale factors determining the similarity of the spatial bifurcations for this type of critical behavior in a neighborhood of the critical point. At the same time the solution of the RG equation, if it can be found, is usually found only at the critical point itself

$$GU = S'GGSU, \tag{3.20}$$

where the operator G is invariant relative to the action of the renormalization group. In addition, the solutions of the RG equations linearized near the stationary point G can be used to find the scaling constants. In the general case this is not sufficient. With some restrictions on the structure of the operator F_N, however, this problem can be solved. For this one must be able to calculate the "preceding," increasingly higher order iterations, from the "following" iterations of the action of F_N directly adjacent to the stationary point of the RG and thus to predict the behavior of the system as a function of the parameter in an increasingly larger neighborhood of the critical point.

In order for such a calculation to be possible the stationary point of the RG equation must have stretching, i.e., unstable, directions. The action of the operator F_N in a small neighborhood of the critical point determines the behavior of the system in an increasingly larger neighborhood only along such directions. We stress here that the set of unstable directions in the function space where the operator F_N is defined cannot be continuous. Otherwise the critical behavior is no longer universal—arbitrarily small changes in the seed operator F_N result in completely different similarity laws. Thus the stationary point of the RG equation describing the universal behavior at the critical point must be a saddle point. In addition, to determine the similarity laws it is necessary to know only the perturbations of the operator F_N to which the eigenvalues (multipliers) of the linearized problem which are greater than unity correspond. In what follows we shall term them real. These multipliers themselves are the constants sought which determine the scale similarity under transformations which are specified by the perturbing operators corresponding to these multipliers.

We shall make use of these considerations to analyze the RG equation (3.18). The stationary point of this equation is

$$G = \begin{Bmatrix} f_N \\ \varphi_N \end{Bmatrix} = \begin{Bmatrix} g \\ 0 \end{Bmatrix}. \tag{3.21}$$

Here the function g is identical to the universal Feigenbaum function (period doubling),[155] which is the solution of the functional equation

$$g(U) = agg(U/a). \tag{3.22}$$

We shall investigate the RG equation (3.18) in a neighborhood of the stationary point (3.21). Representing $F_N(A_j, A_{j-1})$ in the form

$$F_N(A_j,\ A_{j-1}) = g(A_j) + \mu\,[h_N(A_j) + \gamma\tilde{\varphi}_N(A_j,\ A_{j-1})], \tag{3.23}$$

we obtain for the functions h_N and $\tilde{\varphi}_N$ in the first approximation in μ

$$h_{N+1}(A_j) = ag'g\left(\frac{A_j}{a}\right)h_N\left(\frac{A_j}{a}\right) + h_N g\left(\frac{A_j}{a}\right); \tag{3.24}$$

$$\varphi_{N-1}(A_j,\ A_{j-1}) = ag'g\left(\frac{A_j}{a}\right)\tilde{\varphi}_N\left(\frac{A_j}{a},\ \frac{A_{j-1}}{a}\right)$$
$$+\tilde{\varphi}_N\left[g\left(\frac{A_j}{a}\right),\ g\left(\frac{A_{j-1}}{a}\right)\right]. \tag{3.25}$$

The equation (3.24) is simply the Feigenbaum equation linearized at the stationary point $g(A)$ and therefore it has one real eigenvalue $\delta = 4.669$, corresponding to the eigenfunction $h_0(A) = 1 + O(A^2)$. The equation (3.25), however, is identical to the RG equation describing the transition to chaos in a system to two coupled parabolic maps.[162] This equation, according to Ref. 162, has two real eigenvalues: $\nu_1 = a = -2.5029...$ and $\nu_2 = 2$. The value of ν_1 corresponds to the eigenfunction

$$\tilde{\varphi}_1(A_j,\ A_{j-1}) = (A_j - A_{j-1})\,\Phi_1(A_j,\ A_{j-1}),\ \Phi_1(A_j,\ A_{j-1}) \sim 1.$$

Disturbances of this type can be interpreted as the introduction of an inertial coupling between point-like elements. The value $\nu_2 = 2$ corresponds to the eigenfunction $\tilde{\varphi}_2(A_j, A_{j-1}) = (A_j^2 - A_{j-1}^2)\Phi_2(A_j,\ A_{j-1})$, where $\Phi_2(A_j, A_{j-1}) \sim 1$ which is responsible for the introduction of the dissipative coupling.

Taking into account the eigenfunctions which correspond only to real eigenvalues Eq. (3.17) of the flow system can be written in the following universal form:

$$A_j(n+2^N) = g(A_j(n)) + \mu\delta^N h_0(A_j(n)) + \gamma c_1(A_j(n) - A_{j-1}(n))\Phi_1(A_j(n), A_{j-1}(n)) + \gamma c_2(A_j^2(n) - A_{j-1}^2(n))\Phi_2(A_j(n), A_{j-1}(n)). \quad (3.26)$$

where c_1 and c_2 are constants which determine the value of the inertial and dissipative couplings, respectively. It follows directly from the form of the equations obtained that in a neighborhood of the critical point the effect the RG transformation reduces to increasing the critical parameter μ by a factor of $\delta = 4.669...$, the inertial coupling by a factor of γ, and the dissipative coupling by a factor of 2. For the system (3.17) this result was first obtained approximately in Ref. 163.

A characteristic feature of the systems studied in this section is that the coupling between the elements is unidirectional. In such systems there exist strongly nonuniform stationary regimes (for example, with the boundary 2^N-cycle–chaos). The RG procedure is also formally applicable to such solutions, since unlike Ref. 164 here the spatial uniformity of the solution at the critical point is not fundamental. This nontrivial circumstance makes it possible to obtain from (3.25) the similarity laws for the characteristics of these regimes. In particular, the following similarity laws can be obtained.

1. The similarity law for the period of the cycle $T(\mu,\gamma)$ in an element after which chaos appears. Since under the action of the RG transformation the time scale and the magnitude of the coupling γ are doubled ($c_1 = 0$) and the critical parameter μ is increased by a factor of δ we have the following similarity law for $T(\mu,\gamma)$: $T(\mu,\gamma) \sim \gamma^{-1}\tilde{f}_0(\mu/\gamma^\alpha)$, $\alpha = \ln\delta/\ln 2$.

2. Similarity laws for the number of spatial bifurcations and the number j^*, from which chaos arises. Since under the action of the RG transformation both these quantities do not change, for them the following similarity laws must hold: $N_k(\mu,\gamma) \sim \tilde{f}_1(\mu/\gamma^\alpha)$, $j^*(\mu,\gamma) \sim \tilde{f}_2(\mu/\gamma^\alpha)$, where $\tilde{f}_{0,1,2}$ are certain functions.

3.5. Effect of external concentrated forcings on dynamical structures. Order-chaos transitions

The nearly spatially uniform chaotic regime established in a flow system from sequentially coupled structures with sufficiently large j may be unstable with respect to the synchronizing action of an external periodic field applied at the boundary of the system. We shall demonstrate this for the example of a unidirectional chain described in Eqs. (3.15) with $\Phi(A,\varepsilon) = A - (1+i\beta)|A|^2A$ and $\varkappa = 0$:

$$\frac{dA_j}{dt} = [1 - (1+i\beta)|A|^2]A_j + \gamma(A_j - A_{j-1}). \quad (3.27)$$

In the absence of a synchronizing action stabilization of turbulence occurs in this chain—a spatially nonuniform chaotic regime, in which the dimension, entropy, and other average characteristics no longer depend on j for $j > \bar{j}$, is established along the chain.

Now, suppose a synchronizing action is applied at the start of the chain:

$$A_0(t) = A_s e^{i\omega_s t}. \quad (3.28)$$

The chain should be most sensitive to synchronization at the frequency ω_s close to the partial frequencies ω_p of its constituent elements, i.e., (taking into account the complex coupling γ) at the frequency $\omega_s \approx \omega_p = \beta(1 - \mathbf{Re}\,\gamma) + \mathrm{Im}\,\gamma/\mathbf{Re}\,\gamma$. The intensity $I_j = |A_j|^2$ in the stationary spatially uniform regime of synchronization is described by the map

$$I_j(1 - I_j)^2 = \frac{|\gamma|^2}{1+\beta^2} I_{j-1}, \qquad I_0 = A_s^2. \quad (3.29)$$

This map has for any value of β and γ a stable stationary point $I_1^0 = 1 + |\gamma|(1+\beta^2)^{-1/2}$, and for any amplitude of the external field there exists a trajectory of the map which lies entirely in the region of stability. Moreover, the regime of full synchronization—(3.29) also turns out to be globally stable, i.e., the infinite-dimensional phase space of the system (3.27) and (3.28) with $\omega_s = \omega_p$ does not contain any other attracting sets.[166]

The time over which the regime of synchronization is established can, however, be very long—it is determined not only by the parameters of the system but also by the initial degree of excitation of its constituent elements. Since the oscillations of the elements are not synchronized, if the spread in the initial conditions is sufficiently large a chaotic regime should be rapidly established in the system. Synchronization of this regime, starting with the first element, will gradually encompass the elements "downstream"—a propagating front of synchronization forms. In the case when the mismatch between the frequency of the external field and the partial frequency of the oscillations of the elements of the chain is greater than the synchronization band, a regular regime of beats arises at the left end of the street; this regime will displace chaos similarly to a one-period regime—a wave of the "beating-chaos" transition forms (Fig. 18).[166] If the duration of the controlling periodic signal is finite, then the moving region of synchronization—a regular spot on the background of turbulence)—will also turn out to be finite in space (in j).

Thus if different asymptotic states (multistability), including also turbulent states, whose realization depends on the initial and/or boundary conditions, are possible in the

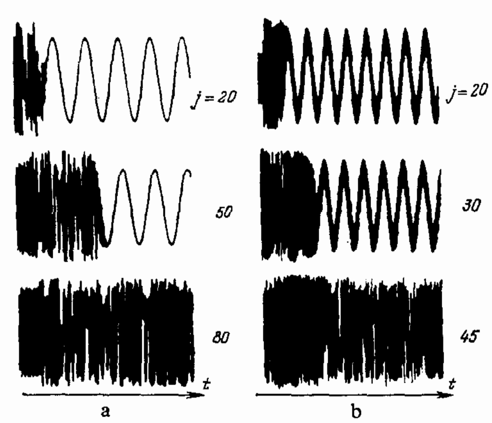

FIG. 18. Waves of a phase transition ($\gamma = 0.7\,(1\text{–}1.7i)$, $\beta = 3.42$). a–Regular oscillations–chaos ($I_0 > 1/2$); b–beats–chaos ($I_0 < 1/2$). (See Ref. 166).

flow, then concentrated forcing may turn out to be quite effective. In this connection there arises the question of how realistic such a situation in formed shear flows is, since in accordance with Townsend's hypothesis,[167,168] which has been confirmed by a number of experiments, in such flows turbulence with universal properties is established in the self-similar region. The dominant structures in this region can be represented in the form of vortex pairs, oriented along the principal axis of the velocity of deformations, making an angle of 45° with the average velocity. These vortices appear owing to the stretching of the starting (nonuniversal) turbulence by the average shear flow and serve as a coupling link between the average flow and the small-scale turbulence, and thus determine its properties. In the self-similar regime the dominant structures—vortex pairs—reach a quasistationary state, which is determined by the condition that intensification (owing to deformations in the average shear flow) is balanced by dissipation (owing to interaction with smaller vortices). Townsend hypothesized that the flow loses any memory of the initial (boundary) conditions—its state depends on the overall geometry and not on the fine details of the applied forces—based on the fact that the completely developed state depends solely on the turbulent energy budget. However a number of later papers contain weighty proofs of the fact that memory of the initial conditions extends into the region where the flow is usually regarded as self-similar. It may be concluded from the results of Ref. 169, which were obtained in a study of wakes behind a porous disk and behind a sphere ($\mathbf{Re} \sim 10^4$) with the same radii and drag, that in the first case there is no shedding of ring-shaped vortices and self-similar Townsend turbulence with dominating vortex pairs does indeed form at sufficiently large distances. At the same time large ring-shaped (possibly also spiral-shaped[170]) vortices shed from the sphere are observed at distances of up to several hundreds of diameters and determine the properties of the flow. In particular, the turbulent Reynolds number $R_T = 31$ is substantially different in this case from the corresponding value $R_T = 4$ in the wake behind a porous disk. The large-scale transverse two-dimensional and ring-shaped vortices in shear layers and jets, already discussed above, are other examples of structures which do not correspond to the mechanism of Townsend self-similarity.

Thus either different asymptotic states (multistability), realized with different initial and/or boundary conditions, or states from which the transition to the asymptotic state occurs at such long times and/or large distances that finite perturbations strongly affect this transition, are possible even under conditions of developed turbulence. This confirms that it is in principle possible to change qualitatively the properties of flows with the help of concentrated forcing. However in experiments performed thus far with weak forcings which are of practical interest[13)] it has been possible to achieve flow control only up to and in the vicinity of the region of transition to turbulence.

Among the many effects observed under concentrated forcing of shear flows (see the reviews Refs. 173–180) the suppression of turbulence is of greatest interest. In subsonic jets such suppression was first observed in Ref. 181. The experiments presented there and subsequent experiments[182–192] showed that the suppression is strongest at the start of the jet and is obtained with high-frequency forcing. It is explained by the fact (see Refs. 189 and 190) that an external high-frequency field initiates in the shear layer of the jet the formation of a regular chain of thin ring-shaped vortices whose spatial period Λ is much shorter than the diameter d of the jet. The most dangerous long-wavelength ($\Lambda \sim d$) disturbances arising against their background have smaller increments than in the case of a continuous shear layer; this is what delays their development and decreases the energy of pulsations on the starting section of the jet ($x \lesssim 8d$). Forcing at frequencies close to the frequencies of the most dangerous disturbances regularizes the flow, but the integrated energy of the pulsations usually does not decrease in the process. Suppression of pulsations is nonetheless also possible in this case, if the amplitude and phase of the forcing are chosen so that the excitations developing naturally in the flow are compensated by the excitations induced by the external action.[147,193–196] Such compensation with the help of concentrated forcing can be realized comparatively simply in the case when the most dangerous excitations have a narrow-band spectrum. In particular, it makes possible complete suppression of self-excited oscillations in a wind tunnel whose working part is open.[147,195,196] The question of the possibility of utilizing this method for suppressing wideband excitations actually leads to the problem of distributed forcing.[194,197,198]

3.6. "Commensurate-incommensurate" transitions

We shall study a stationary periodic lattice of structures subjected to external static forcing which is periodic in space. In this case the flow can transform into new states, stationary or nonstationary, depending on the amplitude and the period of the forcing. Among the newly arising stationary states it is natural to single out three basic states, which are qualitatively different and which transform into one another as a result of bifurcation at the critical values of the parameters—the supercriticality, the amplitude, and the wavelength of the disturbance. The first state is the state of "commensurateness," when the period of the established lattice is related with the spatial period of the disturbance by a rational ratio. The second state is the state of "incommensurateness" and is characterized by the presence of regions in the flow where the period of the lattice is incommensurate with the period of the perturbation. Finally, the third state is the chaotic state when the period of the lattice varies in space in an irregular fashion. Such states can be observed both in static solid-state lattices (in particular, in krypton adsorbed on graphite[199] and in magnetically ordered systems[200]) and in ensembles of hydrodynamic structures discussed here that are formed, for example, under the conditions of Rayleigh-Bénard thermal convection[201,202] or of the electrohydrodynamic instability in thin layers of liquid crystals.[92,203,204] For small excesses above threshold the latter two cases do not differ fundamentally, but because of purely technical difficulties experimental studies have been performed only for liquid crystals.

In thin layers of liquid crystals flow in the form of rolls (Williams domains), whose properties are similar to those of Rayleigh-Bénard convection, arises as a result of the electrohydrodynamic instability when the voltage across the layer V is greater than the critical value V_{cr}. The introduction of an added voltage $\Delta V = (a/2)\, V_{cr} \cos k_1 x$ periodic

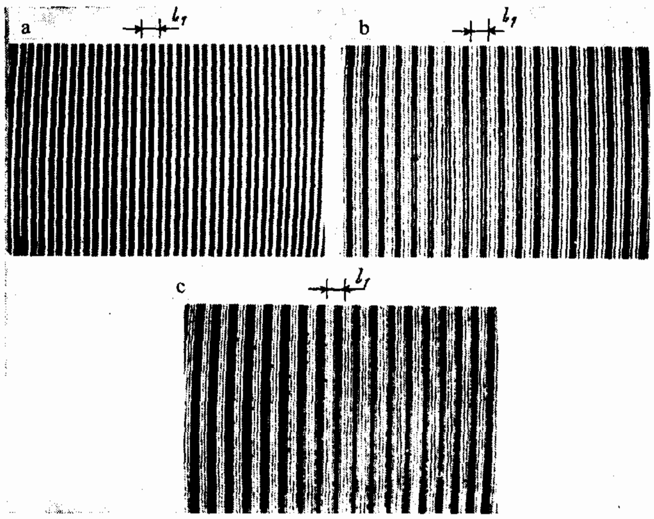

FIG. 19. Commensurate states. a–1/1, $l_0/l_1 = 0.928$, $\alpha = 0.097$; b–1/2, $l_0/l_1 = 0.460$, $\alpha = 0.114$; c–1/3, $l_0/l_1 = 0.370$, $\alpha = 0.114$. (See Ref. 204).

along the layer result in competition between modes with two different scales and, as a consequence, leads to the effects studied here (see Refs. 92 and 203–204). Figure 19 shows as an example[204] the commensurate states m/n in which $n = 1, 2$, and 3 hydrodynamic periods form on $m = 1$ periods of the disturbance. Commensurate states of higher order with a spatial period ml_1 were also observed in the experiment of Ref. 204, but as m was increased three-dimensional effects made it difficult to observe these purely two-dimensional states. When the values of l_0/l_1 differed by large amounts from the ratio of small simple numbers incommensurate phases, characterized by the amplitude and phase of the modulation, arose. In the incommensurate phases shown in Fig. 20 the period of most rolls is dictated by the period of the external forcing as in the commensurate phase 1/1, but regions of local compression of the rolls also occur between them. The shift $\varphi(x_k)$ of the spatial phase of the k th pair of rolls relative to the phase of the external forcing

$$\varphi(x_k) = 2\pi\left(\frac{x_k}{l_1} - k\right) \tag{3.30}$$

turned out to be close to the solution of the equation

$$\frac{d^2\varphi}{dx^2} = c\sin\varphi \tag{3.31}$$

with appropriately chosen constants a, b, and δ:

$$\varphi(x) = 2\pi\left[a - \frac{1}{\pi}\,\mathrm{am}\left(\frac{2b}{s}x + \delta\right)\right]; \tag{3.32}$$

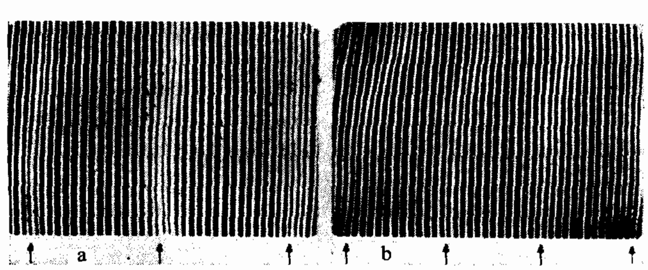

FIG. 20. Incommensurate states. $\alpha = 0.032$; the arrows mark the regions of local compression of rolls. a–$l_0/l_1 = 0.866$; b–$l_0/l_1 = 0.816$. (See Ref. 204).

here $am(u)$ is the amplitude of the elliptic integral of the first kind and s is the distance between the points of compression of the rolls.

The explanation of this phenomenon is as follows. For small excesses above threshold in the absence of external forcing the flow can be described by the GL equations. A spatially periodic external forcing should result in corresponding changes in the symmetry of the amplitude equations. In the two-dimensional case (one-dimensional chains of structures) use of the fact that a small external forcing with the wave number k_1 destroys invariance under arbitrary translations and admits invariance under the group of discrete translations $x \to x + 2\pi N/k_1$ ($k_1 = nk_0/m$, n, m are integers), leads to an amplitude equation of the form[205]

$$\frac{\partial A}{\partial t} = \varepsilon A - |A|^2 A + \frac{\partial^2 A}{\partial x^2} + \alpha (A^*)^{n-1}, \tag{3.33}$$

where α is a small parameter, usually proportional to the mth power of the external forcing. Off resonance $mk_1 = n(k_0 + q)$ $(q \ll k_0)$ a slowly varying function $\exp(inqx)$ must be inserted in the amplitude equation in accordance with perturbation theory:

$$\frac{\partial A}{\partial t} = \varepsilon A - |A|^2 A + \frac{\partial^2 A}{\partial x^2} + \alpha (A^*)^{n-1}\exp(inqx) = -\frac{\delta F}{\delta A^*}, \tag{3.34}$$

where

$$F = \int dx\left\{-\varepsilon |A|^2 + \frac{1}{2}|A|^4 + \left|\frac{\partial A}{\partial x}\right|^2 - \frac{\alpha}{n}\left[(A^*)^n \exp(inqx) + A^n \exp(inqx)\right]\right\}. \tag{3.35}$$

The stationary uniform solutions $A = Q\exp(i\overline{\varphi})$ are determined by the relations $\overline{\varphi} = qx + k\pi/n$ and $\varepsilon - q^2 - Q^2 + \alpha(-1)^k Q^{n-2} = 0$. For $-[\varepsilon - q^2 + \alpha(n-1)Q^{n-2} - 3Q^2] = 2P^2 \gg n\alpha Q^{-2}$ the solutions with even k can be divided into amplitude modes with the decrement $\gamma_A = -2P^2$ and phase modes with the decrement $\gamma_\varphi = -a\alpha Q^{n-2}$. By virtue of the condition $2P^2 \gg n\alpha Q^{-2}$ the changes in the amplitude follow the changes in phase, which are described in this approximation by the following equations:[205]

$$\frac{\partial\varphi}{\partial t} = -V\sin(n\varphi) + \frac{\partial^2\varphi}{\partial x^2} = -\frac{\delta H}{\delta\varphi},$$

$$H = \int\left[-\frac{v}{m}\cos n\varphi + \frac{1}{2}\left(\frac{\partial\varphi}{\partial x}\right)^2 - q\frac{\partial\varphi}{\partial x}\right]dx, \tag{3.36}$$

where $V = \alpha Q^{n-2}$ and $\varphi = \theta - qx$. Comparing (3.31) and (3.36) shows that this approximation describes well the change in the sizes of the structures determined by the phase variable in the stationary case $\partial/\partial t = 0$.

Generalization to the degenerate case, when there are two types of excitations with identical (close) spatial periods, with small excesses above threshold can likewise be made under the most general assumptions. The corresponding equation for $\overline{A} = A\exp(-iqx)$ has the following form in the lowest orders in ε (Refs. 205 and 206):

$$\frac{\partial^2 \overline{A}}{\partial t^2} - \nu\frac{\partial \overline{A}}{\partial t} - \frac{\partial^2 \overline{A}}{\partial x^2} = (\varepsilon - q^2)\overline{A} + 2iq\frac{\partial \overline{A}}{\partial x} - |\overline{A}|^2 A + c_1(\overline{A}^*)^{n-1} \tag{3.37}$$

and in the limit of small mismatches $q^2 \ll \varepsilon, v_1^{2/(4-n)}$ and $|\nu| \ll \varepsilon^{1/2}$ transforms into an equation for the phase:

$$\frac{\partial^2\varphi}{\partial t^2} - \nu\frac{\partial\varphi}{\partial t} - \frac{\partial^2\varphi}{\partial x^2} = -v_1\varepsilon^{(n-2)/2}\sin(n\varphi). \qquad (3.38)$$

The experimental results discussed above and analysis of the amplitude equations (3.34) and (3.37) show that for one-dimensional chains of oriented convective rolls the flow responds in a nontrivial fashion to external forcing, even in the simplest cases. If however, the boundary conditions do not impose strict restrictions on the orientation of the convective rolls, then in a wide region of the parameters of the external forcing the three-dimensional flow is more stable (Fig. 21). Though the possibility for the appearance of three-dimensional flow can apparently be predicted (see the discussion in Ref. 204) from estimates of the Lyapunov functional F, obtained with the corresponding extension of (3.34) taking into account the changes along the second coordinate, this flow itself cannot be described on the basis of the amplitude equations.

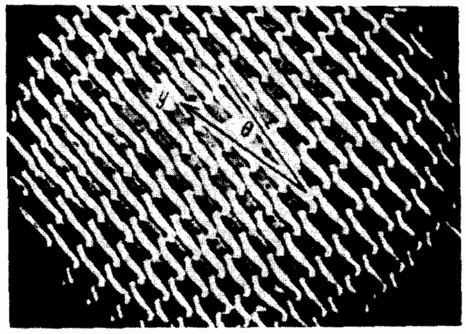

FIG. 21. Three-dimensional incommensurate states with $l_0/l_1 = 0.91$ (see Ref. 204).

3.7. Random walk of defects. Faraday ripples

The development of a dynamical theory of turbulence and the hypothesis proposed in this connection that scenarios of transitions to spatial-temporal chaos are universal stimulated new experiments intended to observe these scenarios.[93,207-214] These experiments confirm, in particular, that the general properties of transitions to spatial-temporal chaos, which are observed in real flows, are similar to those of transitions observed in model equations and in systems of coupled maps. However the direct observation of transition scenarios in an ensemble of structures is often complicated by the fact that the identification of individual structures in a turbulent regime is a very difficult problem. One of the few exceptions in this sense are cells of capillary Faraday ripples, arising on the surface of a deep liquid when the liquid is parametrically excited. These cells are so stable that they can be easily identified in both the transient and turbulent regimes. We shall illustrate using the example of Faraday ripples the scenarios most typical for an ensemble of stable structures of a transition to spatial-temporal chaos.[93,214]

In the experiment under discussion[93,214] a horizontal membrane oscillates uniformly in space at a completely determinate frequency f. Pairs of parametrically coupled capillary-gravity waves arise on the surface of a layer of liquid on the membrane in the oscillating "gravitational" field. For not too high amplitude of the vibrations (pumping) these pairs of waves form an exceptionally regular spatial lattice with square cells. If, however, the amplitude of the oscillations of the membrane (i.e., the critical parameter) is increased, an unexpected phenomenon is observed: spatial-temporal disorder appears, but the cells do not vanish (Fig. 22). The transition from a regular arrangement of cells to a disordered arrangement corresponds to the transition from a discrete spatial spectrum to a continuous spectrum.

Three scenarios of the appearance of spatial-temporal

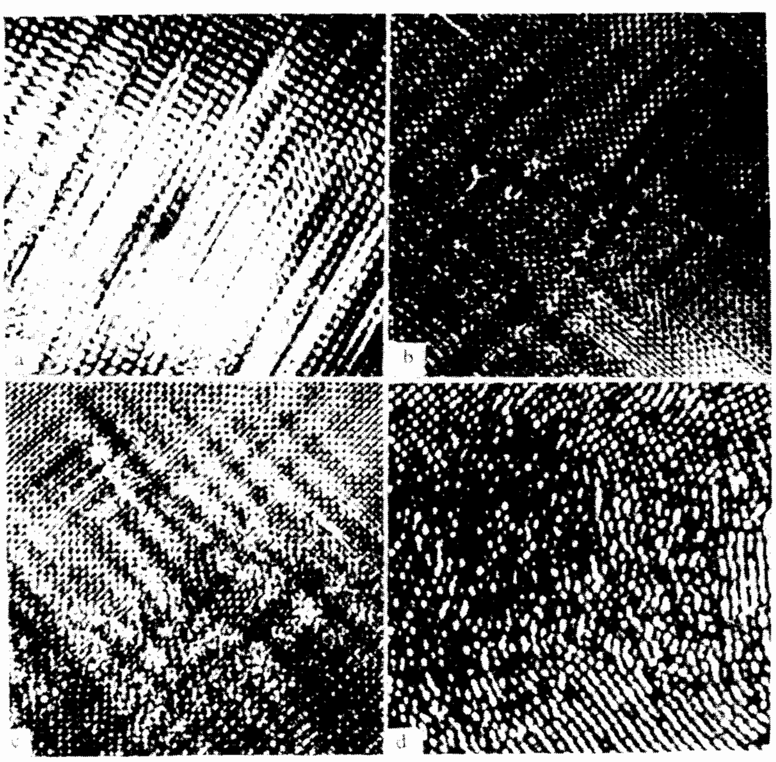

FIG. 22. The structures of capillary ripples on the surface of a liquid under conditions of parametric excitation.[93,214] a–Waves of modulation against the background of square cells. b–Waves of modulation with dislocations. c–Two-dimensional superlattice with dislocations. d–Chaotic motion of unit cells.

chaos were observed in the experiment of Refs. 93 and 214: 1) the appearance of one-dimensional periodic modulation (Fig. 22b) which subsequently became chaotic; 2) the appearance of a two-dimensional "superlattice"—a lattice of the envelope (Fig. 22c); and, 3) the formation of dislocations by the mechanism of competition of one-dimensional waves of modulation with close wave numbers, as discussed in Sec. 2.8 (Fig. 22c). We note that the number of dislocations increases as the critical parameter increases, and the turbulence that is established represents the chaotic dynamics of the interacting dislocations (Fig. 22d).

A similar, though somewhat different, picture of chaotic motion of dislocations is also observed under conditions of thermal convection in a horizontal layer of argon ($\mathrm{Pr} \ll 1$), placed in a cylindrical container (Fig. 23).[212] The difference lies in the fact that here dislocations appear not in the lattice of waves of modulation, but rather in the lattice of the starting structures—Bénard convective rolls. As the Rayleigh number increases the convective rolls at first undergo periodic motions, which then transform into random walks accompanied by the generation, motion, and vanishing of dislocations.

We shall study in greater detail the first scenario of the transition to chaos. A theory which agrees with experiment was constructed for this scenario in Ref. 114. Using the procedure described in Sec. 2.7 a discrete analog of the GL equations can be constructed for the complex amplitude of the wave of modulation from the starting continuous equations, but now in a parametric variant

$$\frac{\partial A_j}{\partial t} = i(hA_j^* - \sigma A_j) + i|A_j|^2 A_j + iQ(A_{j+1} + A_{j-1} - 2A_j), \tag{3.39}$$

where Q is determined in terms of the parameter q, equal to the number of discretization links at the wavelength λ of the wave of modulation: $Q = (v_g/\gamma\lambda)q^2/4\pi$, where v_g and γ are the group velocity and damping decrement of the capillary waves. The system (3.39) replaces the active medium by a chain of coupled parametric generators, each of which is equivalent to an elementary unit of the medium with the characteristic scale λ/q.

The system of equations (3.39) was solved numerically for two types of initial conditions: a) small deviations on the background of a uniform equilibrium state A and b) distributions A_j with high amplitude oscillating rapidly along the chain.

For small excesses above threshold complicated stationary states with a large number of oscillations on the profile A_j appear in the chain. In the case of initial conditions of the type a) the stationary regime is reached through a secondary instability of the periodic spatial modulation.[214] Stationary regimes of a different type are formed with the initial conditions b). Their spatial structure is modelled by the product of a complex function of the coordinates with relatively small changes in phase and rapidly oscillating modulus by a real sign-alternating function. As the critical parameter $\varepsilon = (h-1)$ is increased the troughs between the beats on the profile $|A_j|$ contract. At $h = 1.85$ the stationary state becomes unstable—weak oscillations in time appear. The character of the oscillations indicates that the transition to chaos is realized through intermittency.[215]

The above picture of the chaotic dynamics of modulation spikes is in good qualitative agreement with the experimental results. The computational results for small excesses above threshold predict the formation of large troughs on the modulation of the experimentally observed profile. In

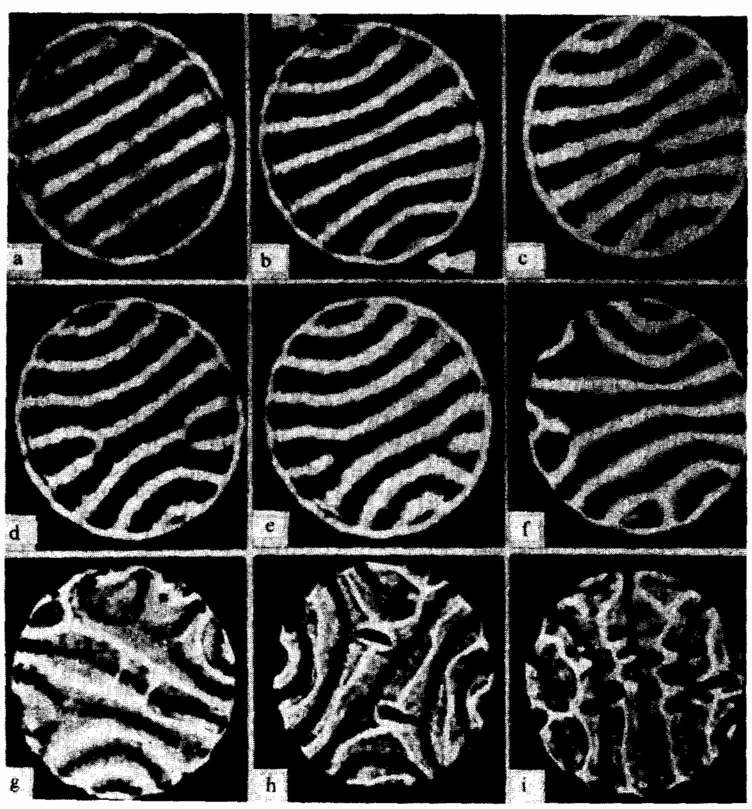

FIG. 23. The transition to turbulence under conditions of thermal convection of argon in a cylindrical cell.[212] a–$\varepsilon = 0.05$–stationary rolls; b–e: $\varepsilon = 0.14$–one-period oscillations with formation of dislocations. f: $\varepsilon = 1$–deformations of the rolls. g: $\varepsilon = 2$–appearance of cross rolls; h: $\varepsilon \approx 4$–formation of pairs of small rolls near dislocations. i: $\varepsilon \approx 4$–nonstationary structures.

addition the displacement times of the dark fringes agree with the restructing times accompanying the establishment of stationary states in the numerical calculation. For example, for $h = 1.4$ ($\varepsilon = 0.4$) this is the time $t \sim 100\gamma^{-1} \approx 3$ s. In real time the fastest restructurings with $h = 2.2$ have the scale $t_2 \approx \tau_2 \gamma^{-1} \approx 0.12$ s, which also agrees with the visual estimates for the regime of developed chaos. As numerical experiments show Eq. (3.39) for the same values of the parameters can describe different established chaotic regimes. This means that its phase space contains simultaneously several different stochastic attractors, the emergence onto one of which is determined by the initial conditions. Visually, in the experiment, to this set of attractors there corresponds a set of spatial images (structures), which are established against the background of capillary ripples with the same value of the critical parameter.

We call attention here to the following important fact. The chaos observed in the experiment of Ref. 214 was almost always two-dimensional. Near the threshold for its appearance, however, it is almost a superposition of one-dimensional, mutually orthogonal, modulation structures; this is what justifies the construction of a one-dimensional theory based on Eq. (3.39).

3.8. Multidimensional chaos. Relation of the dimension of turbulence with the number of collective excitations

For sufficiently large critical parameter (amplitude of vibrations) the properties of the observed turbulence no longer depend on the path by which it appears—turbulence consists of spatial-temporal dynamical chaos in an ensemble of interacting capillary cells. A model theory (see Ref. 216) of such turbulence can be constructed using the discrete analog of Eq. (2.14)

$$\frac{dA_{j,l}}{dt} = A_{j,l} - (1 + i\beta)|A|^2 A_{j,l} + \varkappa(1 - ic)(A_{j,l+1} + A_{j,l-1} + A_{j+1,l} + A_{j-1,l} - 4A_{j,l}) \qquad (3.40)$$

or in the one-dimensional variant—Eq. (3.15). We shall assume that the boundary conditions in the analysis of collective motions in ensembles of the form (3.15) and (3.42) are periodic (respectively):

$$A_j(t) = A_{j+N}(t), \qquad (3.41)$$

$$A_{j,l}(t) = A_{j+N,l}(t), \quad A_{j,l}(t) = A_{j,l+N}(t). \qquad (3.42)$$

Assuming that in some region of the parameters a stable stochastic regime is realized in the ensemble (3.15) or (3.40), we shall determine the dependence of the characteristics of chaos on the parameters of the ensemble—the numbers of elements N and the magnitudes of the couplings $\varkappa$ between the autostructures—elementary cells of Faraday ripples. Assuming that the turbulence established is on the average spatially homogeneous, i.e.,

$$\overline{|A_j|^2}^t = |a|^2, \qquad \overline{A_j^2}^t = a^2, \qquad (3.43)$$

and, in addition, the average pulsations of the intensity are small

$$|A_j|^2 - |a|^2 = z_j, \qquad \overline{z_j^2}^t \ll |a|^4, \qquad (3.44)$$

the Lyapunov exponents of the motion under study on a strange attractor can be calculated explicitly and the dependence of the Lyapunov dimension D_L on the parameter $\varkappa$ can be calculated. In particular, for $\varkappa < 1/4$ we have[216]

$$D_L \lesssim N\left(1 + \frac{1 - 2\varkappa}{4|a|^2 - 1}\right) \qquad (3.45)$$

in the one-dimensional variant and

$$D_L \approx 2N(1 - 2\varkappa)\{[(1 + \beta^2)^{1/2} + 2]|a|^2 - 1\}^{-1} \qquad (3.46)$$

in the case of a square lattice.

It is natural to compare the dimension of stochastic sets in one- and two-dimensional ensembles of structures with the same parameters and the same number elements (Fig. 24). It is obvious that the dimension of chaos in a two-dimensional ensemble with a given coupling between the structures is always less than in a one-dimensional ensemble with the same number of elements. This is explained by the fact that the degree of autonomy of the structures (the dimension of chaos increases as the degree of autonomy decreases) is determined not only by the magnitude of the coupling between the neighbors but also on the number of neighbors: as the number of couplings increases the autonomy of an elementary structure effectively decreases and therefore the collective motions become more ordered. This is what corresponds to the lower value of the dimension.

As the autonomy of the structures increases the number of collective excitations which can exist in ensembles of the form (3.15) and (3.40), as we shall now prove, continuously increases. For this reason it seems obvious that the above-discussed increase in the dimension of chaos as $\varkappa$ decreases should be related with the appearance of new independent motions in the ensemble. Also they should obviously be unstable.

We shall demonstrate the truth of this proposition using the example of the system (3.15) and (3.40), collective excitations in which have the form of steady-state traveling waves:

$$A_j(t) = A^{(n)} \exp[i(\omega^{(n)}t + j\theta^{(n)})]. \qquad (3.47)$$

Substituting (3.47) into (3.15) gives the dependence of the intensity of these waves on the propagation constant

$$|A^{(n)}|^2 = 1 - 4\varkappa \sin^2\frac{\theta^{(n)}}{2} \qquad (3.48)$$

and the dispersion law for these waves is

$$\omega^{(n)} = -\beta + 4\varkappa(\beta + c)\sin^2\frac{\theta^{(n)}}{2}, \qquad (3.49)$$

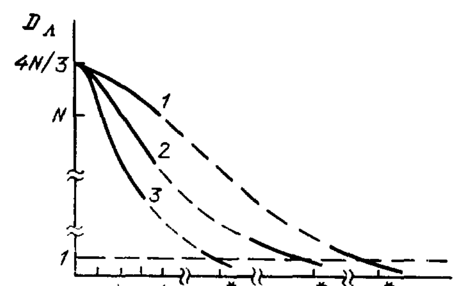

FIG. 24. The Lyapunov dimension D_A of a stochastic set in an ensemble of N autostructures.[216] 1–For a one-dimensional "lattice" ($\varkappa_1^* = N^2/4\pi^2$). 2–For a square lattice ($\varkappa_2^* = \varkappa_1^*/2N$). 3–For a cubic lattice ($\varkappa_3^* = \varkappa_1^*/3N^{4/3}$).

where $\theta^{(n)} = \pm 2\pi n/N$, $n = 0,1,...,N/2$. Immediately above the threshold for the appearance of structures, i.e., for not too large critical parameter, the coupling between the cells is quite strong. The ensemble of structures demonstrates only a trivial regular behavior. The stability of the spatially homogeneous regime is determined by the exponents (see Ref. 216):

$$\lambda^{(i)} = -1 - 4\varkappa \sin^2\frac{\theta^{(i)}}{2} \pm \left[1 - \left(4\varkappa c \sin^2\frac{\theta^{(i)}}{2}\right)^2 + 8\beta\varkappa \sin^2\frac{\theta^{(i)}}{2}\right]^{1/2}, \tag{3.50}$$

whence it follows that for

$$\varkappa > \varkappa_0 = (\beta c - 1)\left[2(1+c^2)\sin^2\frac{\pi}{N}\right]^{-1} \tag{3.51}$$

all $\lambda^{(i)} \leqslant 0$ and the regime of spatially homogeneous oscillations in an ensemble of N cells is stable.

For $\beta c > 1$ as $\varkappa$ decreases (from the value $\varkappa_0$) new collective motions are successively engendered in the system (at $\varkappa = \varkappa_k$) from the trivial equilibrium state $A_j = 0$. In the phase space of the system (3.15) this corresponds to soft generation at $\varkappa = \varkappa_k$ from the states of equilibrium of pairs of limit cycles (corresponding to oppositely propagating waves), and in addition all periodic motions appearing in this manner are unstable. This can be proved by studying the characteristic indices of the trivial equilibrium A_j:

$$\lambda^{(i)} = 1 - 4\varkappa \sin^2\frac{\theta^{(i)}}{2} + 4ic\varkappa \sin^2\frac{\theta^{(i)}}{2}. \tag{3.52}$$

Comparing (3.52) and (3.34) it is not difficult to see that the number of unstable directions in phase space, i.e., the number of positive $\mathbf{Re}\,\lambda^{(i)}$, with given $\varkappa'$ is equal to the number of steady-state waves appearing as $\varkappa$ decreases from $\varkappa_0$ to $\varkappa'$, while the increments of the perturbations along unstable directions are determined by the intensities of these waves: $\mathbf{Re}\,\lambda^{(i)} = |A^{(i)}|^2$. Since the periodic motions appear from the trivial equilibrium in a soft manner, they inherit (at the moment a new unstable direction is engendered) the exponents of the state of equilibrium along the remaining independent directions. For this reason at the moment of creation the periodic motion with $i = 1$ is characterized by one unstable direction (it corresponds to growth of spatially homogeneous disturbances) of the motion, the periodic motion with $i = 2$ is characterized by three unstable directions, etc. If it is now assumed that the newly created unstable directions belong to a strange attractor, then it is easy to interpret the result that the dimension of chaos increases monotonically as the autonomy of the structures increases—as $\varkappa$ decreases, trajectories for which the number of unstable directions is of the order of the number of the created cycle (periodic motion with $\theta = \theta^{(i)}$) appear in the attractor. Thus the number of unstable periodic solutions of the form (3.47) which exist for a given value of $\varkappa$ is the lower limit of the dimension of the attractor.

3.9. Scaling properties of developed turbulence. The fractal structure of the field of dissipation of turbulent energy

One of the most fundamental properties of developed *hydrodynamic turbulence is the existence of an interval of* scales $L \ll l \ll l_d$ (inertial interval) in which the statistical characteristics of the velocity field satisfy a definite scaling law (where L is the global scale of the flow determined by the external forces and/or boundary conditions, while l_d is the scale on which viscous dissipation becomes significant, $l_d \sim L/\mathbf{Re}^{3/4}$). The first and best known example of such scaling is Kolmogorov's $-5/3$ law[217] for the energy spectrum $E(k)$ of the velocity pulsations:

$$E(k) = C\varepsilon k^{-5/3}. \tag{3.53}$$

This universal power-law spectrum is obtained by the method of dimensions[14)] under quite general assumptions about the local homogeneity and isotropy of turbulence for large $\mathbf{Re}$. Here ε is the rate of dissipation of turbulent energy per unit volume and C is Kolmogorov's constant. The simplicity of the dimensional approach, which yields results which agree well with the physical and numerical experiments,[214–224] is amazing given the complicated mathematical structure of the Navier-Stokes equations. Moreover, the *Kolmogorov spectrum is observed in experiments even for* moderate Reynolds numbers and/or in the range of comparatively small wave numbers, for which, with respect to all criteria, turbulence is not isotropic and homogeneous. This is especially surprising, taking into account the fact that such a dimensional approach is not applicable for the Burgers model of turbulence, the equations for which, just like the Navier-Stokes equations, have one dimensional parameter—the viscosity, and in the nonviscous limit—the energy integral.[225] A fundamental feature of Burgers model is that it does not contain internal stochasticity, i.e., stochasticity not related with the external noise; internal stochasticity is characteristic of real three-dimensional hydrodynamic turbulence. Numerical experiments with dynamical systems of high order confirm that the universal scaling laws in the inertial interval are indeed characteristic for any nonlinear systems with an invariant and internal stochasticity which remain in the nonviscous limit and can be determined from analysis of dimensions.[225–227]

It is obvious that the "scaling property" mentioned above does not exhaust all properties of the Navier-Stokes equations and cannot determine the detailed structure of the turbulence, even for extremely large Reynolds numbers. In particular, from the scale invariance of the equations of hydrodynamics of an incompressible liquid (2.4) and (2.5) with respect to the transformations

$$\begin{gathered} r' = \lambda r,\ u' = \lambda^{\alpha/3}u,\ t' = \lambda^{1-\alpha/3},\ t, \\ \left(\frac{p}{\rho}\right)' = \lambda^{2\alpha/3}\frac{p}{\rho},\quad \nu' = \lambda^{1+\alpha/3}\nu \end{gathered} \tag{3.54}$$

in the inertial interval it follows that the exponent α cannot be determined from an analysis of the dimensions without invoking additional hypotheses. Kolmogorov's inertial-interval theory assumes that the rate of dissipation of turbulent energy averaged over a region of size r $\varepsilon \sim \langle(|\Delta u|^3\rangle/r \sim \varepsilon_0(r/r_0)^{\alpha-1}$ does not depend on the dimensions of this region, i.e., $\alpha = 1$. In this case the moments $\langle|\Delta u|^p\rangle$ ($\langle\ \rangle$ indicates spatial averaging) satisfy the following Kolmogorov-Obukhov scaling law:[217,228]

$$\langle|\Delta u|^p\rangle \sim r^{\xi_p}, \tag{3.55}$$

where $\xi_p = p/3$.

In the experiments of Ref. 229, which were performed with large Reynolds numbers, it was found, however, that

$\xi_p \neq p/3$, and this discrepancy increases as p increases. This discrepancy can be eliminated, if it is assumed that the active (from the viewpoint of energy transfer upwards along the spectrum) part of the turbulence is distributed on a fractal subspace. We shall study the physical interpretation of the origin of such fractals for the example of the simplest model, the idea for which was formulated in Refs. 230–233 and which was later termed the β model.

We shall assume that the cascade transfer of energy from large vortices to small vortices does not encompass the entire volume of a large vortex, but rather only the active part of the volume, and we introduce the coefficient $\beta = 2^{D\beta^{-3}}$, equal to the ratio of the volume of the newly formed vortices with scale $l_{n+1} \sim 2^{-(n+1)} l_0$ to the volume of the starting vortex with scale $l_n \sim 2^{-n} l_0$, where l_0 is the characteristic scale of the entire flow. Since in the cascade process energy is transferred at a constant rate,

$$\varepsilon_n = \beta\varepsilon_{n+1}, \qquad \frac{\Delta u_n^3}{l_n} = \frac{\beta \Delta u_{n+1}^3}{l_{n+1}}, \tag{3.56}$$

whence it follows that

$$\Delta u_n \sim l^{1/3} \left(\frac{l}{l_0}\right)^{(D_\beta - 3)/3},$$

$$\langle |\Delta u|^p \rangle \sim r^{\xi_p},$$

$$\xi_p = \frac{p(D_\beta - 2)}{3} + (3 - D_\beta). \tag{3.57}$$

It is easy to show that in accordance with the definition (3.4) D_β is the fractal dimension of the region occupied by active vortices [here, of course, the "physical" transition to the limit under the condition that $r > r_d$ is presumed in (3.4)]. Although in this model the free parameter D_β is not determined, the fact that ξ_p is a linear function of p is an exact consequence of the model. Figure 25 shows the experimental data of Ref. 229, which confirm the linear dependence of ξ_p on p for $p < 7$, but for larger p a deviation from this dependence is observed. As we shall see this can be explained by the multifractal structure of the turbulence.

To construct the multifractal model[234–236] we shall assume that the dissipation is concentration on the sets $S(h)$ with dimension $D(h)$, on each of which the scaling analogous to that studied above but with its own index h holds in the inertial interval:

$$\Delta u(r) \sim r^h.$$

It is natural to assume that the relative number of cubes with edge r on the set $S(h)$ will be proportional to $r^{-D(h)}/r^{-3} = r^{3-D(h)}$, so that

$$\langle |\Delta u|^p \rangle \sim \int d\rho(h)\, r^{ph+3-D(h)} \sim r^{\xi_p}. \tag{3.58}$$

In the limit of small r the weighting function $\rho(h)$ can be assumed to be a slowly varying function, so that the method of steepest descent can be employed to calculate the integral in (3.58); this gives the relations

$$\rho(h) \left(\frac{2\pi}{D^{*}(h)}\right)^{1/2} (\ln r)^{-1/2}\, r^{ph^*+3-D(h^*)} \sim r^{\xi_p}, \tag{3.59}$$

where h^* is determined by the conditions

$$\left.\frac{\partial D(h)}{\partial h}\right|_{h=h^*} = p, \quad \left.\frac{\partial^2 D(h)}{\partial h^2}\right|_{h=h^*} \leqslant 0.$$

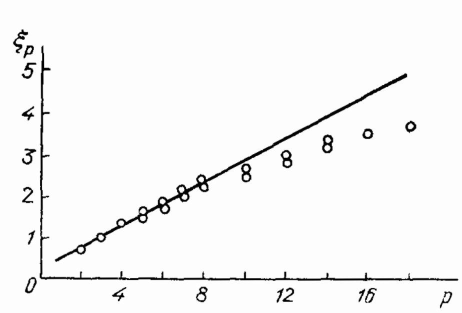

FIG. 25. The dependence (3.54) of the scaling index ξ_p on the number of the moment p in the model of uniform fractals with $D_\beta = 2.83$ (straight line) and the experimental data of Ref. 229 (circles).

For small r it may be assumed that

$$ph^* + 3 - D(h^*) = \xi_p, \tag{3.60}$$

so that the fractal spectrum $D(h)$ can be determined in a parametric form from the measured dependence $\xi_p = \xi(p)$:

$$D(h) = ph + 3 - \xi_p, \tag{3.61}$$

$$h = d\xi_p \,|\, dp. \tag{3.62}$$

In particular, for Kolmogorov turbulence $\xi_p = p/3$; for this reason the fractal spectrum consists of one point $h = 1/3$, at which $D(1/3) = 3$. For the β model $\xi_p = [p(D_\beta - 2)/3] + 3 - D$, $h = (D_\beta - 2)/3$, and naturally $D(h) = D_\beta$. The β model gives the best agreement with experimental data for $p < 7$, if $D = 2.83$. Such a small difference in D from the corresponding value for the Kolmogorov turbulence explains why the $-5/3$ law is observed so consistently in many experiments. Indeed, if the local relation between the scales r and the wave numbers k is employed for approximate calculations and it is assumed that $k \sim r^{-1}$, then we obtain for the spectrum in the β model

$$E(k) \sim k^{(-5/3)-[(3-D)/3]} \approx k^{(-5/3)-(1/18)}.$$

The small correction to the exponent can hardly be reliably measured in experiments, which usually concern a comparatively small range of wave numbers (on a logarithmic scale). The fact that $D \neq 3$ is nonetheless fundamental, since it means that the turbulence is highly inhomogeneous—the relative fraction of the volume occupied by active vortices r^{-D}/r^{-3} approaches zero for sufficiently small values of r. In other words, the structure of this part of the space is the same as that of a Cantor space U. The following simple relation is almost always satisfied in the isotropic case between the dimension D of the set U and the dimension of the sets formed by the intersection of U with a plane S or a line L (see, for example, the discussion in Refs. 132 and 237):

$$D = 1 + D_S = 2 + D_L,$$

which is extremely important for determining the values of D experimentally, since it is often necessary to confine the experiments to one-dimensional measurements. If Taylor's hypothesis is employed in addition to this relation and it is assumed that the temporal realization corresponds to the intersection of frozen-in turbulence and a straight line (for example, the straight line OX along the flow: $\partial/\partial t = -U_0 \partial/\partial x$), then $D_L(h)$ can be determined experimentally. In Ref. 237 such measurements were performed

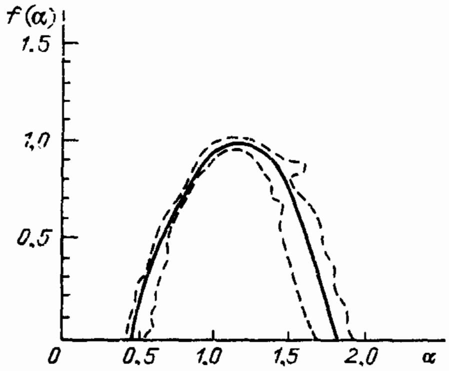

FIG. 26. The average multifractal spectrum for developed turbulence in different flows: in laboratory boundary layer, behind a grid, in the wake of a cylinder, and in the atmospheric boundary layer. The broken curves bound the region containing the experimental points.[237]

for one of the terms appearing in the expression for the dissipation of turbulent energy $\varepsilon \sim (\partial u/\partial x)^2 \sim (U_0 \partial u/\partial x)^2$. The results of measurements of $D_L(h)$ of the spectra of developed turbulence with different flow geometries and Reynolds numbers (Fig. 26) are virtually identical to one another and extend from $h = \alpha_{\min} = 0.51$ to $h = \alpha_{\max} = 1.78$ while the maximum value $f(\alpha_0) = 1$ is reached at $\alpha_0 = 1.117$.[237] It follows from the dependences presented that the greatest dissipation of energy $\varepsilon \sim r^{\alpha-1}$ for small r (singular in the limit $r \to 0$) occurs on fractal subspaces with dimension $f(\alpha < 1) < f(1) \approx 0.95$ (here, as we have already pointed out, the fractals are meant in the physical sense, since it is assumed that all scales of r exceed the Kolmogorov scale l_d).

The results presented above indicate that for large Reynolds numbers most of the volume of the turbulent liquid is passive with respect to energy dissipation, and therefore also with respect to the transfer of energy upwards along the spectrum. In the Navier-Stokes equation for the vorticity

$$\frac{\partial \boldsymbol{\omega}}{\partial t} + \operatorname{rot}(\mathbf{u} \times \boldsymbol{\omega}) = \nu \nabla^2 \boldsymbol{\omega} \tag{3.63}$$

the only nonlinear term directly responsible for this transformation is $\nabla \times (u \times \omega)$. From here it may be concluded that the most probable distributions of the vorticity $\boldsymbol{\omega}(\mathbf{r})$ in developed turbulence are those that minimize this term (with the exception, possibly, of the component describing the trivial transfer of vorticity). Recent studies[238] indicate that this principle for suppressing nonlinearity is not a unique property of the Navier-Stokes equations and is satisfied for a wider class of nonlinear systems. The qualitative interpretation of the suppression of nonlinearity with small dissipation ($\mathbf{Re} \to \infty$) consists of the fact that the system is most likely to be found in the region of phase space (or function space, if we are talking about fields), where its motion is slowest:

$$\frac{\partial}{\partial t} \sim \mathbf{Re}^{-1}.$$

It can be expected that further investigations of this problem will make it possible to formulate more exact variational principles, suitable for finding quasiequilibrium coherent structures with long lifetimes. It is possible that the spiral structures, widely discussed in recent years,[239-243] in which the velocity field and the vorticity are oriented predominantly parallel to one another, belong to this class.

4. CONCLUSIONS

Three directions in the theory of turbulence—statistical, structural, and dynamical—developed in parallel and practically independently, even comparatively recently. The results obtained in each direction pertained to different problems and answered questions arising in qualitatively different experimental situations. Now it seems surprising that such autonomy has existed for so long and an impetus towards and possibilities (!) for constructing a single unified theory appeared only in the last five years.

The interaction of the structural and dynamical approaches to turbulence are especially clear today. This, in particular, is attributable to many experimental successes, which convinced investigators that turbulence with moderate Reynolds numbers is spatial-temporal chaos of interacting structures. Qualitative proof of this fact is provided by experiments in which hydrodynamic flows are visualized; quantitative proof, however, is obtained by special analysis of measurements and comparatively simply in numerical experiments. Thus computer studies of two-dimensional turbulence described by the Navier-Stokes equations with periodic boundary conditions[244] have shown that the dimension of the chaotic set, calculated with the help of the definition of Lyapunov exponents, is usually much less than the number of elementary (harmonic) excitations engendering the flow. This fact has a clear interpretation—the chaotic dynamics of the flow is determined only by the large number of independent (in this case—large-scale) excitations; the rest are strongly coupled with them, i.e., they form coherent structures. This result was obtained previously for turbulence described by the two-dimensional Ginzburg-Landau equations.[216] It can be asserted that the dimension of the chaotic motion—turbulence—is correlated with the number of structures (spiral waves, defects of the wave lattice, etc.), interacting with one another.

The discovery of a relation between the dimension of turbulence for large Reynolds numbers and the number of modes in the inertial interval is of great interest. Here only isolated results have as yet been obtained (see, for example, Ref. 245), but it is precisely in the analysis of multidimensional stochastic sets, which vary very uniquely as the width of the inertial interval increases, that it may be possible to explain the phenomenon of self-similarity of turbulence from the viewpoint of nonlinear dynamics.

We thank I. S. Aranson, A. V. Gaponov-Grekhov, and M. V. Nezlin for fruitful discussions.

[1)] For wave fields it is known as the modulation instability,[11] also sometimes called the Benjamin-Feir instability.[9]

[2)] In the absence of a two-dimensional wave such disturbances with $\mathbf{Re} \lesssim 5772$ decay.

[3)] Here the picture of Ref. 45 is presented. This picture is typical for laboratory experiments, though it is obvious that other transitions are also possible, depending on the properties of the disturbances in the incident flow.

[4)] A remarkable property of this system is its gradient nature. Because of this property the obtained results regarding the instability of "elementary" localized structures can also be extended to a Hamiltonian system of the form $\partial^2 u/\partial t^2 = -\delta F/\delta u$, $\partial^2 v/\partial t^2 = -\delta F/\delta v$. We stress that the stability of the solutions forming at the minimum of the functional F is only a necessary condition for these static solutions to be stable in the Hamiltonian system with the same potential function. In the case when there are no internal resonances (corresponding to the nonlinear excitation of the characteristic degrees of freedom of the localized structure), however, this condition is also sufficient. Direct computer experiments have confirmed the existence of stable three-dimensional "particles" of the type shown in Fig. 6 in the Hamiltonian system presented.

5) The n-dimensional cubes covering the set may turn out to be "almost empty," and because of this it may be that $D < n$. For the usual sets the definition (3.4) gives obvious results. Thus for a set of isolated points we have $N(\varepsilon) = N$ and $D = 0$; for the segment L of a line $N(\varepsilon) = L/\varepsilon$, $D = 1$; for the area S of a two-dimensional surface $N(\varepsilon) = S/\varepsilon^2$, $D = 2$; etc.

6) Of course, the solution of Eqs. (3.6) (with given initial conditions at $t = 0$) actually describes the neighboring trajectory only as long as all distances $l_j(t)$ remain small. This circumstance, however, does not render meaningless the definition (3.7), in which arbitrarily long times are employed. The relative change in the lengths over a long time t enters into (3.7); within the framework of the linear approximation it gives the same result as successive relative changes over time intervals during each of which linearization of the equations is admissible.

7) Taking into account the Lyapunov exponent that equals zero makes a contribution of $+1$ to the dimension D_L, corresponding to the dimension along the trajectory itself.

8) The exact definition of the correlation interval is predicated on passing to the limit $N \to \infty$.

9) It may even happen that in a short realization there is simply not enough time for separate details of the attractor to be manifested.

10) As is well known, the states of matter near the critical point at different temperatures differ only by the spatial scale of long-range correlations. For this reason the thermodynamic functions of one or another state behave similarly and can be obtained from one another by a corresponding scale transformation. This property of critical phenomena is called scaling. Behavior of scaling type is also characteristic of transitions to chaos;[154] the nature of scaling is essentially the same as that of universality as a whole.

11) The significance of the parameter $\varepsilon = \varepsilon_{cr}$ is that of a critical point in the transition to chaos in each individual element.

12) Equation (3.19) for describing a transition to chaos in a medium with diffusion, consisting of elements described by Feigenbaum's mapping, was first studied in Refs. 160 and 161.

13) Such forcings are usually realized with the help of vibrations of the borders forming the flow or vibrating ribbons inserted additionally into the flow. Small pulsations of the flow rate in jets and acoustic irradiation at subsonic velocities can in most cases be classified as concentrated forcings, since the disturbances which they introduce are transformed effectively into modes of the hydrodynamic flow only near the borders.[171,172]

14) The term dimension in this case is employed in its everyday sense and refers to the units of measurement of physical quantities.

[Reviews and articles which contain a detailed discussion of the questions studied here are marked with an asterisk.]

1* F. H. Busse in: Hydrodynamic Instability and the Transition to Turbulence, (Eds.) H. L. Swinney and J. P. Gollub, Springer-Verlag, N.Y., 1985. [Russ. transl., Mir, M., 1984, p.124].

2 L. P. Gor'kov, Zh. Eksp. Teor. Fiz. **33**, 402 (1957) [Sov. Phys. JETP **6**, 311 (1958).

3 V. W. R. Malkus and G. Veronis, J. Fluid Mech. **4**, 225 (1958).

4 A. Schluter, D. Lortz, and F. H. Busse, *ibid.* **23**, 129 (1965).

5 F. H. Busse and J. A. Whitehead, *ibid.* **47**, 305 (1971).

6 F. H. Busse and R. M. Clever, *ibid.* **91**, 319 (1979).

7 R. M. Lever and F. H. Busse, J. Appl. Math Phys. **29**, 711 (1978).

8 W. Eckhaus, Studies in Non-Linear Stability Theory, Springer-Verlag, N.Y., 1965 (Springer Tracts in Natural Philosophy, Vol. 6).

9 J. T. Stuart and R. C. di Prima, Proc. R. Soc. London A **362**, 27 (1978).

10 M. Lowe and J. P. Gollub, Phys. Rev. **55**, 2575 (1985).

11 M. I. Rabinovich and D. I. Trubetskov, Introduction to the Theory of Oscillations and Waves [in Russian], Nauka, M., 1984.

12 F. H. Busse, J. Fluid Mech. **52**, 97 (1972).

13 E. Jakeman, Phys. Fluids **11**, 10 (1968).

14* S. Chandrasekhar and G. S. Ranganath, Adv. Phys. **35**, 507 (1986).

15 M. C. Cross, Phys. Rev. A **25**, 1065 (1982).

16 J. A. Whitehead, Phys. Fluids **26**, 2899 (1983).

17* M. I. Rabinovich, Usp. Fiz. Nauk **125**, 123 (1978) [Sov. Phys. Usp. **21**, 443 (1978)].

18* J. R. Eckman, Rev. Mod. Phys. **53**, 643 (1984).

19* C. D. Andereck, S. S. Liu, and H. L. Swinney, J. Fluid Mech. **164**, 155 (1986).

20 S. Newhouse, D. Ruell, and F. Takens, Commun. Math. Phys. **64**, 35 (1987).

21* J.-P. Eckman and D. Ruelle, Rev. Mod. Phys. **57**, 617 (1985).

22 P. R. Fenstermaher, H. L. Swinney, and J. P. Gollub, J. Fluid Mech. **94**, 103 (1979).

23* E. A. Spiegel, Theoretical Approach to Turbulence, edited by I. L. Dwoyer, M. Y. Hussaini, and R. G. Voigt, Springer-Verlag, N.Y., 1985, p. 303.

24 L. D. Landau and E. M. Lifshitz, Fluid Mechanics, Pergamon Press, N. Y. 1987 [Russ. original, Nauka, M., 1986].

25* S. A. Orszag and A. T. Patera, Transition and Turbulence, (Ed.) R. E. Meyer, Academic Press, N.Y., 1981, p. 127.

26 M. Nishioka, S. Iida, and Y. Ichikawa, J. Fluid Mech. **72**, 731 (1975).

27 D. R. Carlson, S. E. Widnall, and M. F. Peeters, *ibid.* **121**, 487 (1982).

28* J. T. Stuart in: Ref. 25.

29 R. Breidenthal, J. Fluid Mech. **116**, 1 (1981).

30 J. C. Neu, *ibid.* **143**, 253 (1984).

31* S. J. Lin and G. M. Corcos, *ibid.* **141**, 139.

32 J. Jimenez, M. Cogollos, and P. L. Bernal, *ibid.* **152**, 125 (1985).

33 L. P. Bernal and A. Roshko, *ibid.* **170**, 499 (1986).

34* J. C. Lasheras, J. S. Cho, and T. Maxworthy, *ibid.* **172**, 231.

35 T. J. Mueller, R. C. Nelson, and J. T. Kegelman, AJAA J. **19**, 1607 (1981).

36 R. Kobayashi, Y. Kohama, and M. Kurosawa, J. Fluid Mech. **127**, 341 (1983).

37 R. Kobayashi and H. Izumi, *ibid.*, 353.

38* P. Kohama, Phys.-Chem. Hydrodynamics **6**, 659 (1985).

39 Y. Kohama and R. Kobayahsi, J. Fluid Mech. **137**, 153 (1983).

40* M. R. Head and P. Bandyopadhyay, *ibid.* **107**, 297 (1981).

41* J. M. Wallace, Flow of Real Fluids, (Ed.) G. E. A. Meier and F. Obermeir, Springer-Verlag, N.Y., 1985, p. 253.

42* A. E. Perry and M. S. Chang, J. Fluid Mech. **119**, 173 (1982).

43 R. F. Blackwelder, Phys. Fluids **26**, 2807 (1983).

44 A. E. Perry, T. T. Lim, and E. W. Teh, J. Fluid Mech. **104**, 387 (1981).

45 D. R. Williams, H. Fasel, and F. R. Hama, *ibid.* **149**, 179 (1984).

46 V. P. Reutov, Zh. Prikl. Mekh. Fiz. **28**, No. 5, 107 (1987) [J. Appl. Mech. Tech. Phys. (USA) **28**(5), 742 (1987)].

47* G. M. Corcos and F. S. Sherman, J. Fluid Mech. **139**, 29 (1984).

48* G. M. Corcos and S. J. Lin, *ibid.*, 67.

49 I. Wygnanski, D. Oster, H. Fiedler, and B. Dziomba, *ibid.* **93**, 325 (1979).

50 R. Breidenthal, Phys. Fluids **23**, 1929 (1980).

51 A. K. M. F. Hussain and K. B. M. Zaman, J. Fluid Mech. **159**, 85 (1985).

52 L. D. Meshalkin and Ya. G. Sinai, Prikl. Mat. Mekh. **25**, 1140 (1961) [PMM J. Appl. Math. Mech. **25**, 1700 (1961)].

53* A. M. Obukhov, Usp. Mat. Nauk **38**, 101 (1983) [Russ. Math. Surv. **38**, 113 (1983)].

54* V. A. Dovzhenko and F. V. Dolzhanskiĭ in: *Nonlinear Waves. Structures and Bifurcations,* edited by A. V. Gaponov-Grekhov and M. I. Rabinovich [in Russian], Nauka, M., 1987, p. 132.

55* S. S. Moiseev, R. Z. Sagdeev, A. V. Tur, G. A. Khomenko, and V. V. Yanovskiĭ, Zh. Eksp. Teor. Fiz. **85**, 1979 (1983) [Sov. Phys. JETP **58**, 1149 (1983).

56 V. V. Gvaramadze, A. V. Tur, and G. A. Khomenko, "Interaction of a stationary flow with spiral turbulence," Preprint No. 121, IKI AN SSSR, Moscow (1987).

57 G. Sivashinsky and V. Yakhot, Phys. Fluids **28**, 1040 (1985).

58 V. Yakhot and G. N. Sivashinsky, Phys. Rev. A **35**, 815 (1987).

59 V. Yakhot and R. Pelz, Phys. Fluids **30**, 1272 (1987).

60 D. Galloway and V. Frisch, J. Fluid Mech. **180**, 557 (1987).

61 V. Frisch, Z. S. She, and P. L. Sulem, Physica D **28**, 382 (1987).

62 F. H. Busse and J. A. Whitehead, J. Fluid Mech. **66**, 67 (1974).

63 A. Barcilon, J. Brindley, M. Lessen, and F. R. Mobs, *ibid.* **94**, 453 (1979).

64 A. Barcilon and J. Brindley, *ibid.* **143**, 429 (1984).

65 R. Krishnamurti and L. N. Howard, Proc. Natl. Acad. Sci. USA **78**, 1981 (1981).

66* L. N. Howard and R. Krishnamurti, J. Fluid Mech. **170**, 385 (1986).

67 L. D. Landau, Dokl. Akad. Nauk SSSR **44**, 339 (1944).

68 H. R. Brand, P. S. Lomdahl, and A. C. Newell, Phys. Lett. A **118**, 67 (1986).

69 H. R. Brand, P. S. Lomdahl, and A. C. Newell, Physica D **23**, 345 (1986).

70* C. Normand, Y. Pomeau, and M. G. Velarde, Rev. Mod. Phys. **49**, 591 (1977).

71 P. R. Gromov, A. B. Zobnin, M. I. Rabinovich, and M. M. Sushchik, Pis'ma Zh. Tekh. Fiz. **12**, 1323 (1986) [Sov. Tech. Phys. Lett. **12**, 547 (1986)].

72* A. V. Gaponov-Grekhov and M. I. Rabinovich in: Ref. 54, p. 7.

73 M. V. Nezlin, E. N. Snezhkin, and A. S. Trubnikov, Pis'ma Zh. Eksp. Teor. Fiz. **36**, 190 (1982) [JETP Lett. **36**, 234 (1982)].

74* M. V. Nezlin, Usp. Fiz. Nauk **150**, 3 (1986) [Sov. Phys. Usp. **29**, 807 (1986)].

[75]A. V. Gaponov-Grekhov, A. S. Lomov, and M. I. Rabinovich, Pis'ma Zh. Eksp. Teor. Fiz. **44**, 242 (1986) [JETP Lett. **44**, 310 (1986)].
[76]O. V. Vashkevich, A. V. Gaponov-Grekhov, A. B. Ezerskiĭ, and M. I. Rabinovich, Dokl. Akad. Nauk SSSR **293**, 563 (1987) [Sov. Phys. Dokl. **32**, 197 (1987)].
[77]H. Haken, Advanced Synergetics: Instability Hierarchies of Self-Organizing Systems and Devices, Springer-Verlag, N. Y., 1983 [Russ. transl., Mir, M., 1985].
[78]A. V. Gaponov-Grekhov, A. S. Lomov, G. V. Osipov, and M. I. Rabinovich, "Origin and Dynamics of Two-Dimensional Structures in Nonequilibrium Dissipative Media" (in Russian), Preprint No. 199, Inst. Appl. Phys. Acad. Sci. USSR, Gor'kiĭ, 1988.
[79]I. S. Aranson, A. V. Gaponov-Grekhov, and M. I. Rabinovich, Izv. Akad. Nauk SSSR, Ser. Fiz. **51**, 1133 (1987) [Bull. Acad. Sci. USSR Phys. Ser. **51**(6), 87 (1987)].
[80]A. S. Lomov and M. I. Rabinovich, Pis'ma Zh. Eksp. Teor. Fiz. **48**, 598 (1988) [JETP Lett. **48**, 648 (1988)].
[81*] J. S. Swift and P. C. Hohenberg, Phys. Rev. A **15**, 319 (1977).
[82]S. Ciliberto and M. A. Rubio, Phys. Rev. **58**, 2652 (1987).
[83]K. A. Gorshkov, A. S. Lomov, and M. I. Rabinovich, Phys. Lett. A **137**, 250 (1989).
[84*] *V. S. L'vov and A. A. Predtechenskiĭ in: Nonlinear Waves: Stochasticity and Turbulence* [in Russian], (Ed.) M. I. Rabinovich, Gor'kii, 1980, p. 57.
[85]A. S. Thomas, J. Fluid Mech. **137**, 233 (1983).
[86*] J. M. Cimbala, H. M. Nagib, and A. Roshko, *ibid.* **190**, 265 (1988).
[87*] I. S. Aranson, A. V. Gaponov-Grekhov, and M. I. Rabinovich, Physica D **33**, 1 (1988).
[88]E. Meiburg and J. C. Lasheras, Phys. Fluids **30**, 623 (1987).
[89*] E. Meiburg and J. C. Lasheras, J. Fluid Mech. **190**, 1 (1988).
[90]J. A. Whitehead, *ibid.* **75**, 715 (1976).
[91]Y. Pomeau, Physica D **23**, 3 (1986).
[92]M. Lowe, J. P. Gollub, and T. C. Lubensky, Phys. Rev. Lett. **51**, 786 (1983).
[93]A. B. Ezerskiĭ, N. I. Korotin, and M. I. Rabinovich, Pis'ma Zh. Eksp. Teor. Fiz. **41**, 129 (1985) [JETP Lett. **41**, 157 (1985)].
[94]A. B. Zobnin, M. I. Rabinovich, and M. M. Sushchik, "Dynamics of defects in a Kármán street of vortices" (In Russian), Inst. Appl. Phys. Acad. Sci. USSR, Gor'kiĭ, 1989.
[95]K. F. Browand and C.-M. Ho, Nucl. Phys. B **2**, 139 (1987).
[96]D. V. Choodnovsky and G. V. Choodnovsky, Nuovo Cimento B **40**, 339 (1977).
[97*] H. Aref, Ann. Rev. Fluid Mech. **15**, 345 (1983).
[98*] S. Qian, Y. C. Lee, and H. H. Chen, Phys. Fluids B **1**, 87 (1989).
[99]H. Lamb, Hydrodynamics, Cambridge Univ. Press, 1932 [Russ. transl., Gostekhizdat, M., 1947].
[100*] P. G. Saffman and G. R. Baker, Ann. Rev. Fluid Mech. **11**, 95 (1979).
[101]B. M. Bubnov and G. S. Golitsyn, Dokl. Akad. Nauk SSSR **281**, 552 (1985) [Sov. Phys. Dokl. **30**, 204 (1985)].
[102*] B. M. Bubnov and G. S. Solitsyn, J. Fluid Mech. **167**, 503 (1986).
[103*] E. J. Hopfinger, F. K. Browand, and Y. Gagne, *ibid.* **125**, 103 (1982).
[104]G. Ahlers and D. S. Cannell, Phys. Rev. Lett. **50**, 1583 (1983).
[105]M. Luke, M. Mihelcic, and B. Kowalski, Phys. Rev. A **35**, 4001 (1987).
[106]A. N. Kolmogorov, I. G. Petrovskiĭ, and N. S. Piskunov, Byul. MGU Ser. Mat. mekh. **1**, 1 (1937).
[107*] E. Ben-Jacob, H. Brand, G. Dee, L. Kramer, and J. S. Langer, Physica D **14**, 348 (1985).
[108]V. G. Kamenskiĭ and S. V. Manakov, Pis'ma Zh. Eksp. Teor. Fiz. **45**, 499 (1987) [JETP Lett. **45**, 638 (1987)].
[109]P. A. Matusov and L. Sh. Tsimring, "Propagation of a front of parametrically excited capillary ripples," (In Russian), Preprint, Inst. Appl. Phys. Acad. Sci. USSR, Gor'kiĭ (1989).
[110]E. D. Siggia and A. Zippelius, Phys. Rev. A **24**, 1036 (1981).
[111]G. Tesauro and M. C. Cross, *ibid.* **34**, 1363 (1986).
[112*] P. Huerre, Nucl. B **2**, 159 (1987).
[113]A. Zippelius and E. D. Sigia, Phys. Fluids **26**, 2905 (1983).
[114*] H. S. Greenside and W. M. Coughran, Phys. Rev. A **31**, 398 (1984).
[115]V. Croquette and A. Pocheau, Lect. Not. Phys. **210**, 104 (1984).
[116]M. C. Cross, Phys. Rev. A **25**, 1065 (1982).
[117]M. S. Heutmaker, P. N. Fraenkel, and J. P. Gollub, Phys. Rev. Lett. **54**, 1369 (1985).
[118*] A. V. Gaponov-Grekhov, A. S. Lomov, G. V. Osipov, and M. Rabinovich, Nonlinear Waves. Part 1, (Eds.) A. Gaponov-Grekhov, M. Rabinovich, and J. Engelbreht, Springer-Verlag, N.Y., 1989, p. 65.
[119]M. Roberts, J. W. Swift, and D. H. Wagner, Contemp. Math. **56**, 283 (1986).
[120]M. Henon, C. R. Acad. Sci. A **262**, 312 (1966).
[121]I. S. Aranson, M. I. Rabinovich, and M. M. Sushchik, Chaos and Order in Nature, (Ed.) H. Haken, Springer-Verlag, N. Y., 1981, p. 54.
[122]L. M. Kuznetsova, M. I. Rabinovich, and M. M. Sushchik, Izv. Akad. Nauk SSSR, Ser. Fiz. Atm. Okeana **19**, 53 (1983) [Izv. Acad. Sci. USSR Atmos. Oceanic Phys. **19**(1) 36 (1983)].
[123*] M. I. Rabinovich and M. M. Sushchik in: Nonlinear Waves: Self Organization [in Russian], edited by A. V. Gaponov-Grekhov and M. I. Rabinovich, Nauka, M., 1983, p. 58.
[124]H. Aref, J. Fluid Mech. **143**, 1 (1984).
[125]J. Chaiken, R. Chevray, M. Tabor, and Q. M. Tam, Proc. R. Soc. London A **408**, 165 (1986).
[126]A. Leonard, V. Rom-Kedar, and S. Wiggins, Nucl. Phys. **B 2**, 179 (1987).
[127]M. Falcioni, G. Paladin, and A. Vulpiani, J. Phys. A **2**, 3451 (1987).
[128]E. A. Novikov and Yu. B. Sedov, Pis'ma Zh. Eksp. Teor. Fiz. **29**, 737 (1979) [JETP Lett. **29**, 677 (1979)].
[129]E. A. Novikov and Yu. B. Sedov, Zh. Eksp. Teor. Fiz. **77**, 588 (1979) [Sov. Phys. JETP **50**, 297 (1979)].
[130]S. L. Ziglin, Dokl. Akad. Nauk SSSR **250**, 1296 (1980) [Sov. Math. Dokl. **21**, 296 (1980)].
[131]J. M. Finn and E. Ott, Phys. Rev. Lett. **60**, 760 (1988).
[132*] K. R. Sreenivasan and C. Meneveau, J. Fluid Mech. **173**, 357 (1986).
[133]F. Ledrappier, Comm. Math. Phys. **81**, 229 (1981).
[134]R. Mane, *Dynamical Systems and Turbulence*, Springer-Verlag, N.Y., 1981, p. 230 (Lecture Notes in Mathematics, Vol. 898).
[135*] *F. Takens, ibid., p. 3661.*
[136]P. Grassberger and I. Procaccia, Phys. Rev. Lett. **50**, 346 (1983).
[137]P. Grassberger, Phys. Lett. A **97**, 227 (1983).
[138]H. G. E. Hentschel and I. Procaccia, Physica D **8**, 435 (1983).
[139]P. Grassberger, Phys. Lett. A **107**, 103 (1985).
[140]M. Halsey, J. Jensen, L. P. Kadanoff, I. Procaccia, and B. I. Shraĭman, Phys. Rev. A **33**, 1141 (1986).
[141*] V. S. Afraĭmovich and A. M. Reĭman *in*: Nonlinear Waves: Dynamics and Evolution [in Russian], (Ed.) A. V. Gaponov-Grekhov and M. I. Rabinovich, Nauka, M., 1989.
[142]P. Grassberger and I. Procaccia, Phys. Rev. A **28**, 2591 (1983).
[143]P. R. Gromov, A. B. Zobnin, M. I. Rabinovich, A. M. Reĭman, and M. M. Sushchik in: Numerical Methods in the Mechanics of Continuous Media [in Russian], (Ed.) G. V. Godiyak, Novosibirsk, 1986, p. 30.
[144]A. Brandstater, J. Swift, H. L. Swinney, A. Wolf, J. D. Farmer, E. Jen, and P. J. Crutchfield, Phys. Rev. Lett. **51**, 1442 (1983).
[145]B. Malraison, P. Atten, P. Berge, and M. Dubuis, J. Phys. (Paris) Lett. **44**, L-897 (1983).
[146]P. R. Gromov, A. B. Zobnin, M. I. Rabinovich, A. M. Reĭman, and M. M. Sushchik, Dokl. Akad. Nauk SSSR **292**, 284 (1987) [Sov. Phys. Dokl. **32**, 8 (1987)].
[147]M. I. Rabinovich and M. M. Sushchik, Laminar-Turbulent Transition: IUTAM Symposium, Novosibirsk, 1984, (Ed.) V. V. Kozlov, Springer-Verlag, N.Y., 1985, p. 375.
[148*] M. M. Sushchik in: Ref. 54, p. 104.
[149]M. Bonett, R. Meynart, J. P. Boon, and D. Olivari, Phys. Rev. Lett. **55**, 492 (1985).
[150]V. V. Kozlov, M. I. Rabinovich, M. P. Ramaganov, A. M. Reĭman, and M. M. Sushchik, Pis'ma Zh. Tekh. Fiz. **13**, 986 (1987) [Sov. Tech. Phys. Lett. **13**, 411 (1987)].
[151]V. V. Kozlov, M. I. Rabinovich, M. P. Ramazanov, A. M. Reĭman, and M. M. Sushchik, Phys. Lett. A **128**, 479 (1988).
[152*] R. J. Deissler and K. Kaneko, *ibid.* **119**, 397 (1987).
[153]Yu. S. Kachanov, V. V. Kozlov, and V. Ya. Levchenko, Formation of Turbulence in a Boundary Layer [in Russian], Nauka, Novosibirsk, 1982.
[154]M. Feigenbaum, J. Stat. Phys. **21**, 669 (1979).
[155*] M. J. Feigenbaum, Los Alamos Science **1**, 4 (1980) [Russ. transl., Usp. Fiz. Nauk **141**, 343 (1983)].
[156]P. Manneville and Y. Pomeau, Physica D **1**, 219 (1980).
[157]M. J. Feigenbaum, L. P. Kadanoff, and S. J. Shenker, *ibid.* **5**, 370 (1982).
[158]Ya. G. Sinaĭ and K. M. Khanin, *Renormalization Group*, (Eds.) D. V. Shirkov, D. I. Kazakov, and A. A. Vladimirov, World Scientific, Singapore, 1988, p. 251.
[159]I. S. Aranson and M. I. Rabinovich, "Renormalization group description of the spatial development of turbulence," Preprint No. 152, Inst. Appl. Phys. Acad. Sci. USSR, Gor'kiĭ (1987).
[160]S. P. Kuznetsov and A. S. Pikovskiĭ, Izv. Vyssh. Uchebn. Zaved., Radiofiz. **28**, 308 (1985) [Radiophys. Quantum Electron. **28**, 205 (1985)].
[161]S. P. Kuznetsov, *ibid.* **29**, 889 (1986) [*ibid.* **29**, 679 (1986)].
[162]S. P. Kuznetsov, *ibid.* **28**, 991 (1985) [*ibid.* **28**, 681 (1985)].
[163]V. S. Anishchenko, I. S. Aranson, D. E. Postnov, and M. I. Rabinovich, Dokl. Akad. Nauk SSSR **286**, 1120 (1986) [Sov. Phys. Dokl. **31**, 169 (1986)].
[164]S. P. Kuznetsov, Izv. Vyssh. Uchebn. Zaved., Fiz., No. 6, 87 (1984) [Sov. Phys. J. **27**, 522 (1984)].
[165]A. V. Gaponov-Grekhov, M. I. Rabinovich, and I. M. Starobinets, Pis'ma Zh. Eksp. Teor. Fiz. **39**, 561 (1984) [JETP Lett. **39**, 688

(1984)].
[166]I. S. Aranson, A. V. Gaponov-Grekhov, M. I. Rabinovich, and I. M. Starobinets, Zh. Eksp. Teor. Fiz. **90**, 1707 (1986) [Sov. Phys. JETP **63**, 1000 (1986)].
[167]A. A. Townsend, The Structure of Turbulent Shear Flow, Cambridge University Press, 2nd Ed., 1976 [Russ. transl. of first ed., Inostr. Lit., M., 1959].
[168]A. A.Townsend, J. Fluid Mech. **41**, 13 (1970).
[169]P. M. Bevillaqua and P. S. Lykoudis, *ibid.* **89**, 589 (1978).
[170]E. Achenbach, *ibid.* **62**, 209 (1974).
[171]C. K. W. Tam, *ibid.* **89**, 257 (1987).
[172]C. K. W. Tam, *ibid.*, 373.
[173]A. S. Ginevskiĭ, E. V. Vlasov, and A. V. Kolesnikov, *Aeroacoustic Interactions* [In Russian], Mashinostroenie, M., 1978.
[174*] E. V. Vlasov and A. S. Ginevskiĭ, Akust. Zh. **26**, 1 (1980) [Sov. Phys. Acoust. **26**, 1 (1980)].
[175*] A. D. Mansfel'd, M. I. Rabinovich, and M. M. Sushchik, *Proceedings of the 2nd All-Union Symposium on the Physics of Acoustodynamic Phenomena and Optoacoustics* (in Russian), Nauka, M., 1982, p. 12.
[176*] A. S. Ginevskii and E. V. Vlasov, in: *Models of the Mechanics of Continuous Media* [in Russian], Novosibirsk, 1983, p. 91.
[177*] A. K. M. F. Hussain, Phys. Fluids **26**, 2816 (1983).
[178*] A. K. M. F. Hussain, J. Fluid Mech. **173**, 303 (1986).
[179*] C. M. Ho and P. Huerre, Ann. Rev. Fluid Mech. **16**, 365 (1984).
[180*] E. V. Vlasov and A. S.Ginevskiĭ, *Progress in Science and Technology, Series on the Mechanics of Liquids and Gases,* [in Russian], VINITI, Acad. Sci. USSR, M., 1986, Vol. 20, p. 3.
[181]E. V. Vlasov and A. S. Ginevskiĭ, Izv. Akad. Nauk SSSR, Ser. Mekh. Zhidk. Gaza No. 4, 133 (1967) [Fluid Dynamics (1967)].
[182]E. V. Vlasov and A. S. Ginevskiĭ, *ibid.* No. 6, 37 (1973) [*ibid.* (1973)].
[183]S. I. Isataev and S. B. Tarasov, *ibid.* No. 2, 164 (1971) [*ibid.* (1971)].
[184]V. I. Furletov, *ibid.*, No. 5, 166 (1969) [*ibid.* (1969)].
[185]N. N. Ivanov, *ibid.* No. 4, 182 (1970) [*ibid.* (1970)].
[186]N. N. Ivanov, Zh. Prikl. Mekh. Tekh. Fiz., No. 1, 58 (1972) [J. Appl. Mech. Tech. Phys. (USA) **13**(1), 48 (1972)].
[187]O. I. Navoznov and A. A. Pavel'ev, Izv. Akad. Nauk SSSR, Ser. Mekh. Zhidk. Gaza No. 4, 18 (1980) [Fluid Dynamics (1980)].
[188]A. A. Pavel'ev and V. I. Tsyganok, *ibid.* No. 6, 36 (1982) [Fliud Dynamics (1982)].
[189]A. V. Kudryashov, A. D. Mansfel'd, M. I. Rabinovich, and M. M. Sushchik, Dokl. Akad. Nauk SSSR **277**, 61 (1984) [Sov. Phys. Dokl. **29**, 530 (1984)].
[190]A. V. Kudryashov, A. D. Mansfel'd, M. I. Rabinovich, and M. M. Sushchik, Ultrasonic Diagnostics [in Russian], Inst. Appl. Phys. Acad. Sci. USSR, Gor'kiĭ, 1983, p. 182.
[191]A. K. M. F. Hussain and M. A. Z. Hasan, J. Fluid Mech. **150**, 159 (1985).
[192]A. K. M. F. Hussain and K. B. M. Q. Zaman, *ibid.* **101**, 493 (1980).
[193]H. W. Liepman and D. M. Nosenchuck, *ibid.* **118**, 201 (1982).
[194]A. S. Thomas, *ibid.* **137**, 233 (1983).
[195]P. R. Gromov, A. B. Zobnin, S. V. Kiyashko, M. I. Rabinovich, and M. M. Sushchik, "Self-excited oscillations in a wind tunnel with an open working part," (in Russian), Preprint No. 135, Inst. Appl. Phys. Acad. Sci. USSR, Gor'kiĭ, 1986.
[196]P. R. Gromov, A. B. Zobnin, S. V. Kiyashko, and M. M. Sushchik, Akust. Zh. **34**, 349 (1988) [Sov. Phys. Acoust. **34**, 206 (1988)].
[197]J. A. Domaradzki and R. W. Metcalfe, Phys. Fluids **30**, 695 (1987).
[198]P. W. Carpenter and A. D. Garrad, J. Fluid Mech. **170**, 199 (1986).
[199]B. Bak, Rep. Prog. Phys. **45**, 587 (1982).
[200]S. Aubry, Physica D **7**, 240 (1983).
[201]D. Pal and R. E. Kelly, *Proceedings of the 6th International Heat Transfer Conference*, National Res. Council of Canada, Toronto, 1978, Vol. 2, p. 235.
[202]R. E. Kelly and D. Pal, J. Fluid Mech. **86**, 433 (1978).
[203]M. Lowe and J. P. Gollub, Phys. Rev. A **31**, 3893 (1985).
[204]M. Lowe, B. S. Albert, and J. P. Gollub, J. Fluid Mech. **173**, 253 (1986).
[205]P. Coulett, Phys. Rev. Lett. **56**, 724 (1986).
[206]C. Elphick, J. Phys. A **19**, L877 (1986).
[207*] V. S. Lvov, A. A. Predtechensky, and A. I. Chernykh, Nonlinear Dynamics and Turbulence, (Eds.) G. I. Barenblatt *et al.*, Pitman, Boston, 1983, p. 238.
[208]Yu. N. Belyaev, A. A. Monakhov, S. A. Shcherbakov, and I. M. Yavorskaya, Dokl. Akad. Nauk SSSR **279**, 51 (1984) [Sov. Phys. Dokl. **29**, 872 (1984)].
[209]P. Coulett, C. Elphick, and D. Repaux, Phys. Rev. Lett. **58**, 431 (1987).
[210]S. Ciliberto and M. A. Rubio, *ibid.*, 2652.
[211]S. Ciliberto and P. Bigazzi, *ibid.* **60**, 286 (1988).
[212]A. Pocheau, V. Croquette, and P. le Gal, Phys. Rev. Lett. **55**, 1094 (1985).
[213]V. Croquette, P. le Gal, and A. Pocheau, Phys. Scripta **113**, 135 (1986).
[214*] A. B. Ezerskiĭ, M. I. Rabinovich, V. P. Reutov, and I. M. Starobinets, Zh. Eksp. Teor. Fiz. **91**, 2070 (1986) [Sov. Phys. JETP **64**, 1228 (1986)].
[215]Y. Pomeau and P. Manneville, Comm. Math. Phys. **79**, 189 (1980).
[216]I. S. Aranson, A. V. Gaponov-Grekhov, and M. I. Rabinovich, Zh. Eksp. Teor. Fiz. **89**, 92 (1985) [Sov. Phys. JETP **62**, 52 (1985)].
[217]A. N. Kolmogorov, Dokl. Akad. Nauk SSSR **30**, 299 (1941).
[218]R. J. Taylor, Austr. J. Phys. **8**, 535 (1955).
[219]M. M. Gibson, J. Fluid Mech. **15**, 161 (1963).
[220]M. S. Uberoi and P. Freymyth, Phys. Fluids **12**, 1359 (1969).
[221]F. H. Champagne, V. G. Harris, and S. Corsin, J. Fluid Mech. **41**, 81 (1970).
[222*] F. H. Champagne, *ibid.* **86**, 67 (1978).
[223]M. E. Bracket *et al.*, Phys. Rev. Lett. **57**, 683 (1986).
[224]A. Babino *et al.*, J. Fluid Mech. **183**, 379 (1987).
[225]S. Kida and M. Sugihare, J. Phys. Soc. Jpn. **50**, 1785 (1981).
[226]M. Yamada and K. Ohkitani, Phys. Rev. Lett. **60**, 983 (1988).
[227]M. Yamada and K. Ohkitani, Phys. Lett. A **134**, 165 (1988).
[228]A. M. Obukhov, Dokl. Akad. Nauk SSSR **32**, 22 (1941).
[229]F. Anselmet, Y. Gagne, E. J. Hopfinger, and A. R. Antonia, J. Fluid Mech. **140**, 63 (1984).
[230]E. A. Novikov and R. W. Stewart, Izv. Akad. Nauk SSSR, Ser. Geofiz. No. 3, 408 (1964) [Izv. Acad. Sci. USSR Geophys. Ser. No. 1, 245 (1964)].
[231]E. A. Novikov, Dokl. Akad. Nauk SSSR **184**, 1072 (1969) [Sov. Phys. Dokl. **14**, 104 (1969)].
[232]E. A. Novikov, Prikl. Mat. Mekh **35**, 266 (1970) [PMM J. Appl. Math. Mech. **35**, 231 (1970)].
[233]R. H. Kraichman, J. Fluid Mech. **63**, 305 (1974).
[234]U. Frisch and G. Parisi, *Turbulence and Predictability in Geophysical Fluid Dynamics and Climate Dynamics*, (Eds.) M. Ghil, R. Benzi, and G. Paris, North-Holland, Amsterdam, 1984, p. 84.
[235]R. Benzi, G. Paladin, G. Parisi, and A. Vulpiani, J. Phys. A **17**, 3521 (1984).
[236]G. Paladin and A. Vulpiani, Phys. Rep. **156**, 147 (1987).
[237]C. Meneveau and K. R. Sreenivasan, Nucl. Phys. B **2**, 49 (1987).
[238]R. H. Kraichnan and R. Panda, Phys. Fluids **31**, 2395 (1988).
[239]A. Tsinober and E. Levich, Phys. Lett. A **99**, 231 (1983).
[240]E. Levich, Phys. Rep. **151**, 129 (1987).
[241]R. B. Pelz, V. Yakhot, S. A. Orszag, L. Shtilman, and E. Levich, Phys. Rev. Lett. **54**, 2505 (1985).
[242]E. Kit, A. Tsinober, J. L. Balint, J. M. Wallace, and E. Levich, Phys. Fluids **30**, 3323 (1987).
[243]M. M. Rogers and P. Moin, *ibid.*, 2662.
[244]R. Grappin and J. Leorat, Phys. Rev. Lett. **50**, 1100 (1987).
[245]R. Grappin, J. Leorat, and A. Pouquet, J. Phys. (Paris) **47**, 1127 (1986).

Translated by M. E. Alferieff